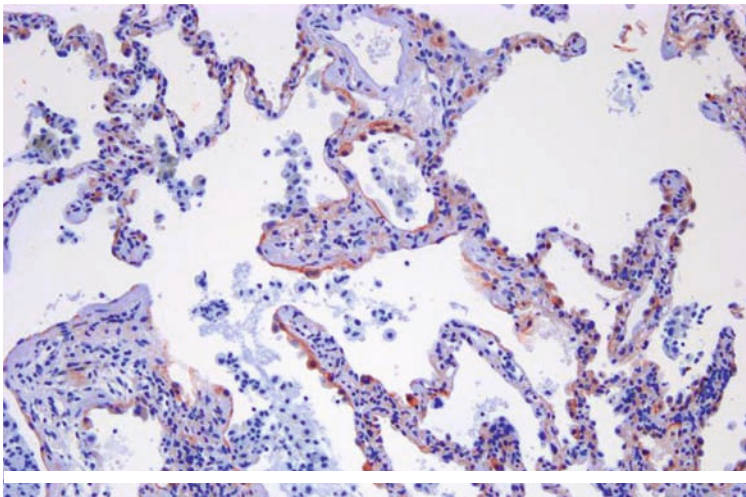


Role of the WNT/ β -catenin signal pathway in idiopathic and experimental pulmonary fibrosis

NISHA BALSARA



INAUGURAL-DISSERTATION zur Erlangung des Grades eines **Dr. med. vet.**
beim Fachbereich Veterinärmedizin der Justus-Liebig-Universität Gießen



édition scientifique
VVB LAUFERSWEILER VERLAG

Das Werk ist in allen seinen Teilen urheberrechtlich geschützt.

Jede Verwertung ist ohne schriftliche Zustimmung des Autors oder des Verlages unzulässig. Das gilt insbesondere für Vervielfältigungen, Übersetzungen, Mikroverfilmungen und die Einspeicherung in und Verarbeitung durch elektronische Systeme.

1. Auflage 2013

All rights reserved. No part of this publication may be reproduced, stored in a retrieval system, or transmitted, in any form or by any means, electronic, mechanical, photocopying, recording, or otherwise, without the prior written permission of the Author or the Publishers.

1st Edition 2013

© 2013 by VVB LAUFERSWEILER VERLAG, Giessen

Printed in Germany



édition scientifique
VVB LAUFERSWEILER VERLAG

STAUFENBERGRING 15, D-35396 GIESSEN
Tel: 0641-5599888 Fax: 0641-5599890
email: redaktion@doktorverlag.de

www.doktorverlag.de

aus dem Institut für Veterinär-Physiologie
Fachbereich Veterinärmedizin
Justus-Liebig-Universität Gießen
Betreuer: Prof. Dr. Rüdiger Gerstberger
und
aus dem Zentrum für Innere Medizin
Medizinische Klinik und Poliklinik II,
Fachbereich Humanmedizin
Universitätsklinikum Gießen und Marburg - Standort Gießen
Betreuer: Prof. Dr. Oliver Eickelberg

Role of the WNT/ β -catenin signal pathway in idiopathic and experimental pulmonary fibrosis

INAUGURAL-DISSERTATION
zur Erlangung des Grades eines
Dr. med. vet.
beim Fachbereich Veterinärmedizin
der Justus-Liebig-Universität Giessen

eingereicht von

Nisha Balsara

Tierärztin aus Offenbach am Main

Giessen 2013

mit Genehmigung des Fachbereichs Veterinärmedizin
der Justus-Liebig-Universität Gießen

Dekan: Prof. Dr. Dr. h.c. M. Kramer

Gutachter: Prof. Dr. R. Gerstberger
Prof. Dr. O. Eickelberg

Tag der Disputation: 17.06.2013

FOR MY PARENTS

I TABLE OF CONTENTS

I	TABLE OF CONTENTS	5
II	LIST OF FIGURES	8
III	LIST OF TABLES	10
IV	LIST OF ABBREVIATIONS	11
V	SUMMARY	19
VI	ZUSAMMENFASSUNG	21
1	INTRODUCTION	23
1.1	Diffuse parenchymal lung diseases.....	23
1.2	Idiopathic pulmonary fibrosis.....	24
1.2.1	Definition and epidemiology	24
1.2.2	Clinical features, radiological characteristics and therapy options	26
1.2.3	Histopathological characteristics	27
1.2.4	Pathomechanism of idiopathic pulmonary fibrosis	27
1.3	WNT signalling	31
1.3.1	The canonical WNT/ β -catenin signalling pathway.....	31
1.4	WNT signalling in the lung	34
1.4.1	Lung development and homeostasis	34
1.4.2	Lung cancer.....	36
1.5	WNT signalling in fibrotic disorders	37
2	AIMS OF THE STUDY	38
3	MATERIALS AND METHODS	39
3.1	Materials.....	39
3.1.1	Equipment.....	39
3.1.2	Chemical reagents	40
3.1.3	Antibodies.....	42
3.1.4	Recombinant proteins	43
3.1.5	Human tissues	43
3.1.6	Animal tissues.....	44
3.1.7	Primary cells	44
3.2	Methods.....	44
3.2.1	Animal model of bleomycin-induced pulmonary fibrosis in mice.....	44
3.2.2	WNT reporter mice (TOPGAL).....	45
3.2.3	Isolation of primary mouse alveolar epithelial type II (ATII) cells	45
3.2.4	Supernatants	48

3.2.5	RNA isolation and measurement	48
3.2.5.1	RNA isolation from lung homogenates	48
3.2.5.2	RNA isolation from cultured cells.....	48
3.2.6	cDNA synthesis	49
3.2.7	Quantitative real-time polymerase chain reaction (qRT-PCR)	50
3.2.8	DNA agarose gel electrophoresis.....	52
3.2.9	Immunohistochemistry	52
3.2.10	Immunocytochemistry	54
3.2.11	Western blot analysis	55
3.2.12	[³ H]-thymidine proliferation assay.....	57
3.2.13	Whole genome microarray.....	58
3.2.14	Enzyme linked-immuno-sorbent assay (ELISA)	58
3.2.15	Statistical analysis	59
4	RESULTS.....	60
4.1	Analysis of the canonical WNT/ β -catenin signalling pathway in idiopathic pulmonary fibrosis	60
4.1.1	Expression of the canonical WNT/ β -catenin signalling pathway in idiopathic pulmonary fibrosis.....	60
4.1.2	Localisation of the canonical WNT/ β -catenin signalling pathway in idiopathic pulmonary fibrosis.....	63
4.1.3	Activity of the canonical WNT/ β -Catenin signalling pathway in idiopathic pulmonary fibrosis.....	72
4.2	Analysis of the canonical WNT/ β -catenin signalling pathway in experimental pulmonary fibrosis	74
4.2.1	Expression of the canonical WNT/ β -catenin signalling pathway in experimental pulmonary fibrosis.....	74
4.2.2	Localisation of the WNT/ β -catenin signalling pathway in experimental pulmonary fibrosis.....	77
4.3	Functional analysis of the WNT/ β -catenin signalling pathway	87
4.3.1	Purity and phenotype of primary mouse alveolar epithelial type II (ATII) cells	88
4.3.2	Expression of Wnt3a-induced target genes in primary mouse alveolar epithelial type II (ATII) cells	91
4.3.3	Proliferative effects of Wnt3a stimulation on primary mouse alveolar epithelial type II (ATII) cells	92
4.3.4	Whole genome microarray analysis on Wnt3a-induced primary mouse alveolar epithelial type II (ATII) cells.....	94
4.4	Analysis of the novel WNT target genes IL1 β and IL6 <i>in vitro</i> and <i>in vivo</i>	98
4.4.1	ELISA analysis for quantification of IL1 β and IL6	98
5	DISCUSSION	103

5.1	Conclusions and future perspectives.....	116
6	APPENDIX.....	118
6.1	List of human (q)RT-PCR primers.....	118
6.2	List of mouse (q)RT-PCR primers.....	121
6.3	Characteristics of IPF patients.....	124
6.4	List of antibodies.....	125
6.4.1	Primary antibodies.....	125
6.4.2	Secondary antibodies.....	126
6.5	Microarray gene list.....	127
7	REFERENCES.....	129
8	DECLARATION.....	139
9	ACKNOWLEDGEMENTS.....	140

II LIST OF FIGURES

- figure 1.1: Classification scheme of diffuse parenchymal lung diseases (DPLDs)
- figure 1.2: Survival curves in different interstitial lung diseases (ILDs)
- figure 1.3: Origins of myofibroblasts in idiopathic pulmonary fibrosis (IPF)
- figure 1.4: Original and new hypotheses for the pathogenesis of idiopathic pulmonary fibrosis (IPF)
- figure 1.5: An overview of the canonical WNT signalling pathway
- figure 4.1: Gene expression profile of canonical WNT signalling components in idiopathic (IPF)
- figure 4.2.1 +
figure 4.2.2: Localisation of WNT1 in idiopathic pulmonary fibrosis (IPF)
- figure 4.3.1 +
figure 4.3.2: Localisation of WNT3A in idiopathic pulmonary fibrosis (IPF)
- figure 4.4.1 +
figure 4.4.2: Localisation of GSK3 β in idiopathic pulmonary fibrosis (IPF)
- figure 4.5.1 +
figure 4.5.2: Localisation of CTNNB1 in idiopathic pulmonary fibrosis (IPF)
- figure 4.6: Protein expression of canonical WNT signalling components in idiopathic pulmonary fibrosis (IPF)
- figure 4.7: Gene expression profile of canonical WNT signalling components in experimental pulmonary fibrosis
- figure 4.8.1 +
figure 4.8.2: Localisation of Wnt1 in experimental pulmonary fibrosis
- figure 4.9.1 +
figure 4.9.2: Localisation of Wnt3a in experimental pulmonary fibrosis
- figure 4.10.1 +
figure 4.10.2: Localisation of Gsk3 β in experimental pulmonary fibrosis
- figure 4.11.1 +
figure 4.11.2: Localisation of Ctnnb1 in experimental pulmonary fibrosis

- figure 4.12: Gene expression profile of canonical WNT signalling components in alveolar epithelial type II (ATII) cells from bleomycin-induced mouse lungs
- figure 4.13
(A+B): Purity and phenotype of primary mouse alveolar epithelial type II (ATII) cells
- figure 4.14: mRNA expression of Wnt3a-induced target genes of the canonical WNT/ β -catenin signalling pathway in primary mouse alveolar epithelial type II (ATII) cells
- figure 4.15: Proliferative effect induced by Wnt3a in primary mouse alveolar epithelial type II (ATII) cells
- figure 4.16: Whole genome expression analysis
- figure 4.17: mRNA expression of potential Wnt3a-induced target genes in primary mouse alveolar epithelial type II (ATII) cells
- figure 4.18: Protein quantification in supernatants from Wnt3a-stimulated primary mouse alveolar epithelial type II (ATII) cells
- figure 4.19: Protein quantification in conditioned media from bleomycin-treated primary mouse alveolar epithelial type II (ATII) cells
- figure 4.20: Protein quantification in mouse bronchoalveolar lavage fluids (BALFs)
- figure 4.21: Protein quantification in human bronchoalveolar lavage fluids (BALFs)

III LIST OF TABLES

- table 3.1: Composition of culture media for isolation of primary mouse alveolar epithelial type II (ATII) cells
- table 3.2: Composition of mixture for complementary deoxyribonucleic acid (cDNA) synthesis
- table 3.3: Composition of mixture for quantitative reverse transcription real time polymerase chain reaction ((q)RT-PCR)
- table 6.1: Human primer sequences and amplicon sizes
- table 6.2: Mouse primer sequences and amplicon sizes
- table 6.3: Characteristics of idiopathic pulmonary fibrosis (IPF) patients with usual interstitial pneumonia (UIP) pattern
- table 6.4.1: List of primary antibodies
- table 6.4.2: List of secondary antibodies
- table 6.5: List of selected target genes found in the microarray

IV LIST OF ABBREVIATIONS

α	Alpha (first letter of the Greek alphabet)
β	Beta (second letter of the Greek alphabet)
γ	Gamma (third letter of the Greek alphabet)
Δ	Delta (fourth letter of the Greek alphabet)
λ	Lambda (eleventh letter of the Greek alphabet)
μCi	microcurie (1 μCi = 3.7×10^4 dpm; measure/unit of radioactivity)
μg	microgram (10^{-6} g)
μl	microlitre (10^{-6} l)
μm	micrometre (10^{-6} m)
<	less-than sign
-	minus sign (mathematical symbol for negative/less)
+	plus sign (mathematical symbol for positive/more)
%	percentage (per cent = “per hundred”)

A

A549	adenocarcinomic human alveolar basal epithelial cells (a cell line)
ACTA2	alpha smooth muscle actin (α -SMA, a protein)
AIP	acute interstitial pneumonia
ANGII	angiotensin II (oligopeptide/hormone)
AP1	activating protein 1
APC	adenomatous polyposis coli (protein)
APS	ammonium persulfate
ATI	alveolar epithelial type I cell (type I pneumocyte)
ATII	alveolar epithelial type II cell (type II pneumocyte)
ATS	American Thoracic Society
AXIN2	axis inhibition protein 2 or conductin (protein)
AZ	“AktENZEICHEN” (= file reference)

B

β -TrCP	E3 ubiquitin ligase β -transducin repeat-containing protein
BALF	bronchoalveolar lavage fluid
bp	base pair
BSA	bovine serum albumin
BW	body weight

C

C57BL/6	common inbred strain of laboratory mice ("C57 black 6")
$^{\circ}\text{C}$	degree Celsius
Ca^{2+}	calcium
CamKII	calmodulin kinase II
cAMP	cyclic adenosine monophosphate
Cdh1	E-cadherin
CD	cluster of differentiation (used for identification of cell surface molecules)
cDNA	complementary deoxyribonucleic acid
CFA	cryptogenic fibrosing alveolitis
CK	casein kinase
CK1 γ	casein kinase 1 γ (serine/threonine protein kinase)
CO	carbon monoxide
CO ₂	carbon dioxide
COP	cryptogenic organising pneumonia
CRD	cysteine-rich domain
CREB	cAMP response element-binding (cellular transcription factor)
C _t	cycle of threshold in (q)RT-PCR
CTGF	connective tissue growth factor
CTNNB1	β -catenin
Cy	cyanine (synthetic fluorescent dyes)

D

DAPI	4',6-diamidino-2-phenylindole
ddH ₂ O	double distilled water
DIP	desquamative interstitial pneumonia
Dkk	dickkopf
DL _{CO}	diffusing capacity of the lung for carbon monoxide
DLT	double lung transplantation
DMEM	Dulbecco's modified eagle medium
DNA	deoxyribonucleic acid
DNase	deoxyribonuclease (enzyme/nuclease)
dNTP	deoxynucleoside triphosphate
DPBS	Dulbecco's phosphate buffered saline
DPLD	diffuse parenchymal lung disease
dpm	disintegrations per minute (measure of radioactivity)
dsDNA	doublestranded deoxyribonucleic acid
DVL	dishevelled

E

ECAD	E-cadherin
ECM	extracellular matrix
EDTA	ethylenediaminetetraacetic acid
e.g.	for example
EGTA	ethylene glycol tetraacetic acid
ELISA	enzyme linked-immuno-sorbent assay
EMT	epithelial-to-mesenchymal transition
ERS	European Thoracic Society
et al.	and others (et alii)

F

FAP	familial adenomatous polyposis
FBS	fetal bovine serum
f.c.	final concentration
Fc	fragment crystallizable region (region of an antibody)
FCS	fetal calf serum

FZD	frizzled
FITC	fluorescein-5-isothiocyanate
G	
g	g-force (m/sec ² , acceleration)/gramm
GBP	GSK binding protein
GSK3β	glycogen synthase kinase 3 beta
GTP	guanosine-5'-triphosphate (purine nucleotide)
H	
h	hours
³ H	tritium/hydrogen-3 (a radioactive isotope)
HDAC	histone deacetylases
HEPES	4-(2-hydroxyethyl)-1-piperazine ethane sulfonic acid (buffering agent)
HPRT	hypoxanthine phosphoribosyltransferase
HRCT	high-resolution chest computed tomography
HRP	horseradish peroxidase
I	
IF	immunofluorescence
IgG	immunoglobulin G (antibody molecules)
IHC	immunohistochemistry
IL	interleukin
IL1β	interleukin 1 beta
IL1R	interleukin 1 receptor
IL1RA	interleukin 1 receptor accessory protein
ILD	interstitial lung disease
IIP	idiopathic interstitial pneumonia
int-1	integration 1
i.p.	intraperitoneal
IPF	idiopathic pulmonary fibrosis

J

JNK c-Jun N-terminal kinase

K

kDA kilo Dalton

kg kilogram

KGF keratinocyte growth factor

L

l liter

LacZ structural gene encoding β -galactosidase

LAM lymphangioliomyomatosis

LEF lymphoid enhancer-binding factor

LIP lymphocytic interstitial pneumonia

log logarithm

LRP lipoprotein receptor-related protein

M

mg milligram (10^{-3} g)

MgCl₂ magnesium chloride

min. minutes

ml milliliter (10^{-3} l)

mM millimolar (a unit of concentration)

mm millimeter (10^{-3} m)

mmHg millimetre of mercury

MMP matrix metalloproteinase

MMTV mouse mammary tumor virus

mRNA messenger RNA

MuLVs murine leukemia viruses (retroviruses)

N

NaCl sodium chloride

NaOH sodium hydroxide

ng nanogram (10^{-9} g)

nm	nanometer (10^{-9} m)
NOV	nephroblastoma overexpressed
NSCLC	non-small cell lung cancer
NSIP	nonspecific interstitial pneumonia
O	
O ₂	oxygen
OCLN	occluding (tight junction protein)
OD	optical density
P	
p	p-value (probability of obtaining a test statistic)
panCK	pan-cytokeratin
PaCO ₂	partial pressure of carbon dioxide
PaO ₂	partial pressure of oxygen
Pbgd	porphobilinogen deaminase
PBS	phosphate-buffered saline
PBST	phosphate-buffered saline + 0.1 % Tween 20
PCP	planar cell polarity
PCR	polymerase chain reaction
PFA	paraform aldehyde
pg	picogram (10^{-12} g)
pH	measure of the acidity or basicity of an aqueous solution
PKA	protein kinase A
PKC	protein kinase C
Q	
qRT-PCR	quantitative reverse transcription real time PCR
R	
Rac	protein of the family of GTPases
RB-ILD	respiratory bronchiolitis-associated interstitial lung disease

Rho	protein of the family of GTPases
rmWnt3a	recombinant mouse protein Wnt3a
RNA	ribonucleic acid
RNase	ribonuclease (enzyme/nuclease)
ROX	an internal fluorescence dye
RT	reverse transcriptase/transcription
RT-PCR	reverse transcription PCR
S	
SDS	sodium dodecyl sulfate
SDS-PAGE	sodium dodecyl sulfate polyacrylamide gel electrophoresis
sem	standard error of mean
SLT	single lung transplantation
SMA	smooth muscle actin
SP-C	surfactant protein C
SPF	specific pathogen-free
SPP1	secreted phosphoprotein 1/osteopontin
ssDNA	single stranded
SYBR Green I	N',N'-dimethyl-N-[1]-1-phenylquinolin-1-ium-2-yl]-N-propylpropane-1,3-diamine (cyanine dye)
T	
TAE	tris-acetate-EDTA
TBST	tris-buffered saline and Tween 20 (mixture)
TCF	T-cellspecific transcription factor
TEMED	N,N,N,N'-tetramethyl-ethane-1,2-diamine
TGFβ1	transforming growth factor β1
TIMPs	tissue inhibitors of metalloproteinases
Tjp1	tight junction protein 1
TLC	total lung capacity
TNF	tumor necrosis factor
TRIS	tris(hydroxymethyl)-aminomethan
t-test	Student's t-test (statistical hypothesis test)

Tween20 polysorbate 20 (polysorbate surfactant)

U

U units

UDG uracil-DNA glycosylase

UIP usual interstitial pneumonia

USA United States of America

UV ultraviolet (light)

V

VA alveolar volume

VC vital capacity

v/v volume fraction (volume/volume)

W

WB Western blot

Wg wingless

Wisp Wnt1-inducible signalling protein

Wnt signal protein (hybrid of Wg and Int)

w/v mass concentration (mass/volume)

X

Y

Z

Further, not listed abbreviations are taken from the valid IUPAC-Nomenclature.

V SUMMARY

Human idiopathic pulmonary fibrosis (IPF) is a progressive and fatal lung disease of unknown origin, which is refractory to any currently available therapy. It is characterised by initial alveolar epithelial cell injury and hyperplasia, enhanced fibroblast/myofibroblast proliferation and activation and increased deposition of extracellular matrix (ECM) in the lung interstitium. These key features, ultimately lead to architectural distortion of the normal lung parenchyma and due to severe loss of function, to respiratory failure. However, the molecular mechanisms underlying alveolar epithelial type II (ATII) cell dysfunction are still poorly understood.

This study is based on the hypothesis that the WNT/ β -catenin signalling pathway, which is essential for organ development, is aberrantly activated in ATII cells in idiopathic and experimental pulmonary fibrosis. The role of canonical WNT signalling was elucidated by determining the expression, function and activity of the pathway.

An increased expression of most WNT/ β -catenin signalling components was demonstrated in pulmonary fibrosis. The mRNA expression was analyzed in lung homogenates of IPF and donor patients, as well as in lung homogenates and ATII cells isolated from the lungs of bleomycin- and saline-treated mice. Immunohistochemical analysis localized increased protein expression of WNT signalling largely in alveolar and bronchial epithelium of IPF patients, as well as of bleomycin-treated mice. This result was confirmed by quantitative real-time (q)RT-PCR of primary human and mouse ATII cells, demonstrating an increase of cell-specific functional WNT signalling. To elucidate active WNT/ β -catenin signalling in IPF, western blot analysis demonstrated that several WNT components were expressed and functional in ATII cells. Furthermore, WNT3A treatment significantly increased ATII cell proliferation. WNT3A treatment of ATII cells *in vitro* caused a significantly increased expression of WNT target genes and, most interestingly, the interleukins IL1 β and IL6. The occurrence of IL1 β and IL6 in conjunction with increased WNT/ β -catenin signalling was corroborated in primary ATII cells isolated from the lungs of bleomycin- and saline-treated mice and *in vivo* in BALF by orotracheal application of WNT3A. In addition, IL1 β and IL6 were increased in BALF samples from IPF patients.

In summary, this study shows that WNT signalling is expressed and localised in idiopathic and experimental pulmonary fibrosis, in particular in alveolar ATII cells. Reversal and/or inhibition predominantly of the WNT/ β -catenin signalling pathway, but equally the use of neutralising antibodies or inhibitors of IL1 β /IL6 may represent a valid therapeutic option in human lung fibrosis.

VI ZUSAMMENFASSUNG

Die häufigste und schwerwiegendste Form der idiopathischen interstitiellen Pneumonien (IIP) beim Menschen ist die idiopathische pulmonale Fibrose (IPF). Es handelt sich um eine therapierefraktäre, progressiv und tödlich verlaufende Lungenerkrankung mit unbekannter Ätiologie. Die initiale Schädigung des Alveolarepithels und eine daraus resultierende abnormale Wundheilung charakterisieren diese Erkrankung. Eine verstärkte Proliferation und Aktivierung von Fibroblasten/Myofibroblasten und die vermehrte Ansammlung von extrazellulärer Matrix (ECM) im Lungeninterstitium sind zusätzliche Begleiterscheinungen. Dies führt letztendlich zu einem kompletten Umbau bzw. einer Zerstörung des normalen Lungengewebes und aufgrund des funktionellen Verlustes zum respiratorischen Versagen. Die molekularen Mechanismen, die den veränderten Schädigungs- und Reparaturprozessen des Alveolarepithels zugrunde liegen und demnach für die Entwicklung von IPF verantwortlich sind, sind allerdings größtenteils noch unklar.

Der kanonische WNT Signaltransduktionsweg, benannt nach dem Liganden „WNT“, hat in der Organentwicklung eine besondere Bedeutung, spielt aber auch eine essentielle Rolle bei verschiedenen Erkrankungen. Das Signalprotein „WNT“ fungiert als lokaler Mediator, und der Name setzt sich zusammen aus den Genen Wingless (Wg) und Integration 1 (Int-1). Die vorliegende Arbeit basiert auf der Hypothese, dass der WNT/ β -catenin Signalweg in alveolaren Epithelzellen Typ II (ATII) in der idiopathischen sowie experimentellen pulmonalen Fibrose differenziell reguliert und aktiviert vorliegt.

In dieser Studie wurden neben humanem und murinem Lungenhomogenat, zusätzlich ATII Zellen aus gesunden bzw. fibrotischen murinen Lungen isoliert und untersucht. Mit Hilfe der quantitativen real-time reversen Transkriptase-Polymerase-Kettenreaktion ((q)RT-PCR) konnte eine gesteigerte Expression des WNT Signalweges nachgewiesen werden. Die verschiedenen WNT Komponenten, darunter auch das Protoonkogen WNT1, waren auf Transkriptionsebene im humanen und murinen fibrotischen Lungengewebe bzw. in daraus isolierten ATII Zellen zum Teil signifikant reguliert. Dabei auffallend war allerdings eine deutlich verminderte Expression des Proteins WNT3A, ein weiteres Mitglied der Sekretionsproteine aus der WNT Familie. Darüber hinaus konnte mittels Immunohistochemie eine

gesteigerte Proteinexpression in Bronchial- und Alveolarepithelzellen von gesunden und IPF Patienten sowie von gesunden und mit Bleomycin behandelten Mäusen, lokalisiert werden. Neben WNT1 und WNT3A wurde auch β -catenin (CTNNB1), ein intrazelluläres Schlüsselmolekül des WNT/ β -catenin Signalweges, exprimiert. Auch der zusätzliche Nachweis in primären murinen ATII Zellen hebt die Zellspezifität des Signalweges hervor. Ebenso konnte die Aktivierung des WNT/ β -catenin Signalweges in Lungengewebe von IPF Patienten durch Western Blot Analyse gezeigt werden. Zusätzlich bewirkte der Einsatz von rekombinantem murinen Wnt3A Protein eine zeitabhängige Regulation von bestimmten Wnt-spezifischen Zielgenen, wie cyclinD1 und WNT1-inducible-signaling pathway protein 1 (Wisp1), in primären murinen ATII Zellen. Weitere Versuche ergaben, dass WNT3A eine signifikant erhöhte Expression von bestimmten WNT-spezifischen Zielgenen bewirkte, welche unter anderem für die Interleukine IL1 β und IL6 kodieren. Der direkter Zusammenhang zwischen der gesteigerten Expression von spezifischen Interleukinen und die Aktivierung des WNT/ β -catenin Signalweges konnte mit Hilfe eines Microarrays verdeutlicht werden. Neben veränderten Genexpressionsprofilen, konnte bei primären murinen ATII Zellen, die mit rekombinantem murinen Wnt3A Protein stimuliert wurden, auch eine gesteigerte Zellproliferation beobachtet werden. Dabei wurden mittels [³H]-Thymidin Inkorporation die Effekte auf Proliferationsebene untersucht. Diese Beobachtung bestätigte sich in mit WNT3A stimulierten murinen ATII Zellen anhand von (q)RT-PCR, sowie in bronchoalveolären Lavage (BALF) Proben von IPF Patienten und Bleomycin behandelten Mäusen mittels ELISA.

Zusammenfassend konnte gezeigt werden, dass der WNT Signalweg bei der idiopathischen und experimentellen Lungenfibrose, vornehmlich in ATII Zellen lokalisiert sowie exprimiert wird. Demnach spielt dieser Signaltransduktionsweg eine potentiell erhebliche Rolle im Rahmen der Pathogenese der Erkrankung. Eine generelle Hemmung des WNT/ β -catenin Signalweges, aber auch die spezifische Verwendung von neutralisierenden IL1 β /IL6 Antikörpern, könnte einen möglichen therapeutischen Ansatz in der Behandlung der IPF darstellen.

1 INTRODUCTION

1.1 Diffuse parenchymal lung diseases

Diffuse parenchymal lung diseases (DPLDs), commonly also termed interstitial lung diseases (ILDs), are a group of acute and chronic disorders that involve inflammation and fibrosis of the alveoli, distal airways, and septal interstitium of the lungs, subsequently leading to distortion of the normal lung architecture and respiratory failure. In ILDs, the lung interstitium, primarily the space between the basement membranes of epithelium and endothelium, is injured. ILDs consist of two different subgroups: firstly, pulmonary disorders, which develop on the basis of known causes and secondly, pulmonary disorders of unknown origin. Occupational or environmental exposures, inherited conditions, drugs or infections are few of the possible known causes associated with pulmonary disorders. Furthermore, ILDs occur in association with systemical diseases, such as connective tissue diseases, collagen vascular diseases, or sarcoidosis. The group of idiopathic pulmonary disorders comprises eosinophilic pneumonia, pulmonary Langerhans' cell histiocytosis/histiocytosis X and lymphangioleiomyomatosis, as well as the more common idiopathic interstitial pneumonias (IIPs) [1, 2].

The group of IIPs is divided into seven diverse entities: idiopathic pulmonary fibrosis (IPF), non-specific interstitial pneumonia (NSIP), cryptogenic organizing pneumonia (COP), acute interstitial pneumonia (AIP), respiratory bronchiolitis-associated interstitial lung disease (RB-ILD), desquamative interstitial pneumonia (DIP) and lymphoid interstitial pneumonia (LIP). The different forms are mainly differentiated by clinical, radiological and histological features [1, 3].

1.2 Idiopathic pulmonary fibrosis

1.2.1 Definition and epidemiology

Idiopathic pulmonary fibrosis (IPF; also termed cryptogenic fibrosing alveolitis (CFA)) is the most common and severe form among the IIPs. It is a chronically progressive, devastating and life-threatening lung disease with unknown etiology, for which no effective therapy exists at present [1, 4]. IPF occurs worldwide, more commonly in male gender and the rates of prevalence and incidence are associated predominantly with increasing age.

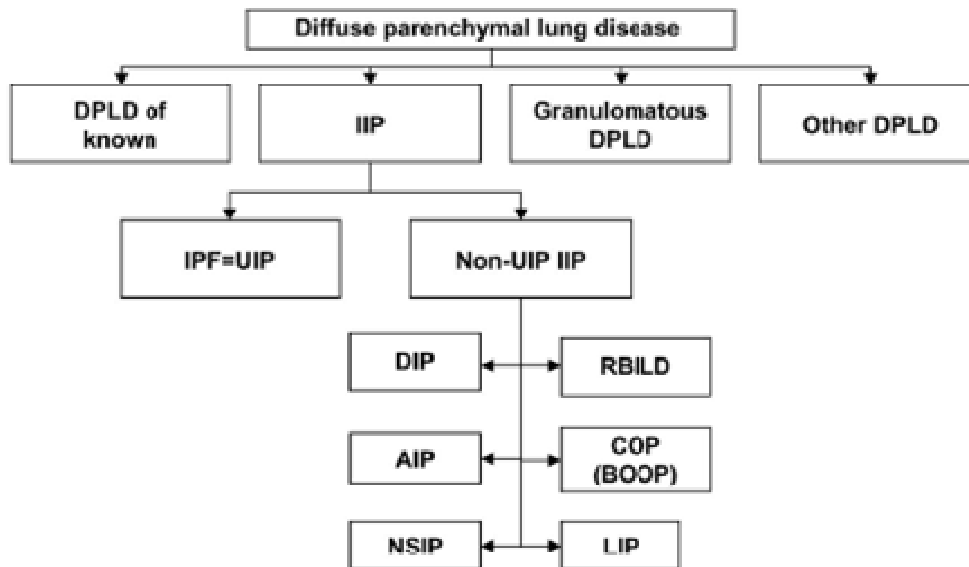


figure 1.1: Classification scheme of diffuse parenchymal lung diseases. The group of diffuse parenchymal lung diseases (DPLDs) consist of disorders of known origin, idiopathic interstitial pneumonias (IIP), granulomatous lung disorders and other forms of DPLDs. The IIPs are divided in idiopathic pulmonary fibrosis/usual interstitial pneumonia (IPF=UIP) and other IIPs (non-UIP IIPs), which include desquamative interstitial pneumonia (DIP), respiratory bronchiolitis-associated interstitial lung disease (RBILD), acute interstitial pneumonia (AIP), cryptogenic organizing pneumonia/bronchiolitis obliterans organizing pneumonia (COP/BOOP), non-specific interstitial pneumonia (NSIP) and lymphoid interstitial pneumonia (LIP) [modified scheme; derived from reference [1]].

The rate of prevalence in the United States is estimated at 13 to 20 cases per 100,000 annually, suggesting that IPF is more common than previously assumed. The majority of patients are between 50 to 70 years old (mean age over 65 years). The estimated incidence rate per year is 7 to 10 cases per 100,000 in the United States, with increasing tendency [5]. Many risk factors, like medication, chronic aspiration, environmental exposures (e.g. metal/wood dust), infectious agents, bacterial or viral infections (e.g. hepatitis C, adenovirus, Epstein - Barr virus), physical trauma (mechanical ventilation) or genetic components have been suggested to correlate with IPF. However, further investigations are required to reveal the coherence. There is no evidence of race or ethnicity predispositions. At present, cigarette smoke, the most potential risk factor, is strongly associated with IPF [4, 6-8]. IPF patients have a significantly worse prognosis, due to unresponsiveness to currently available therapy options. The median survival time is between 2.5 to 3.5 years from the time of diagnosis [1, 9, 10].

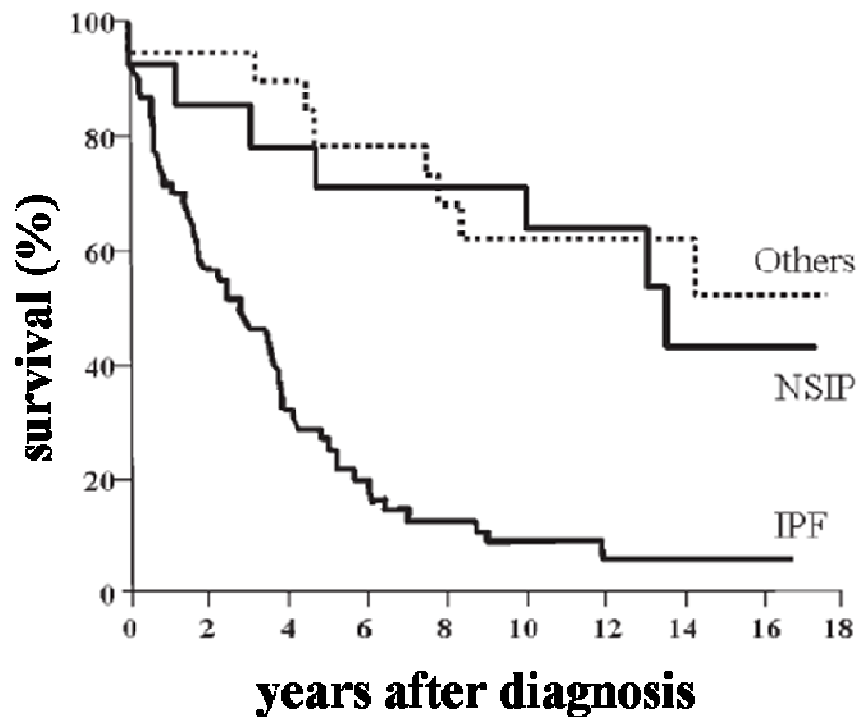


figure 1.2: Survival curves in different interstitial lung diseases (ILDs). The scheme shows the survival curves of patients with idiopathic pulmonary fibrosis (IPF) compared with patients with non-specific interstitial pneumonia (NSIP) and with

other diffuse parenchymal lung diseases. IPF patients had a significantly reduced median survival time [modified scheme; derived from reference [3]].

1.2.2 Clinical features, radiological characteristics and therapy options

Clinically, the most prominent and typical symptoms an IPF patient presents are dyspnoea and non-productive cough for a minimum period of 3 months. A chest auscultation gives frequent evidence of Velcro-type crackles during the inspiration phase in the basal parts of the lung. Often digital clubbing can be observed. An analysis of bronchoalveolar lavage fluids (BALFs) shows a strong increase of neutrophils [1, 4, 11, 12]. Recurrent respiratory infections and acute exacerbations are frequent and often responsible for rapid deterioration. In the course of the disease, a lung function test mostly depicts a restrictive pattern, as lung compliance is reduced and impaired gas exchange is noticeable. These facts inevitably lead to decreased physical capacity and loss of life quality. Respiratory failure is the most frequent cause of death, and has been reported to account for over 80% of all fatalities; bronchogenic carcinoma, ischemic heart disease, infection, and pulmonary embolism are also common causes of mortality. In more advanced stages, IPF patients develop severe pulmonary hypertension, peripheral edema and cor pulmonale, resulting in right heart failure [1]. In chest radiographs and high-resolution chest computed tomography (HRCT) peripheral, basal and subpleural parts of the lung are affected, with involvement of other lung parts in advanced disease. A decreased lung volume, bilateral reticular abnormalities, diffuse areas of “ground-glass” opacities associated with traction bronchiectasis and peripheral “honeycombing” are characteristic radiological findings in HRCT [1, 13-15].

The treatment strategies have been based on the concept that inflammation leads to injury and fibrosis. Anti-inflammatory and immunosuppressive therapies are often used in the treatment of IPF; however, such treatment has not been demonstrated to improve survival or quality of life. Oral corticosteroids alone or in combination with immunosuppressives, such as azathioprine and cyclophosphamide, usually used in cases of other IIP forms, showed no or limited effects in IPF. Currently, as no other alternatives are available, several studies preferably suggest a combination of low dose prednisolone and azathioprine with concomitant antioxidant treatment [16]. Accordingly, a conventional therapy for IPF provides only marginal benefit [3, 17,

18]. It has to be pointed out that lung transplantation is currently the best and only therapeutic intervention shown to prolong survival in IPF. Although the survival rate is improved, many patients die, being waitlisted, due to rapidly progressive or severe disease and additionally are often referred late in the course of their disease. Until some years ago, single lung transplantation (SLT) has been the standard procedure for patients with IPF and has produced good results. In the most recent years, a larger application of double lung transplantation (DLT) has been observed worldwide, probably related to higher survival rates. The mean life expectancy in patients with IPF after lung transplantation is about 65-70% at 1 year and 40% at 5 years [19-22].

1.2.3 Histopathological characteristics

To diagnose IPF, it is important to perform a surgical lung biopsy [1]. IPF is associated with a classic histopathological pattern - the usual interstitial pneumonia (UIP). UIP is characterised by alternating areas of normal lung parenchyma parts, interstitial inflammation, honeycomb cysts and fibrosis, resulting in dramatic irreversible disruption of the normal lung architecture. The typical distribution of pathological changes affects the subpleural, basal, and predominantly peripheral areas of the lung [1, 23, 24]. Alveolar epithelial cell injury with hyperplastic type II cells and abnormal regeneration/re-epithelialisation, as well as enhanced extracellular matrix (ECM) deposition in the lung interstitium and increased fibroblast/myofibroblast proliferation and activation, are observed as histological abnormalities in IPF. Only mild inflammation is present in these areas. The hallmark lesions of UIP/IPF are fibroblast foci, prominent aggregates of organised activated myofibroblasts that localise next to hyperplastic type II cells. The number of fibroblast foci has been reported, as an important factor for the individual prognosis of a patient, to correlate with survival in IPF; increasing numbers are related to impaired lung function, resulting in higher mortality [25, 26].

1.2.4 Pathomechanism of idiopathic pulmonary fibrosis

Even though the pathogenesis of IPF is still a topic of controversy, it is widely accepted that the activated fibroblast/myofibroblast represents the key effector cell type in IPF lungs [27, 28]. The role of fibroblasts implies the maintenance of matrix

homoeostasis, as well as synthesis and degradation of several extracellular molecules. Myofibroblast accumulation, activation and impaired apoptosis are characteristic features in the pathogenesis of IPF [29]. Finally, the structural remodelling leads to the loss of alveolar function. Three hypotheses have been proposed, suggesting the cellular origin of the activated myofibroblasts in IPF lungs. The relative contribution of the possible pathways is still unclear [27, 30]. Initially, it was hypothesised that profibrotic cytokines and growth factors influence resident lung fibroblasts to proliferate and differentiate into myofibroblasts. Recently, a second possibility was proposed, emphasising that epithelial cells undergo trans-differentiation into fibroblasts by a process termed epithelial-mesenchymal transition (EMT). The third theory suggests that circulating fibrocytes, derived from the bone marrow, may serve as precursor cells for myofibroblasts. However, the evidence that fibrocytes are able to differentiate into fully activated myofibroblasts is still insufficient [29].

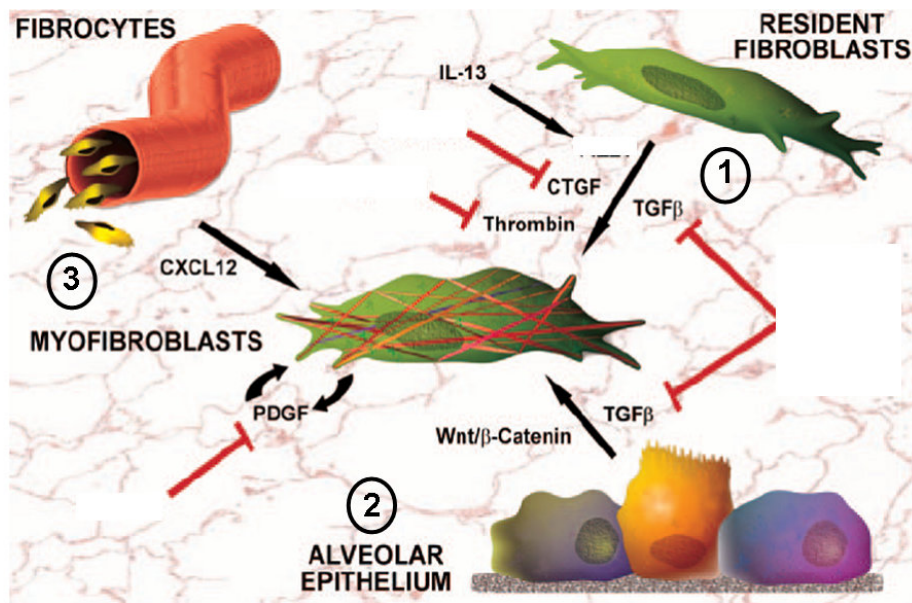


figure 1.3: Origins of myofibroblasts in idiopathic pulmonary fibrosis. Myofibroblasts play a crucial role in idiopathic pulmonary fibrosis (IPF). These effector cells are thought to arise from the following: proliferation and differentiation of resident fibroblasts (1), epithelial-mesenchymal transitions (2) or recruitment of circulating fibrocytes (3). Various cytokines, like interleukin 13 (IL-13) and chemokine ligand 12 (CXCL12), growth factors, like transforming growth factor β (TGF β) and platelet-derived growth factor (PDGF), and signalling pathways,

including the WNT/ β -catenin pathway, are able to mediate these processes (shown in black arrows). A number of potential therapeutic approaches are investigated, which may have an influence on certain pathway components, like connective tissue growth factor (CTGF) or thrombin (shown in red) [modified scheme; derived from reference [29]].

Although fibroblasts represent the key effector cells in IPF, the initial trigger is still unclear. The classic theory describes an unknown stimulus triggering chronic inflammation, which finally leads to fibrosis [31, 32]. This concept was supported by the observations that local inflammation was present in UIP lungs and that BALFs of IPF patients exhibited increased numbers of inflammatory cells [25, 33]. This dysregulation, induced by repeated tissue remodelling processes, finally results in fibrosis. However, the use of conventional anti-inflammatory treatment strategies provided no successful effects in IPF. Furthermore, histological studies at different stages of the disease, revealed only mild to moderate degrees of inflammation in UIP lungs. In fact, the observed increase of neutrophils in BALFs of IPF patients was suggested to be a consequence of the disease, not a cause. All these findings provide evidence that the role of inflammation is not predominantly relevant in the pathogenesis of IPF [10, 33-35].

Following these observations, a novel hypothesis has emerged proposing that the development of IPF is based on the premise of abnormal wound repair, resulting from an inadequate alveolar epithelial regeneration and slow re-epithelisation in response to repetitive unidentified epithelial injuries [10]. As a consequence, this dysregulated communication between mesenchymal and epithelial pulmonary components leads to a denuded and disrupted basement membrane. The release of several enzymes, profibrotic cytokines and growth factors by damaged epithelial cells promotes activation, proliferation and migration of fibroblasts into the alveoli. The formation of fibroblast foci leads to excessive ECM deposition, which in turn destroys the normal lung structure, ultimately causing fibrosis [10, 31, 33]. However, local inflammation occurs in the course of IPF, which makes it obvious, that it is not possible to totally exclude the inflammation theory from the pathogenesis. Rather, the current view demonstrates that the pathogenesis of IPF is complex and several hypotheses are valid for the mechanism leading to the disease [32, 34, 36].

As a result of the complex pathogenesis mentioned above, IPF can be described as a disease of disturbed epithelial-mesenchymal crosstalk. Epithelial-mesenchymal interactions are responsible for the maintenance of the alveolar unit, and are essential for normal lung function and gas exchange. However, an impaired crosstalk between alveolar epithelial type (AT) II cells and fibroblasts has recently been shown to contribute to the pathomechanism of IPF [36]. Several soluble mediators, such as transforming growth factor (TGF) β 1, angiotensin II, or interleukin (IL)1 β , were released by ATII cells and have been assigned a clear pathogenic role in experimental and idiopathic pulmonary fibrosis [37, 38]. Most recently, the WNT target gene WISP1 has been identified as a novel mediator of epithelial-mesenchymal interaction [39]. The WNT signalling pathway is essential to organ development, a process that can be recapitulated in organ failure. An aberrant activation of the WNT/ β -catenin signalling pathway during adult homeostasis leads to pathological events resulting in cancer, but may also be associated with the development of IPF.

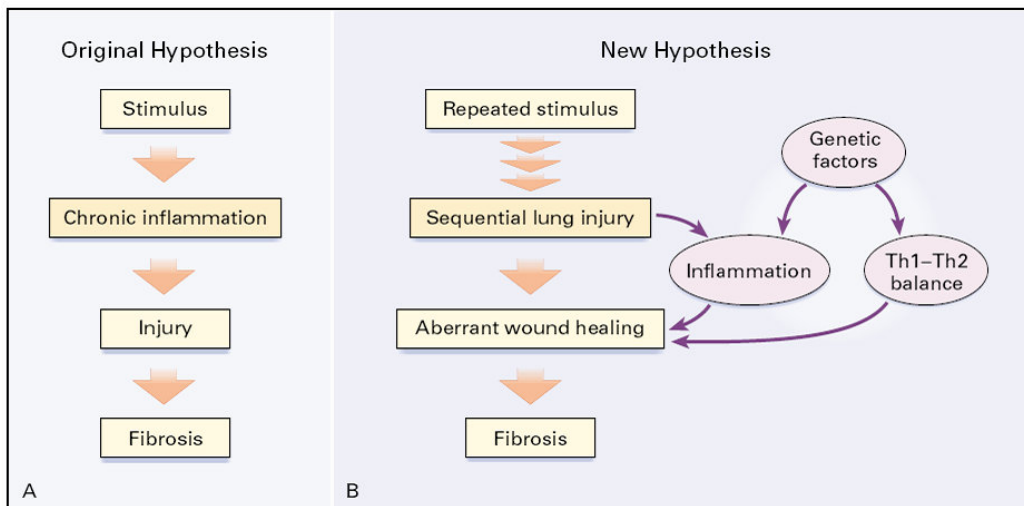


figure 1.4: Original and new hypotheses for the pathogenesis of idiopathic pulmonary fibrosis (IPF). Originally (panel A), idiopathic pulmonary fibrosis was viewed as an inflammatory response, which leads to chronic lung injury and thus to fibrosis. Newer insights (panel B) suggest that idiopathic pulmonary fibrosis results from repetitive acute lung injury, inducing aberrant wound-healing as a response and leading to pulmonary fibrosis. Several interacting factors that modify the fibrotic response include genetic factors and environmental inflammatory triggers [derived from reference [31]].

1.3 WNT signalling

WNT signalling plays a pivotal role during development of organisms as well as in maintenance and regeneration during adulthood. Signal transduction in the cytoplasm of different target cells leads to altered expression of various target genes and subsequently can influence several cell functions, such as proliferation, migration, differentiation, polarity, growth and cell fate specification [40-43]. Developmental defects are caused as a consequence of dysregulated active WNT signalling during embryogenesis. Aberrant WNT signal transduction in adult tissue promotes various diseases, including degenerative and inflammatory disorders, cancer and fibrosis [39, 43-45]. Currently, four different WNT signalling pathways are known: first, the canonical WNT/ β -catenin signalling pathway, which triggers WNT ligand binding to cell surface receptors, resulting in β -catenin stabilisation and translocation to the nucleus for target gene expression. Second, the non-canonical WNT/calcium (WNT/ Ca^{2+}) signalling pathway, which activates protein kinase C (PKC) and calmodulin kinase (CamKII) II by intracellular Ca^{2+} release. Third, the planar cell polarity (PCP) pathway, also termed c-Jun N-terminal kinase (JNK) pathway, which is a β -catenin independent and non-canonical pathway, like the WNT/ Ca^{2+} signalling pathway. It acts through small GTPases, like Rho/Rac, resulting in activation of activating protein1 (AP1) and is implicated in cytoskeletal organisation and epithelial cell polarity. Recently, a fourth pathway was discovered, particularly regulating muscle development. Thereby, the transcription factor CREB is phosphorylated by protein kinase A (PKA) [42, 44].

1.3.1 The canonical WNT/ β -catenin signalling pathway

The best characterised WNT signalling pathway is the β -catenin dependent or canonical WNT signalling pathway, which is the first discovered and best understood pathway. The transcriptional regulator β -catenin acts as an intracellular key molecule [42, 44, 45].

The canonical WNT/ β -catenin signalling pathway is modulated by multiple extracellular, cytoplasmic and nuclear signalling molecules. The WNT signalling molecules belong to a large family of secreted glycoproteins that play an important role as ligands in receptor-mediated signalling pathways. WNT proteins, generally

350 - 400 amino acids long, contain a signal domain followed by a highly conserved sequence of cysteines, and are usually quite insoluble and hydrophobic due to extensive palmitoylation of the mature protein. This post-translational modification is critical for proper WNT signalling [45, 46]. In mammals 19 WNT members are identified at present: WNT1, 2, 2B, 3, 3A, 4, 5A, 5B, 6, 7A, 7B, 8A, 8B, 9A, 9B, 10A, 10B, 11 and 16. Many WNT proteins share a high amino-acid sequence homology, in particular those that are grouped within similar subfamilies. Basically, the WNT genes have been divided into two classes, those that induce β -catenin signalling, and those that activate other pathways. Known WNT ligands that trigger the canonical pathway are: WNT1, 2, 2B, 3, 3A, 7A, 7B, 8, 10 [41, 42]. The first representative of the WNT gene family was int-1 in mice and wingless in fruit flies (*Drosophila melanogaster*). Int1 was first identified in a retrovirus causing mammary tumors in mice (mouse mammary tumor virus; MMTV). The preferred integration place for MMTV was the int-1 gene, a proto-oncogene. Wingless was named after the phenotype of the *Drosophila* mutant, where the gene is defect and results in wingless flies. By cloning and sequencing both these genes, a homology could be shown and therefore the terms int-1 and wingless (wg) were combined to the new term WNT [47-49].

In the absence of WNT ligands, the cytoplasmic β -catenin level is low because the molecule is destined to 26S proteasome-mediated degradation by a so-called degradation/destruction complex. This “destruction complex” is comprised of the scaffolding protein axin and the adenomatous polyposis coli protein (APC) as well as the glycogen synthase kinase 3 β (GSK3 β) as central elements. The serine/threonine kinases GSK3 β and casein kinase 1 γ (CK1 γ) are responsible for constitutive phosphorylation of β -catenin, which is recognised by the E3 ubiquitin ligase β -transducin repeat-containing protein (β -TrCP) and targeted for ubiquitination and final proteosomal degradation [42, 45]. As a consequence, in the nucleus prospective target genes of the pathway are repressed by interaction with members of the T-cell-specific transcription factor/lymphoid enhancer-binding factor (TCF/LEF) family. The TCF/LEF transcription factors form a complex with the associated co-repressor Groucho. These repressing effects are mediated by histone deacetylases (HDAC) and accordingly avoid transcription [42, 43]. When WNT ligands are present and WNT/ β -catenin signalling is activated, the degradation pathway is inhibited. In this case, WNT proteins are released from the surface of signalling cells and act on target cells

by binding to two distinct membrane receptors, the frizzled (FZD) and low density lipoprotein receptor-related proteins 5 and 6 (LRP5/6) at the cell surface [42, 45]. Thereby, the seven transmembrane receptor FZD and single pass transmembrane co-receptor LRP5/6 build a complex. The FZD proteins are the corresponding primary cell surface receptors for the WNT ligands. These seven transmembrane spanning receptors belong to the family of serpentine receptors and possess a long extracellular N-terminal extension, termed as cysteine-rich domain (CRD). WNT proteins directly bind to the CRD. There are 10 FZD members currently known to interact with WNT ligands [40, 46, 50]. In addition to the interactions between WNT and FZD, WNT signalling also requires the presence of the long single pass transmembrane co-receptor LRP5/6, which builds a complex with FZD. They are composed of a small intracellular domain and a large extracellular domain. A hallmark of LRP6 is a cytoplasmic tail with a central proline-rich motif (PPPSP). After phosphorylation by GSK3 β and CK1 γ , this part serves as binding site for axin [41, 43, 51].

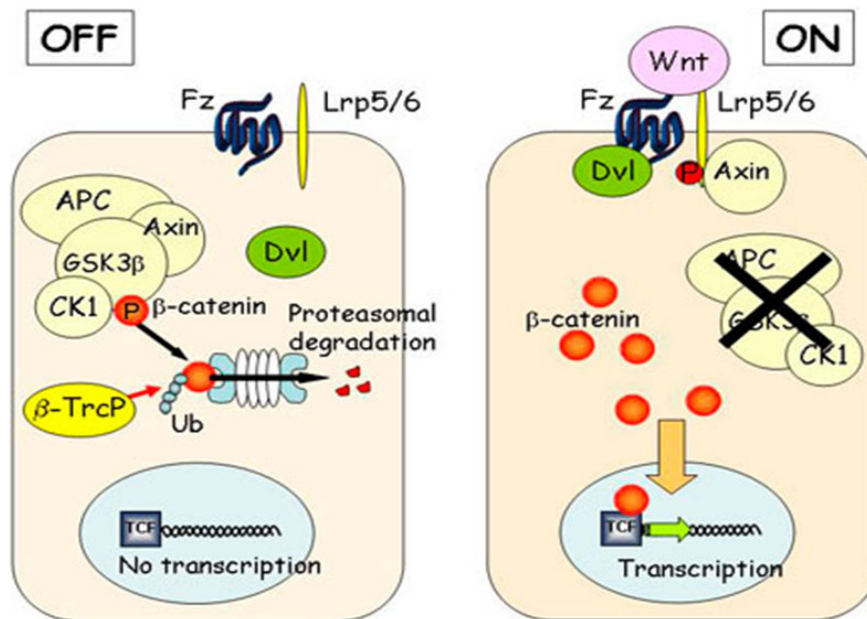


figure 1.5: An overview of canonical WNT signalling. On the left side of the figure, in the absence of WNT ligands (= OFF), there is no interaction of frizzled (Fz) and the lipoprotein receptor-related protein (Lrp5/6) receptor. Axis inhibition protein (Axin), glycogen synthase kinase 3 β (GSK3 β), adenomatous polyposis of the colon (APC) protein and casein kinase 1 (CK1) form a "destruction complex," and β -catenin

is phosphorylated, which is recognised by the E3 ubiquitin ligase β -transducin repeat-containing protein (β -TrcP) and targeted for ubiquitination (Ub) and final proteosomal degradation. On the right side of the figure, in the presence of WNT ligands (= ON), after binding to Fz, the signal is transduced to dishevelled (Dvl) and the Lrp5/6 receptor is activated. Axin is removed from the "destruction complex" and interacts with Lrp5/6. Without Axin the degradation complex is inactive. β -catenin moves into the nucleus, binds to the transcription factor TCF/LEF on DNA, and activates transcription of a protein. "P" represents phosphate [scheme derived from <http://www.umcutrecht.nl/subsite/cmc-utrecht/People/Staff/Madelon-Maurice>].

After the WNT ligands bind to the receptors, the signal is transduced to dishevelled (DVL), another intracellular pathway protein with the ability to interact with Axin. In detail, WNT activation promotes phosphorylation of LRP5/6 by GSK3 β and CK1 γ , which leads to the recruitment of Axin to the plasma membrane, directly binding to the cytoplasmic tail of LRP5/6. Without Axin the degradation complex is inactive. At the same time GSK binding protein (GBP) binds to GSK3 β and prevents the interaction between GSK3 β and Axin. β -catenin is not phosphorylated anymore and therefore cannot be recognised by β -TrCP. Consequently, hypophosphorylated β -catenin accumulates in the cytoplasm. The increased stability and elevated levels of free β -catenin lead to its nuclear translocation and subsequently β -catenin induces transcription of WNT target genes mediated by interactions with TCF/LEF transcription factors. Once in the nucleus, β -catenin replaces Groucho and thereby converts the "repressor complex" into a transcriptional "activator complex" [42, 43, 45, 52].

1.4 WNT signalling in the lung

1.4.1 Lung development and homeostasis

It has been demonstrated that WNT signalling in general plays an important role in the development of various organ systems, such as brain, limb, mammary glands, skin or cardiovascular system. Recent observations revealed that the WNT/ β -catenin signalling pathway additionally plays a fundamental role in lung development.

Several WNT components of the canonical pathway are expressed in a highly cell-specific fashion in the developing lung. Recently, Gross and colleagues proved that WNT/ β -catenin signalling is of particular importance in lung regeneration. Additionally, it was shown that inadequate expression of WNT2/2B in mouse embryos leads to complete lung agenesis [53]. The knowledge of functional importance of WNT signalling during the early development of lung epithelium is largely derived from transgenic animal models. Transgenic mice with epithelial-specific overexpression of WNT5A exhibited reduced epithelial branching morphogenesis and distal air space enlargement [45, 54, 55]. In mice, loss of WNT7B function leads to lung defects during different stages of development, which affects epithelial and mesenchymal cells. These defects arise as a result of aberrant autocrine and paracrine signalling mechanisms [56]. Additionally, it has been shown that WNT7B expression has a positive influence on embryonic lung growth [57]. Several studies revealed active canonical WNT signalling throughout lung development, which subsequently disappeared over time [58, 59]. A lack of β -catenin has severe consequences, as it is the intracellular key molecule of the canonical WNT pathway and cell adhesion processes. It may not only result in dysregulated WNT signalling, but also distorted cell adhesion. An appropriate gas exchange is not ensured, as the distal airways show misguided development [60, 61]. In general, various observations reflect the relevance of WNT signalling in lung development and indicate its possibly strong involvement in pathological processes in the adult organ.

Equally, in the adult lung, most WNT components, including canonical and noncanonical WNT pathway molecules, are expressed. In addition, the expression of several WNT proteins in lung epithelial cell lines was demonstrated [62]. Therefore, WNT signalling may be of great importance not only during organ development, but also in homeostasis. Aberrant WNT signalling inevitably results in abnormalities and diseases. Large numbers of knock-out experiments in mice in the past revealed diverse phenotypes, thereby implicating dysregulated WNT/ β -catenin signalling as a possible consequence in various human diseases. An aberrant signalling pathway is due to altered expression and function, mostly linked to constant activation, or mutations in various components of the pathway. Thus, uncontrolled WNT/ β -catenin signalling may be a hallmark of several diseases [45].

1.4.2 Lung cancer

The role of WNT signalling in correlation with various types of cancer has been widely investigated. The involvement of the canonical WNT signalling pathway is obvious, as many WNT target genes are involved in proliferation, apoptosis and cell cycle regulation, functions that are dysregulated during cancerogenesis [43, 63, 64]. The most famous example is a mutation in the APC gene, which is of inherited nature and leads to familial adenomatous polyposis (FAP), a disorder characterized by precancerous polyps. A constitutive activation of the pathway can also be caused by sporadic truncation of APC or mutations in β -catenin, a condition that inevitably leads to colorectal cancer [44, 45, 65]. Axin2 is an example for mutations in intracellular WNT pathway components that also lead to cancer. A predisposition to colon cancer exists, due to activated β -catenin signalling [66]. Various mutations in WNT signalling pathway components have been also shown in hepatocellular, pancreatic, ovarian, prostate and breast cancer [44].

The role of canonical WNT/ β -catenin signalling, especially in lung cancer has yet to be established. Accordingly, dysregulated WNT signalling in cancer has been largely derived from initial colon cancer studies, and more recently focused especially on non-small cell lung cancer (NSCLC). It has been shown that mutations of APC or β -catenin are frequently associated with colon cancer, whereas such mutations seem to be rare in lung cancer. In NSCLC, overexpression of WNT1 and 2, as well as DVL was shown [67-71]. WNT5A gene expression was reported to be higher in squamous cell carcinoma than adenocarcinoma, suggesting that WNT5A expression may be responsible for more aggressive forms of NSCLC [72]. Additionally, some target genes of the canonical pathway, including matrix metalloproteinases (MMPs), have been reported to be upregulated in invasive cancer forms [73]. In general the involvement of the WNT/ β -catenin signalling pathway is suggested to play a role in lung cancer, as inhibition of WNT signalling is able to affect and arrest cell growth in lung cancer [74].

1.5 WNT signalling in fibrotic disorders

Furthermore WNT/ β -catenin signalling contributes to the development of fibrotic diseases that are characterised by pathologic tissue remodelling.

Recently it was shown, that WNT4 and canonical WNT signalling contributes to the pathogenesis of renal fibrosis. Tumor progression was affected by inhibition of the signalling cascade [75, 76]. The expression of WNT and FZD was recently demonstrated in experimental liver fibrosis. The activation of hepatic stellate cells is a key feature in the pathogenesis of liver fibrosis. However, WNT antagonists were able to influence and inhibit this activation [77].

Chilosi and colleagues reported increased levels of β -catenin in ATII cells and fibroblasts [78], indicating an aberrant activation of WNT signal transduction in IPF [79]. Unbiased microarray screens have revealed an increased expression of several WNT genes, WNT receptors and WNT regulators, in IPF lungs compared with transplant donor lungs or other interstitial lung diseases [80-82]. In addition, several WNT target genes, such as WNT1-inducible signalling protein (WISP) 1, matrix metalloproteinase (MMP) 7, or osteopontin were identified in IPF lungs [39, 81, 83].

2 AIMS OF THE STUDY

Recent studies provided evidence for the reactivation of developmental programs in IPF [82]. The contribution of WNT/ β -catenin signalling to the development and progression of IPF, however, remains to be elucidated. Further investigation is required to evaluate the functional significance of active WNT/ β -catenin signalling in the diseased lung due to IPF and to identify the cell-specific mechanisms that may drive fibrogenesis. This study aimed to answer the following key question:

“Is the WNT/ β -Catenin pathway expressed and activated under conditions of IPF?”

To answer this question, the expression of canonical WNT pathway components was assessed in lung samples obtained from human IPF patients and in a mouse model of experimental pulmonary fibrosis. In addition, the functional effects of WNT signalling on primary mouse alveolar epithelial type (AT) II cells were analysed.

The specific aims of this study were:

- (1) to determine alterations of WNT/ β -catenin signalling at both, gene and protein expression levels in lung tissue of human patients suffering from idiopathic pulmonary fibrosis and in experimental pulmonary fibrosis.
- (2) to assess the localisation of WNT/ β -catenin signalling in lung tissue of human patients suffering from idiopathic pulmonary fibrosis and in experimental pulmonary fibrosis.
- (3) to analyse cellular functions of activated WNT/ β -catenin signalling in primary mouse AT II cells.
- (4) to identify novel WNT target genes in primary mouse ATII cells performing unbiased whole genome microarray analysis.

3 MATERIALS AND METHODS

3.1 Materials

The following equipment, chemicals reagents, antibodies and recombinant proteins were purchased from the companies indicated.

3.1.1 Equipment

ABI PRISM 7500 detection system	Applied Biosystems, USA
Bioanalyser 2100	Agilent Technologies, USA
Bacteriological petri dishes	BD Biosciences, USA
Cover slides	BD Falcon, USA
Culture slides	BD Falcon, USA
Developing machine X Omat 2000	Kodak, USA
Electrophoresis chambers	Bio-Rad, USA
Film cassette	Sigma-Aldrich, Germany
Filter 10, 20, 100 µm	Sefar, Germany
Fluorescence microscope LEICA AS MDW	Leica, Germany
Fusion A153601 reader Packard	Bioscience, Germany
Gel blotting paper 70 x 100 mm	Bioscience, Germany
GenePix 4100A scanner	Molecular Devices, USA
GS-800TM calibrated densitometer	Bio-Rad, USA
Indwelling I.V. cannula 20 G11/4", pink (Vasocan [®])	B. Braun, Germany
Light microscope LEICA DMIL	Leica, Germany
Light microscope Olympus BX51	Olympus, Germany
Liquid-β-scintillation counter (1600 TR, Liquid scintillation analyser)	Canberra Packard Central Europe GmbH, Austria
Measuring vials	Roth, Germany
MicroSprayer [®] aerosoliser - model IA-1C	Penn-Century, USA
Mini spin centrifuge	Eppendorf, Germany

Multifuge centrifuge, 3 s-R	Heraeus, Germany
Nanodrop [®] ND-1000	Peqlab, Germany
Neubauer counting chamber	Roth, Germany
PCR-thermocycler	MJ Research, USA
Petri dishes	Greiner Bio-One, Germany
Quantity One software	Bio-Rad, USA
Radiographic film X-Omat LS	Sigma-Aldrich, Germany
Stericup [®] filter unit 0.22 µm, 33 mm, 150 ml,	
GP Express [™] PLUS (PES) membrane	Millipore, USA
Sterilizing filter unit 0.22 µm, Millex [®] -GP	Millipore, USA
Tissue culture plates: 6, 12, 48 well	Greiner Bio-One, Germany
Vortex machine	Eppendorf, Germany

3.1.2 Chemical reagents

Agarose	Invitrogen, UK
Agarose	Roth, Germany
Bleomycin sulphate (Bleomycin HEXAL [®])	Hexal, Germany
Bovine serum albumin (BSA)	Sigma-Aldrich, Germany
Citrate buffer 20x	Invitrogen, UK
D-(+)-glucose	Sigma-Aldrich, Germany
DAPI [4',6-Diamidino-2-phenylindole dihydrochloride]	Sigma-Aldrich, Germany
Deoxyribonuclease I (DNase I)	Sigma-Aldrich, Germany
Dispase	BD Biosciences, USA
DNA ladder (100 bp, 1kb)	Promega, USA
DNA loading buffer (blue/orange dye) 6x	Promega, USA
Dulbecco's Modified Eagle's Medium (DMEM)	Sigma-Aldrich, Germany
Dulbecco's phosphate buffered saline 1x (DPBS 1x)	PAA Laboratories, Austria
Dulbecco's phosphate buffered saline 10x (DPBS 10x)	PAA Laboratories, Austria
DuoSet [®] ELISA development kit; human IL-1β	R & D Systems, USA
DuoSet [®] ELISA development kit; mouse IL-1β	R & D Systems, USA

DuoSet [®] ELISA development kit; mouse IL-6	R & D Systems, USA
Ecotainer [®] NaCl 0.9 %	B. Braun, Germany
EDTA/EGTA	Promega, USA
Ethanol	Roth, Germany
Ethidium bromide	Bio-Rad, USA
Fluorescence mounting medium	Dako, Denmark
Fetal bovine serum “GOLD” (FBS)	PAA Laboratories, Austria
Hematoxylin (Mayer’s Hematoxylin)	Sigma-Aldrich, Germany
Heparinsodium	
(Heparin-Natrium-25000-ratiopharm [®])	Ratiopharm, Germany
HEPES [2-(-4-2-hydroxyethyl)- piperazinyl-1-ethansulfonate]	PAA Laboratories, Austria
Histostain [®] PLUS kit	Zymed Laboratories, USA
Hydrogene peroxide (H ₂ O ₂)	Roth, Germany
Isofluran	CP-Pharma, Germany
Ketamin hydrochloride (Ketavet [®])	Pfizer, USA
L-glutamine	PAA Laboratories, Austria
Low input RNA T7 kit	Agilent Technologies, USA
Methanol	Roth, Germany
MgCl ₂ (25 mM)	Invitrogen, Germany
MuLV reverse transcriptase	Applied Biosystems, USA
Narcofen [®] (Pentobarbitalsodium)	Merial, Germany
Nile Red	Sigma-Aldrich, Germany
Paraformaldehyde (PFA)	Roth, Germany
PCR nucleotide mix	Promega, USA
PCR buffer II (without MgCl ₂)10x	Applied Biosystems, USA
Penicillin/Streptomycin	PAA Laboratories, Austria
Platinum [®] SYBR [®] green qPCR SuperMix-UDG	Invitrogen, Germany
Proteome profiler TM ; mouse cytokine array	
Panel A array kit	R & D Systems, USA
Quick start Bradford protein assay	Bio-Rad, USA
Random hexamers	Promega, USA
RNase-free DNase Set	Qiagen, Germany
RNase inhibitor	Applied Biosystems, USA

RNase ZAP	Sigma-Aldrich, Germany
RNeasy mini kit	Qiagen, Germany
Roti-quick-kit	Roth, Germany
Rotiszint® Eco plus (scintillation liquid)	Roth, Germany
Sodium chloride 0.9 %	B. Braun, Germany
TAE buffer	Roth, Germany
TEMED [Tetramethyl ethylene diamine]	Bio-Rad, USA
Xylazin hydrochlorid (Rompun® 2 %)	Bayer Vital, Germany
[³ H] thymidine	Amersham Bioscience, USA

3.1.3 Antibodies

Alexa Fluor 555 anti-mouse IgG	Invitrogen, USA
Alexa Fluor 555 anti-rabbit IgG	Invitrogen, USA
Alexa Fluor 555 anti-rat IgG	Invitrogen, USA
Alpha (α)-smooth muscle actin [Acta2]	Sigma-Aldrich, USA
β -catenin	Cell Signaling Technology, USA
Biotinylated anti-mouse IgG	Invitrogen, USA
Biotinylated anti-rabbit IgG	Invitrogen, USA
CyclinD1 [CCND1]	Millipore, USA
E-cadherin [Cdh1]	BD Biosciences, USA
FITC-conjugated anti-mouse IgG	Dako, USA
GSK3 β	Cell Signaling Technology, USA
HRP-conjugated anti-mouse IgG	Thermo Scientific, USA
HRP-conjugated anti-rabbit IgG	Thermo Scientific, USA
HRP-conjugated anti-rat IgG	Thermo Scientific, USA
Lamin A/C	Santa Cruz Biotechnology, USA
LRP6	Cell Signaling Technology, USA
Pan-cytokeratin (pan-CK)	Dako, USA
Phospho-GSK3 β	Cell Signaling Technology, USA
Phospho-LRP6	Cell Signaling Technology, USA
Prosurfactant protein C [proSP-C]	Chemicon International, USA
Purified rat anti-mouse CD16/CD32	BD Biosciences, USA
Purified rat anti-mouse CD45	BD Biosciences, USA

Tight junction protein 1 (ZO-1)	Zymed Laboratories, USA
WNT1	Abcam, UK
WNT3A	Invitrogen, USA

For further details concerning the use of the antibodies see appendix/chapter 6/table 6.4.1 and 6.4.2..

3.1.4 Recombinant proteins

KGF	(a kind gift from Dr. Veronica Grau (ULCG, Germany))
TGFβ1	R & D Systems, USA
WNT3A	R & D Systems, USA

3.1.5 Human tissues

Lung tissue biopsies were obtained from nine control subjects (organ donors; four females, five males; mean age 42 ± 10 years) and 12 IPF patients with histologically identified usual interstitial pneumonia (UIP) pattern (two females, 10 males; mean age = 58 ± 8 years; mean vital capacity (VC) = $48 \% \pm 7 \%$; mean total lung capacity (TLC) = $50 \% \pm 5 \%$; mean diffusion capacity of the lung for carbon monoxide per unit of alveolar volume (DL_{CO}/VA) = $23 \% \pm 3 \%$; ventilated volume of oxygen per minute (V_{O_2}) = 2 - 4 l/min; partial pressure of oxygen in the arterial blood (Pa_{O_2}) = 49 - 71 mmHg, partial pressure of carbon dioxide in the arterial blood (Pa_{CO_2}) = 33 - 65 mmHg). Individual patient characteristics are shown in detail (see appendix/table 6.3). Samples were immediately snap-frozen in liquid nitrogen or placed in 4 % (w/v) paraformaldehyde after explantation. The study protocol was approved by the Ethics Committee of the Justus-Liebig-University of Giessen, School of Medicine (AZ 31/93). Informed consent was obtained in written form from each subject for the study protocol.

3.1.6 Animal tissues

All animal studies in this project were performed in accordance with the guidelines of the Ethics Committee of the Justus-Liebig-University of Giessen, School of Medicine and approved by the local authorities (Regierungspräsidium Giessen, no. V54 – 19 c 20/15 (1) GI20/10 no. 49/2005). Six to eight week old specific pathogen-free (SPF) adult female C57BL/6N mice, minimum 18-20 g in body weight, were used throughout this study (supplied by Charles River, Sulzfeld, Germany). The mice were held in groups at an average room temperature of 26 °C, a humidity of 50-60 % and an alternating day and night light interval of 12 hours. The animals had free access to water and rodent laboratory chow. After exposure to saline or bleomycin, lungs were surgically excised and collected to process for embedding and sectioning, used for isolation of primary alveolar epithelial type (AT) II cells or immediately snap-frozen in liquid nitrogen for further analyses.

3.1.7 Primary cells

Primary mouse alveolar epithelial type (AT) II cells were isolated from saline- and bleomycin-treated, as well as from healthy untreated animals, as described in 3.2.3.

3.2 Methods

3.2.1 Animal model of bleomycin-induced pulmonary fibrosis in mice

Bleomycin is an effective chemotherapy drug, used for the treatment of some types of cancer. The possible side effects of repeated systemic administration may result in lung inflammation that can progress to fibrosis. As bleomycin-induced pulmonary fibrosis is easily reproduced in many different mammalian species (mice, rats etc.), an experimental model using this drug was adopted with the aim to investigate the cellular and molecular basis of interstitial lung fibrosis.

In order to perform the experiments, specific pathogen-free adult female C57BL/6N mice were used. Anesthesia was initiated by intraperitoneal injection of a mixture of ketamin (10 %), xylazin (2 %) and sodium chloride (NaCl) (1:1:2.5 - in a final volume of 20 µl) and maintained by inhalation with isofluran (3.5 vol.%) for approximately

10-15 seconds. Then, mice were intubated under microscopic control with a self-made tracheal tube, using a peripheral venous catheter cut to size. In further preparation steps, bleomycin sulphate was dissolved in sterile 0.9 % saline solution (NaCl) (5 U/kg body weight (BW) → dissolved in 3 ml NaCl). According to exact body weight, a single dose of 0.09 - 0.1 U was administered as a solution with NaCl in a total volume of 200 µl per animal orotracheally *via* microsyringe on day 0. Control mice received 200 µl of pure saline solution for comparison. Mice were euthanised at days 7, 14 and 21 after saline, or bleomycin exposure by an overdosed intraperitoneal (i.p.) injection of a mixture, containing Narcoren® (16 %), Heparin® (5000 I.E.) and NaCl (1:1:1 - in a final volume of 300 µl) and lung tissue was used for further analyses.

3.2.2 WNT reporter mice (TOPGAL)

Specific pathogen-free (SPF), four to eight week old mice were used in this study (supplied by Jackson Laboratories, Bar Harbor, USA). The mice had free access to water and rodent laboratory chow. The TOPGAL mice were previously described in detail [84]. The following primers were used for the identification of transgenic animals: Lac(Z)-F5'-gttgagctgcacggcagatacacttgctga-3'; Lac(Z)-R5'-gccactgggtgtggccataattcattcgc-3'.

3.2.3 Isolation of primary mouse alveolar epithelial type II (ATII) cells

Primary mouse alveolar epithelial type II (ATII) cells were isolated from specific pathogen-free adult female C57BL/6N mice.

Briefly, mice were euthanised by an overdosed intraperitoneal (i.p.) injection of a mixture, containing Narcoren® (16 %), Heparin® (5000 I.E.) and NaCl (1:1:1 - in a final volume of 300 µl). A midline incision was placed from the umbilicus to the chin. The trachea was exposed by a midline neck incision; a shortened 21-gauge cannula was inserted, firmly ligated, and lungs were lavaged twice with sterile saline (300 µl). The abdomen was opened, the renal artery was separated and a pneumothorax was induced by disruption of the diaphragm. The thoracic cavity was opened carefully to avoid puncturing of the lung. To exclude a contamination with immune cells, the thymus was carefully removed. An incision was placed at the left cardiac auricle and the lung was manually perfused through the right heart ventricle with sterile saline

until it was visually free of blood. Next, a total volume of 1.5 ml sterile dispase (5000 caseinolytic units), a proteolytic enzyme, was instilled *via* the trachea to release ATII cells. This was followed by a 400 μ l instillation of 1% low-melting-point agarose in DMEM, maintained in liquid form in a water bath at 55 °C. The agarose solution was allowed to solidify for two minutes inside the lungs and the respiratory organ was then extracted from the thorax, externally blood rinsed, placed in a falcon tube and incubated in 1.0 ml dispase solution for 45 min. at room temperature. After this incubation period, lungs were transferred into a petri dish with plus (+) medium (see table 3.1) and were gently teased with forceps to aid cell separation. Therefore, the lung tissue was carefully dissected from upper airways and large vessels and cells were extracted by obliteration of the lungs. This was followed by subsequent washing steps of the cell suspension with plus (+) medium and filtration through 100, 20 and 10 μ m nylon mesh filters, and centrifugation for 10 minutes at 15 °C and 200 g to collect cells and exclude debris. The resulting pellets were dispersed with minus (-) medium (see table 3.1). Following dispase disaggregation, a purification method, based on the differential adherence of immune cells and other contaminating cells to IgG antibody-coated petri dishes was performed. Petri dishes were coated a day before with a mixture of CD16/32 (15 μ l/dish) and CD45 (15 μ l/dish) specific antibodies diluted in Dulbecco's Modified Eagle's Medium (DMEM), and incubated overnight at 4 °C to allow the antibodies to adhere onto the petri dishes. For a negative selection of lymphocytes and macrophages, the cell suspension was first incubated on the coated dishes for 35 minutes at 37 °C for the attachment of contaminating cells bearing Fc receptors. This was followed by a 45 minute incubation of the cell suspension containing unattached cells at 37 °C in non-coated cell culture dishes for negative selection and attachment of fibroblasts. The unattached cells, mainly comprising ATII cells, were then collected and cell counting was performed using Nile Red staining, which identifies lamellar bodies, a characteristic organelle in ATII cells. The Nile Red staining was performed as follows: 20 μ l of cell suspension was dispensed in 500 μ l DMEM containing a 1:20 dilution of a Nile Red solution. The mix was vortexed and incubated for one minute at room temperature. Stained cells were counted with a Neubauer chamber under a light microscope. Freshly isolated ATII cells were directly analysed by immunofluorescence for characteristics of ATII cell purity and morphology. Cell purity was routinely assessed

by positive staining for the ATII cell marker prosurfactant protein C (pro-SPC) and negative staining for the fibroblast cell marker alpha-smooth muscle actin (Acta2). The phenotypic cell characterization was investigated by the specific epithelial cell marker proteins pan-CK, TJP1 and E-cadherin (ECAD). Finally, ATII cells were kept in minus (-) medium, supplied with 10 % fetal bovine serum “GOLD” (FBS) for 24 to 30 hours to allow attachment and seeded on 6-, 12- and 48-well plates, or chamber slides, depending on the experiment. All cultures were maintained in an atmosphere at 5 % CO₂, 95 - 100 % humidity and 37 °C. After adherence time, cells were kept in minus (-) medium with reduced FBS content of 0.1 % for at least 12 hours to synchronize their metabolic activity before treatment.

	Reagent	Volume/weight	Final concentration
minus (-) medium	DMEM	500 ml	-
	HEPES	26 ml	10 mM
	D-(+)-glucose	1.8 g	3.6 mg/ml
	Penicillin/streptomycin	5 ml	1 %
	L-glutamin	10 ml	2 %
plus (+) medium	DMEM	500 ml	-
	HEPES	26 ml	10 mM
	D-(+)-glucose	1.8 g	3.6 mg/ml
	Penicillin/streptomycin	5 ml	1 %
	L-glutamin	10 ml	2 %
	DNase I	20 mg	0.04 mg/ml

table 3.1: Composition of culture media for the isolation of primary mouse alveolar epithelial type II (ATII) cells obtained from specific pathogen-free adult female C57BL/6N mice.

3.2.4 Supernatants

Primary mouse alveolar epithelial type II (ATII) cells were isolated and cultured in minus (-) medium supplemented with 10 % FBS for 24 hours. After adherence time, culture media and non-adherent cells were removed; attached cells were washed twice with DPBS, and replenished with minus (-) medium at reduced FBS content of 0.1 % for at least 12 hours to synchronize their metabolic activity before treatment with recombinant WNT3A. After indicated time-points of treatment, supernatant was collected and centrifuged for 5 min. at 4 °C and 1.500 g to remove cellular debris. Finally, supernatants were transferred to sterile eppendorf tubes and used for ELISA analysis.

3.2.5 RNA isolation and measurement

In order to isolate total RNA from human or animal tissue samples and animal cells, two different methods were applied.

3.2.5.1 RNA isolation from lung homogenates

Human and mouse lung tissue were ground into a powder under liquid nitrogen with a mortar and pestle, and total RNA was extracted using Roti-quick-kit from Roth®. Further steps were performed according to the manufacturer's protocol.

3.2.5.2 RNA isolation from cultured cells

Extraction of total RNA from primary mouse ATII cells was performed according to the manufacturer's protocol using the RNeasy mini kit from QIAGEN®. During the isolation procedure, a RNase-free DNase set was used, as DNase digestion is recommended to avoid contamination with DNA in RNA solutions. DNA removal is of importance for certain applications (e.g. (q)RT-PCR) that are sensitive to very small amounts of DNA.

The concentration and quality of isolated RNA was determined by measurement of the optical density of the obtained sample, using a NanoDrop® ND-1000 spectrophotometer. The maximum absorbance of nucleic acids is at a wavelength of 260 nm (A260), whereas that of proteins at a wavelength of 280 nm (A280). An absorbance of one unit at 260 nm corresponds to 44 µg of RNA per ml (A260 = 1 → 44 µg/ml). The ratio of absorbance at 260 and 280nm (A260/280) is used to assess the

attachment of the random hexamers	20 °C for 10 min.
reverse transcription	43 °C for 75 min.
inactivation of the reverse transcriptase	99 °C for 5 min.
cooling	4 °C

The random hexamers have a random base sequence and serve as primers that attach to single stranded RNA. The reverse transcriptase starts to add dNTPs in 5' → 3' direction to the strand. The synthesised cDNA was either used directly for polymerase chain reaction or stored at -20 °C.

3.2.7 Quantitative real-time polymerase chain reaction (qRT-PCR)

Quantitative real-time polymerase chain reaction (qRT-PCR) is a variation of the conventional PCR allowing simultaneous amplification and quantification of specific DNA fragments. The method of fluorescence measurement is one possible way to specifically detect double-stranded DNA (dsDNA). Here, the reaction mix for qRT-PCR includes a fluorescent dye, SYBR® Green I that binds sequence independently and specifically to any newly synthesized dsDNA during the PCR reaction.

Reagent	Volume
Platinum® SYBR® Green qPCR SuperMix-UDG	12.5 µl
MgCl ₂ (50mM)	1.0 µl
Forward primer	0.5 µl
Reverse primer	0.5 µl
ROX reference dye	0.5 µl
ddH ₂ O	8.0 µl
Σ 23 µl + 2 µl cDNA = 25 µl (total mixture per well)	

table 3.3: Composition of mixture for quantitative reverse transcription real time polymerase chain reaction ((q)RT-PCR).

The reaction cycle is divided into three phases: 1.) denaturation, 2.) annealing, and 3.) elongation. During denaturation, the dsDNA is separated into single-stranded DNA (ssDNA), so, SYBR® Green I is unable to bind and no fluorescent signal is

detectable. During the annealing phase, primers bind to the complementary ssDNA and SYBR® Green I binds directly to the short dsDNA segments, resulting in steadily increasing fluorescence intensity. In the elongation phase, the complete product is synthesized by a thermostable DNA-dependent DNA polymerase.

The maximum of fluorescent signal and accumulation of target product is detected after each cycle at the end of elongation, as the level of fluorescence produced by the dye is proportional to the amount of amplified DNA.

In order to perform the experiments, all components were mixed as follows and the volume was adjusted to 23 µl with distilled, autoclaved water.

The (q)RT-PCR reaction was performed for 45 cycles according to the following protocol, using the appropriate primers indicated (table 6.1 and 6.2).

activation of polymerase enzyme	50 °C for 2 min.
first denaturation	95 °C for 5 min.
second denaturation	95 °C for 5 sec.
annealing	59 °C for 5 sec.
extension	72 °C for 30 sec.
dissociation step 1	95 °C for 15 sec.
dissociation step 2	60 °C for 1 min.
dissociation step 3	95 °C for 15 sec.
dissociation step 4	60 °C for 15 sec.

The gene expression was analysed using the AB 7500 fast real-time PCR system. To obtain a relative measure for the quantification of the mRNA level of the gene of interest, all results were normalised to the relative expression of an ubiquitously, constantly and equally expressed gene that is free of pseudogenes (= reference gene). Hypoxanthine phosphoribosyltransferase (HPRT) 1 in human tissue/cells and porphobilinogen deaminase (Pbgd) in mouse tissue/cells, respectively, were used as reference genes in all (q)RT-PCR determinations. The relative mRNA level of a target gene was presented in ΔC_t values ($\Delta C_t = C_t \text{ reference gene} - C_t \text{ target gene}$). A commonly-employed method of DNA quantification by real-time PCR relies on plotting fluorescence against the number of cycles on a logarithmic scale. A threshold for detection of DNA-based fluorescence is set slightly above background. The number of cycles at which the fluorescence exceeds the threshold is called the threshold cycle (C_t). During the exponential amplification phase, the sequence of the

DNA target doubles every cycle. Relative changes in transcript levels compared to healthy/untreated controls were shown as $\Delta\Delta C_t$ values ($\Delta\Delta C_t = \Delta C_t$ disease/treated - ΔC_t healthy/untreated control). All $\Delta\Delta C_t$ values correspond approximately to the binary logarithm of the fold change. The specific amplification of the PCR products was confirmed by melting curve analysis and gel electrophoresis.

3.2.8 DNA agarose gel electrophoresis

Agarose gel electrophoresis is a method to separate and visualize DNA fragments according to their size. Negatively charged nucleic acids are moved through the electric field in the gel. The shorter a molecule is, the faster it moves through the gel, what means, that after a certain time period short molecules have covered a longer distance than longer ones.

This method was used to assess the products of (q)RT-PCR. Agarose gels (2 %) were prepared, by mixing 3 g of agarose with 150 μ l TAE buffer 1 \times and heated up for 3 minutes. Then 0.5 μ g/ μ l ethidium bromide was added to make the products visible, as it is a fluorescent dye that intercalates with the DNA. Then the gel was cooled down to solidify. The DNA samples and empty control samples were mixed with 6x DNA loading buffer, before loading them onto the gel. A 100 bp and 1000 bp ladder were used for size control. Then electrophoresis was run constantly for 60 - 90 min. at 100 V/cm in 1 \times TAE buffer. Separated nucleic acids were visualized at short wavelength with UV-light ($\lambda = 257$ nm).

3.2.9 Immunohistochemistry

Immunohistochemistry (IHC) represents a histological method to localise cell- and tissue-specific antigens at the level of thin tissue sections. In order to detect and visualise e.g. cellular expression of particular proteins, antibodies/antisera specifically directed against these antigens are used *in situ*. Serial sections of respective tissue samples are incubated with an antigen-specific primary antibody. A biotinylated secondary antibody is used against the primary antibody. The subsequent incubation with streptavidin creates an enzyme-conjugated complex, which can be visualised by addition of a chromogen substrate after its oxidative conversion. The experiments were performed according to the following protocol. At first, 3 μ m thin sections by

using a microtome were sliced from 4 % paraformaldehyde-fixed, paraffin embedded human and mouse lung tissue samples and mounted on slides. In order to remove paraffin before immuno-staining, slides were kept for incubation in an oven at 50 °C overnight and subsequently were transferred to xylene three times for 10 minutes each. After rehydration in decreasing ethanol concentrations (100 %, 95 % and 70 %), each twice for 5 minutes, and a washing step with Dulbecco's phosphate buffered saline (DPBS) 1x twice for 5 minutes each, tissue sections were treated for paraformaldehyde removal and antigen retrieval was performed. Therefore, slides were placed in slide boxes with citrate buffer 1x (pH 6.0, 6.5 mM) and then placed on a cooker in a pot with water boiled for 25 minutes at 300 °C. They were then kept for another 10 minutes at 50 °C, followed by a cooling step for five minutes. After cooling down, slides were washed twice for five minutes in DPBS 1x again. Endogenous peroxidase activity was quenched by incubation with 3 % (v/v) H₂O₂ twice for 10 minutes each. After another washing step with DPBS 1x (as described earlier), serum blocking solution (Histostain PLUS kit), derived from a species different than the source of the intended primary antibody, was put onto the slides for 10 minutes and kept at room temperature. Finally, the primary antibodies were applied to the slides, diluted appropriately in blocking solution and DPBS 1x, and the slides were stored at 4 °C overnight.

dilution for primary antibody:

DPBS 1x

serum blocking solution

primary antibody solution (depending on the respective dilutions for each antibody used in the experiment (see appendix/table 6.4.1)).

The following day, the slides were first kept for 30 minutes at room temperature and then washed twice for 5 minutes in DPBS 1x. Immune complexes were visualized by incubation, using the species-appropriate secondary biotinylated antibodies for 10 minutes at room temperature (Histostain PLUS kit; see appendix/table 6.4.2). Slides were then incubated with HRP-enzyme conjugated streptavidin for 10 minutes at room temperature. The tissue was stained for a maximum of 10 minutes at room temperature, by using AEC Single Solution chromogen, until red colour staining was visible under a microscope. After each incubation step, a washing step in DPBS 1x was performed as described earlier. Slides were counterstained with hematoxylin for

eight minutes at room temperature, followed by a washing step in running tap water for 10 minutes. Finally, tissue sections were covered with glycerol gelatine (mounting medium) and a cover slide. Slides were stored at room temperature and light protected until use. The stained tissue sections were viewed with an Olympus BX51 light microscope and pictures were taken with an attached DP25 digital camera at 2 different magnifications (10x and 40x) and analysed.

3.2.10 Immunocytochemistry

Immunocytochemistry (ICC) is applied to visualise the localisation of particular antigens at the level of single cells, grown as primary cultures or derived from cell lines, by using enzymes or fluorophores (fluorescent dyes), again coupled to the respective secondary antibodies. This method is based on antigen-specific binding of primary antibodies to the respective antigen and the use of specific fluorochrome-labelled secondary antibodies against the primary antibodies. For the experiments, freshly isolated primary mouse ATII (ATII) cells were plated at a density of 15×10^4 /well in 8-well chamber slides in 10 % FCS culture medium (500 μ l/well). Attachment, synchronisation and stimulation of ATII cells were performed according to the protocol (see chapter 3.2.3). Cells were then washed three times with DPBS 1x and fixed with ice-cold 100 % methanol (200 μ l/well) for five minutes. After each incubation step, a washing step was performed. To block unspecific antibody binding sites, cells were incubated with 3 % (m/vol) BSA in DPBS 1x (200 μ l/well) for a minimum of two hours. Cells were then incubated with the respective primary antibody, diluted in 0.1 % (m/vol) BSA in DPBS 1x (200 μ l/well), at 4 °C overnight.

dilution for primary antibody:

DPBS 1x

BSA

primary antibody solution (depending on the respective dilutions for each antibody used in the experiment (see table 6.4.1)).

Indirect immunofluorescence was performed the following day by incubation with FITC- or Alexa Fluor 555-conjugated secondary antibodies, diluted in DPBS 1x containing 0.1 % BSA (200 μ l/well), which were used at room temperature and light protected for two hours.

dilution for secondary antibody:

DPBS 1x

BSA

secondary antibody solution (depending on the respective dilutions for each antibody used in the experiment (see table 6.4.2)).

Nuclei were visualized by 4',6-diamidino-2-phenylindole dihydrochloride (DAPI) staining (1:1000 dilution). Cells were incubated with DAPI, diluted in DPBS 1x containing 0.1 % BSA (100 µl/well), at room temperature, light protected for five minutes. After incubation with DAPI, the cells were then fixed with 4 % (m/vol) paraformaldehyde (PFA) (100 µl/well) at room temperature, light protected for seven minutes. Finally, the chamber of the culture slide was removed and cells were covered with glycerol gelatine (mounting medium) and a cover slide. Slides were stored at 4 °C and light protected until use. The stained cells were viewed with a fluorescence microscope equipped with appropriate filter sets, and pictures were taken and image analysis was performed with the Leica Q Win program.

3.2.11 Western blot analysis

The Western blot represents a semi-quantitative analytical technique, which is used for protein detection in crude samples of tissue homogenates and allows identification of specific proteins by exposing all proteins present on a SDS-gel after electrophoretic separation to a specific antibody.

In this study, Western blot analysis was performed on whole protein extracts of lung homogenates from donor transplants and IPF patients. For protein extraction, the human lung tissue was homogenized in liquid nitrogen by a pestle and 1 ml tissue lysis buffer per 0.1 g of tissue was added. After five minutes of incubation, the tissue lysate was passed several times through an RNase-free syringe with a 0.9 mm needle for further homogenization. The samples were incubated on ice for 60 minutes and meanwhile vortexed every five minutes. Protein extracts were clarified by centrifugation for 15 minutes at 4 °C and 16000 g; the resulting supernatant containing the proteins was collected and either used directly or stored at -20 °C.

lysis buffer:

20 mM Tris pH 7.5

150 mM NaCl
1 mM EDTA
1 mM EGTA
1% Triton X-100
2 mM Na₃VO₄
1:25 Complete™, protease inhibitor mix

The protein quantification of each sample was determined by using the Quick start Bradford protein assay (a colorimetric protein assay). For measurement, each protein sample was diluted 1:100 in ddH₂O, of which 10 µl was mixed with 200 µl of the Quick start Bradford dye reagent and transferred respectively to a 96-well plate. Additionally, different dilutions of bovine serum albumin (BSA) (0.05, 0.1, 0.2, 0.3, 0.4, 0.5 and 0.6 µg/µl) were used as protein standards. Equally, negative controls containing the Quick start Bradford dye reagent and 1:100 diluted protein lysis buffer were applied at the same 96-well plate. After an incubation period of 15 minutes, a spectrophotometric measurement was performed with a Fusion A153601 Reader at a wavelength of 570 nm, to measure the absorption. Protein samples, as well as the BSA standards and controls were measured as double values and averaged. The corresponding protein concentrations of each sample were calculated by comparing protein sample values to the BSA standard curve via interpolation. Proteins were separated according to their molecular weight by SDS polyacrylamide gel electrophoresis (SDS-PAGE). For separation, a 10 % resolving gel mixture was poured between two glass plates separated by teflon spacers, to allow polymerisation. The stacking gel was poured on top of the resolving gel, and a teflon comb was inserted into the gel to form wells. Ammonium persulfate (APS) and N,N,N,N'-tetramethylethylenediamine (TEMED) were added at last to initiate the polymerisation of the gels. Prior to loading onto the gel, 20 µg of each protein sample was mixed with 10x SDS gel-loading buffer and denatured at 95 °C for five minutes. Samples were loaded onto the polymerized gel, which consisted of a resolving gel with a 15-well stacking gel on top. 5 µl of protein standards run at the same gel were used as molecular weight size markers. In between the working steps, proteins were kept on ice at all times. After loading the proteins onto the gel, electrophoresis was performed in an electrophoresis chamber filled with 1x SDS-running buffer at 120 V for 90 minutes. After separation of the proteins by SDS-Page, immunoblotting was

performed to detect and visualize specific proteins. The separated proteins were transferred from the polyacrylamide gel onto a nitrocellulose membrane. The protein transfer was performed in transfer buffer at 100 V for 60 minutes. The membrane was incubated in blocking solution for 60 minutes at room temperature followed by incubation with the appropriate primary antibodies (table 6.4.1) diluted in blocking buffer at 4 °C overnight. As blocking buffer, either PBST with 5 % non-fat dry milk or TBST with 5 % BSA were used, depending on the recommendations for the corresponding antibody. The membrane was then washed three times for 10 minutes each with washing buffer and incubated with appropriate horseradish peroxidase-labelled (HRP) secondary antibodies for 60 minutes at room temperature (table 6.4.2). The membrane was washed five times for 10 minutes. After the washing step, the protein detection was performed using chemiluminescence by enhanced chemiluminescent immunoblotting system and exposure to radiographic film. For subsequent application of different antibodies, the membrane was incubated in stripping buffer for seven minutes at 52 °C, repeatedly washed and blocked. Protein visualization was performed as previously described.

3.2.12 [³H]-thymidine proliferation assay

The most commonly cellular proliferation assay used is based on DNA cleavage-dependent incorporation of thymidine, labeled with β -emitting tritium [³H]. An indirect quantification can be done by measuring the incorporated radioactive thymidine. Therefore, freshly isolated primary mouse ATII cells were plated at a density of 15×10^4 /well on 48-well plates in 500 μ l of 10 % FBS culture medium (minus (-) medium with FBS). After 24-30 hours the ATII cells became adherent, were subsequently synchronized in 0.1 % FBS medium for further 12 hours and then stimulated with recombinant mouse Wnt3a protein in 200 μ l/well of 0.1 % FCS medium for 18-24 hours. As [³H]-thymidine (0.5 μ Ci/ml) is being incorporated into the DNA during cell proliferation, it was added to the medium for the last six hours of the experiment. After washing twice with 1x PBS, cells were lysed with 300 μ l/well sodium hydroxide (NaOH) and placed on a shaker for a minimum of 30 minutes. Samples were transferred to separate measuring vials, adding 8 ml of scintillation liquid to each. The relative radioactivity was determined by a liquid- β -scintillation counter, to assess the proliferation rate.

3.2.13 Whole genome microarray

In order to perform whole genome microarray analysis, primary mouse ATII cells were isolated from healthy mouse lungs, treated for 8 and 24 hours with recombinant mouse Wnt3a protein according to the stimulation protocol and directly used. Each isolation obtained primary ATII cells pooled from 6 different mice. Total RNA was extracted as described from three independent groups and the quality assessed by capillary electrophoresis using the Bioanalyzer 2100. All samples contained 0.3 - 1.0 µg RNA, which was preamplified and labelled using the Low input RNA T7 kit according to the manufacturer's instructions. Three samples each (untreated and Wnt3a-treated ATII cells) were labeled with Cy3 and Cy5. The labeled RNA was hybridized overnight to 44K 60mer oligonucleotide spotted microarray slides. The slides were washed with different stringencies, dried by gentle centrifugation, and scanned using the GenePix 4100A scanner. Data analysis was performed with GenePix Pro 5.0 software, and calculated fore- and background intensities for all spots were saved as GenePix results files.

3.2.14 Enzyme linked-immuno-sorbent assay (ELISA)

Enzyme linked-immuno-sorbent assays (ELISA) are used for the quantitative determination of selected soluble proteins. The experiments were performed according to the manufacturer's protocol using the DuoSet® ELISA development kits from R & D Systems. The following sample types were used to measure natural and recombinant human and mouse interleukin 1β (IL1β), and mouse interleukin 6 (IL6): cell culture supernatants from primary mouse ATII cells, untreated and treated with recombinant Wnt3a protein; conditioned media from primary mouse ATII cells, obtained from saline- and bleomycin-treated mice; bronchoalveolar lavage fluid (BALF) from saline- and bleomycin-treated mice, as well as from donor transplants and IPF patients.

At first a 96-well microplate was coated with the appropriate capture antibody, sealed and incubated overnight at room temperature. The following day, the 96-well microplate was washed three times, followed by a drying step to completely remove liquid and unbound material. Next, blocking buffer was added and the 96-well microplate was incubated for one hour at room temperature. The wash/drying step was repeated after each incubation step as before. The samples and standards were

diluted in reagent diluent and added in duplicates to the 96-well microplate, which was sealed and incubated for two hours at room temperature. After removing unbound material, the appropriate detection antibody was added to the 96-well microplate, which was sealed and incubated for two hours at room temperature. Streptavidin-HRP was added and the 96-well microplate was incubated for 20 minutes, light protected at room temperature. After incubation with streptavidin-HRP, the 96-well microplate was incubated with substrate solution for 20 minutes, light protected at room temperature. Finally, a stop solution was added and the optical density of each well was determined using a spectrophotometer. The absorption was measured at a wavelength of 450 nm. Additionally, in order to correct optical imperfections in the 96-well microplate, the absorption was measured at 570 nm and subtracted from readings at 450 nm. The corresponding protein concentrations were calculated by interpolation using the standard curve.

3.2.15 Statistical analysis

All results were presented as means \pm standard error of mean (s.e.m.), if not otherwise stated, and were considered statistically significant when the probability by rejecting the null hypothesis is less than 0.05 (* $p < 0.05$). The mean of indicated groups were compared using the Student's t-test. All ΔC_t values obtained from quantitative RT-PCR were analyzed for normal distribution using the Shapiro-Wilk test. All $\Delta\Delta C_t$ values were analyzed using the two-tailed, one-sample t-test. Intergroup differences of ΔC_t values from IPF patients and bleomycin-treated mice were derived using an one-tailed, two-sample t-test. Proliferation assay data were analyzed using the Wilcoxon rank-sum test and signed-rank test. All p values obtained from multiple tests were adjusted using the procedure from Benjamini & Hochberg.

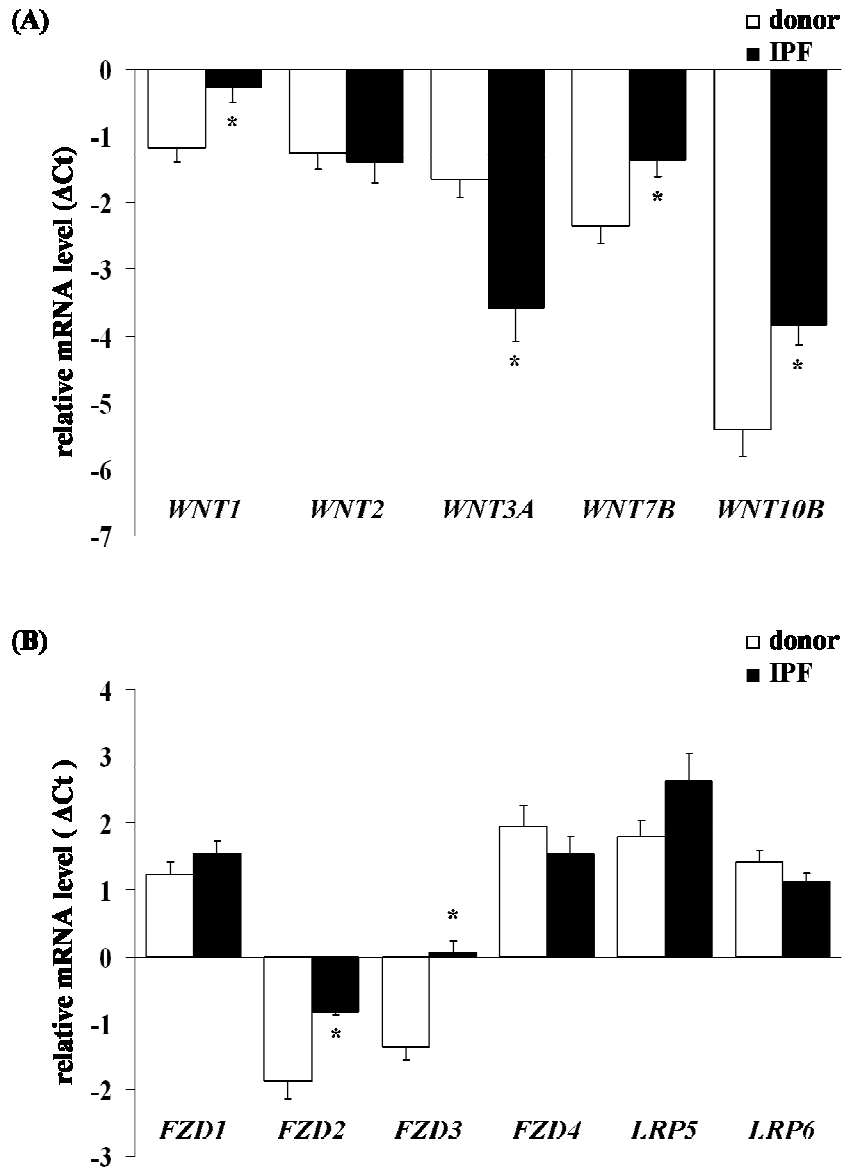
4 RESULTS

4.1 Analysis of the canonical WNT/ β -catenin signalling pathway in idiopathic pulmonary fibrosis

4.1.1 Expression of the canonical WNT/ β -catenin signalling pathway in idiopathic pulmonary fibrosis

In order to investigate the role of the canonical WNT/ β -catenin signalling pathway in IPF, quantitative real time polymerase chain reaction ((q)RT-PCR) was performed to compare the mRNA expression levels of canonical WNT/ β -catenin signalling components in lung tissue samples of healthy transplant donors (= controls) and IPF patients. The total lung homogenates were obtained from twelve (n = 12) healthy transplant donor and IPF lungs, respectively.

First, the canonical WNT ligands WNT1, 2, 3A, 7B and 10B were analysed in this study. As depicted in figure 4.1 (A), WNT1, 2, 3A and 7B were expressed at similar low levels in the human lung, while WNT10B expression in particular was minimal in lung tissue obtained from healthy transplant donors. In IPF lung samples, there was a significant upregulation of WNT1, 7B and 10B mRNA levels compared with healthy transplant donor lung samples (log fold change: 0.90 ± 0.30 , 1.00 ± 0.36 and 1.58 ± 0.50 , respectively). However, WNT3A proved to be significantly downregulated in IPF lung samples as compared to healthy transplant donor lung samples (log fold change: -1.93 ± 0.58). Subsequently, the expression profile of the common WNT receptors FZD1, 2, 3 and 4; as well as the WNT co-receptors LRP5 and 6 was determined. As seen in figure 4.1 (B), the most abundant receptors in the human lung were FZD1 and 4, as well as the co-receptors LRP5 and 6. However, their expression levels were similar in healthy transplant donor and IPF lungs. FZD2 and 3 specific mRNAs were detected at low levels in healthy transplant donor and IPF lungs, but significantly increased under pathological conditions of IPF as compared to healthy transplant donor lung samples (log fold change: 1.04 ± 0.28 and 1.41 ± 0.27 , respectively). Figure 4.1 (C) shows the expression of the WNT cytoplasmic factors AXIN1 and 2, as well as DVL1, 2 and 3, and GSK3 β .



The most abundant cytoplasmic factors in the human lung were Axin1 and 2, as well as DVL3 and GSK3 β . However, AXIN1 was significantly increased in IPF as compared to healthy donor lung samples (log fold change: 0.97 ± 0.30). In figure 4.1 (D), the expression of the main intracellular canonical WNT signal transducer β -catenin (CTNNB1), as well as the WNT-specific transcription factors LEF1, TCF3 and 4 was investigated. CTNNB1 expression was observed in healthy transplant donor and IPF lung tissue, with a significantly increased expression of CTNNB1 in IPF lung samples as compared to healthy transplant donor lung samples (log fold change: 0.79 ± 0.20). All members of the TCF/LEF family of transcription factors, except for TCF1, were expressed in human lung tissue, and LEF1 mRNA was

significantly upregulated in IPF as compared to healthy transplant donor lung samples (log fold change: 0.85 ± 0.27).

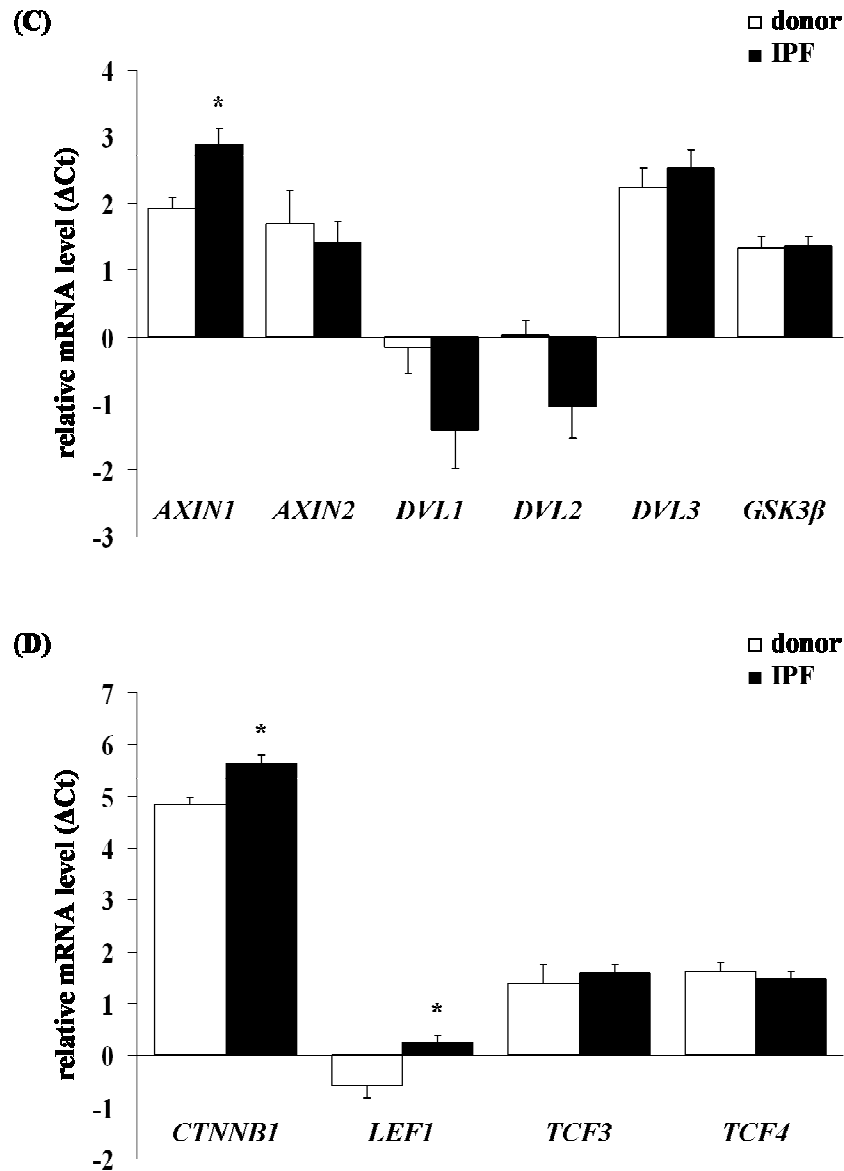


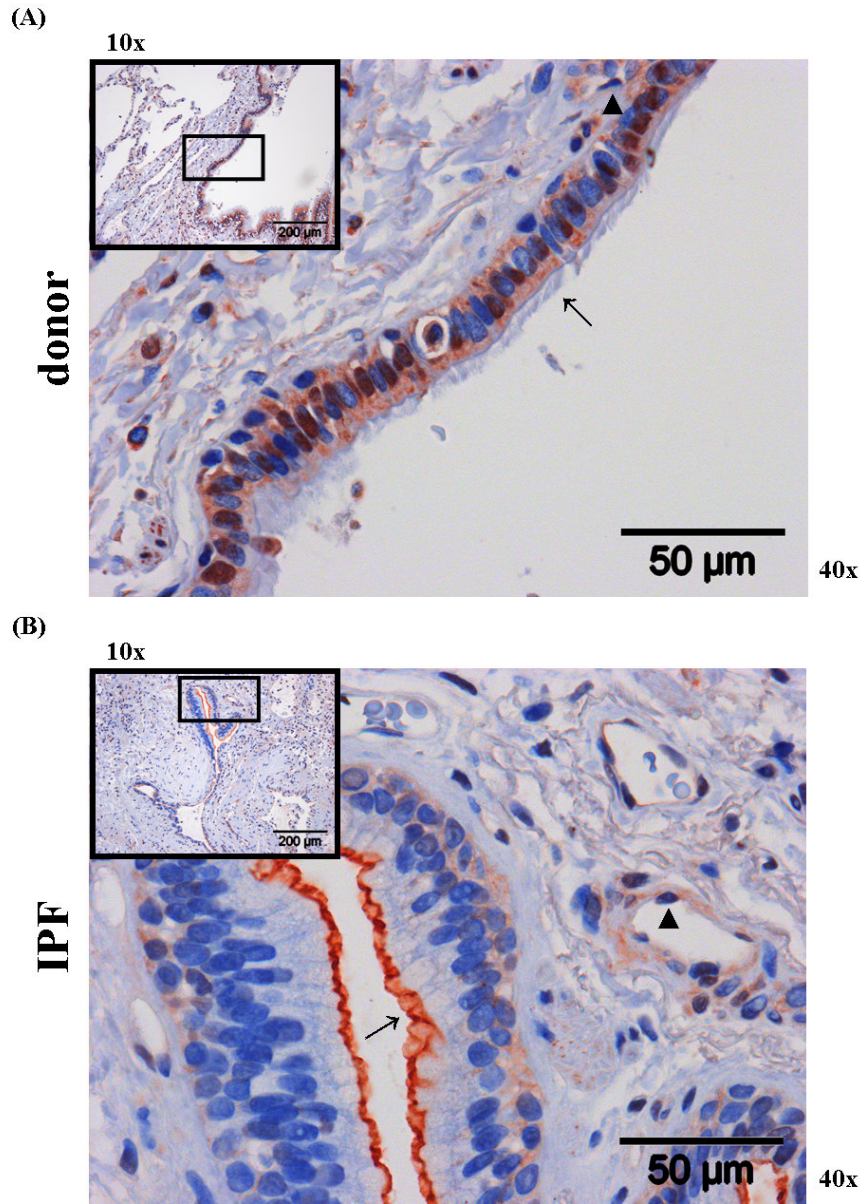
figure 4.1: Gene expression profile of canonical WNT signalling components in idiopathic pulmonary fibrosis (IPF). The relative messenger ribonucleic acid (mRNA) levels of (A) the WNT ligands *WNT1*, *2*, *3A*, *7B* and *10B*, (B) the receptors frizzled *FZD1* - *4*, low density lipoprotein-related proteins *LRP5* and *6*, (C) the cytoplasmic factors axis inhibition protein *AXIN1*, *2*, dishevelled *DVL1* - *3*, and intracellular signal transducer glycogen synthase kinase *GSK3β*, and (D) the intracellular signal transducer *CTNNB1*, lymphoid enhancer-binding factor *LEF1* and

T-cell-specific transcription factors *TCF3* and *4* were assessed in healthy transplant donor and IPF total lung homogenates by quantitative real time polymerase chain reaction ((q)RT-PCR). Data were presented in a bar graph; plotting the results as ΔC_t ($\Delta C_t = C_t$ reference gene - C_t target gene); statistical significance (p/p-value) was presented as * (* = $p < 0.05$), samples of 12 individual isolations were used ($n = 12$). The resulting data for LRP5 and 6 were kindly provided by Eva Pfaff.

4.1.2 Localisation of the canonical WNT/ β -catenin signalling pathway in idiopathic pulmonary fibrosis

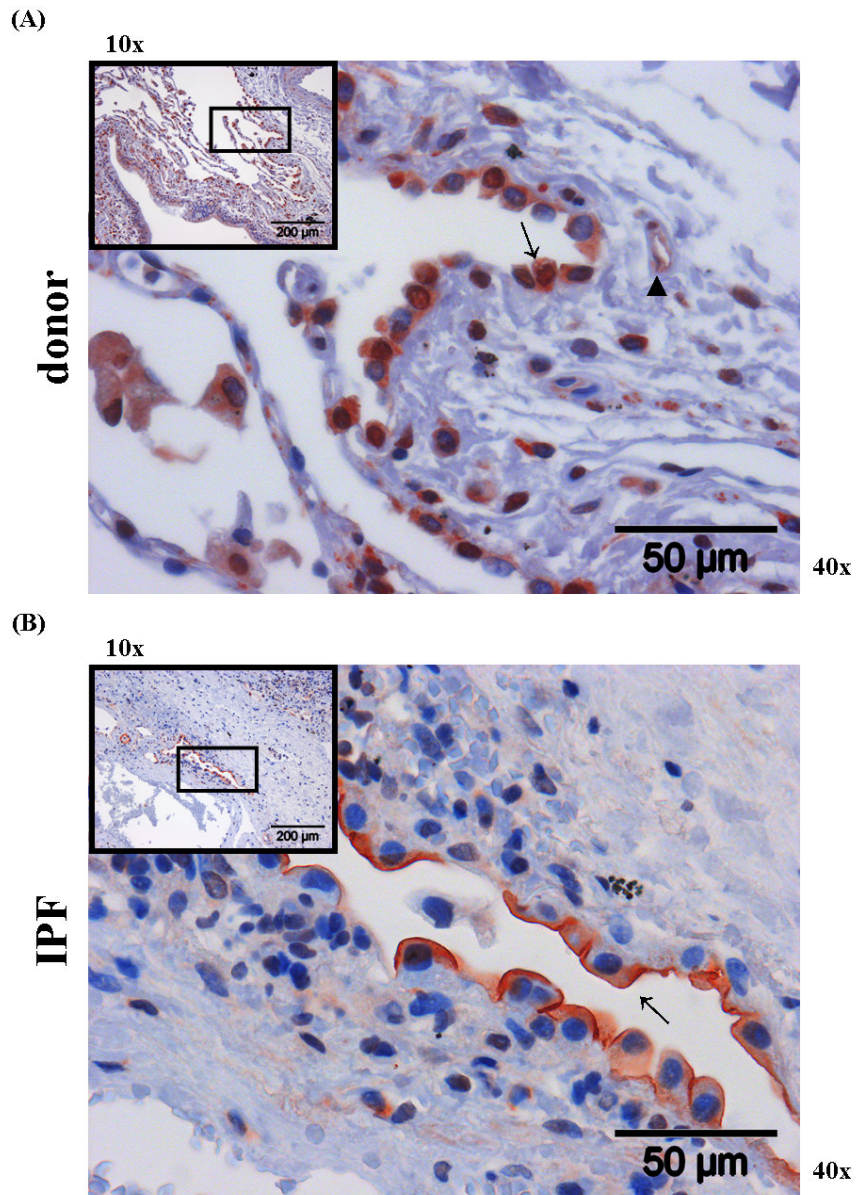
In order to detect the various cell types, which are capable of expressing specific canonical WNT/ β -catenin signalling pathway components, immunohistochemistry (IHC) was performed. The WNT ligands WNT1 and 3A and the main canonical intracellular WNT signal transducers CTNNB1 and GSK3 β were assessed in paraformaldehyde-fixed and paraffin embedded lung tissue sections prepared from biopsies of healthy transplant donors (= controls) and IPF patients. The lung tissue sections were obtained from three ($n = 3$) healthy transplant donor and IPF lungs, respectively.

As shown in figure 4.2.1 (A) and 4.2.2 (A), in healthy transplant donor lung sections WNT1 was mainly expressed in bronchial and alveolar epithelium, with strong staining of alveolar epithelial type II (ATII) cells. Additionally, WNT1 was detected in vascular smooth muscle cells. In IPF lung sections (see figure 4.2.1 (B) and 4.2.2 (B)), WNT1 staining was observed in bronchial epithelial cells and hyperplastic ATII cells, identifiable by their cubic shape. In bronchial epithelial cells of IPF lungs WNT1 showed an apical staining pattern as compared to healthy transplant donor lungs, which indicates increased secretion. WNT1 was also expressed in endothelial cells in IPF tissues. Figure 4.3.1 and 4.3.2 (A and B) shows, that WNT3A protein expression was predominantly detected in ATII cells and selected ciliated bronchial epithelial cells in both, healthy transplant donor and IPF lung tissue sections. In figure 4.4.1 (A) and 4.4.2 (A), GSK3 β exhibits a predominant staining in bronchial epithelial and ATII cells, as well as endothelial cells in healthy transplant donor lung tissue. In figure 4.4.1 (B) and 4.4.2 (B), GSK3 β expression was observed in basal bronchial epithelial and hyperplastic ATII cells in IPF lung tissues.



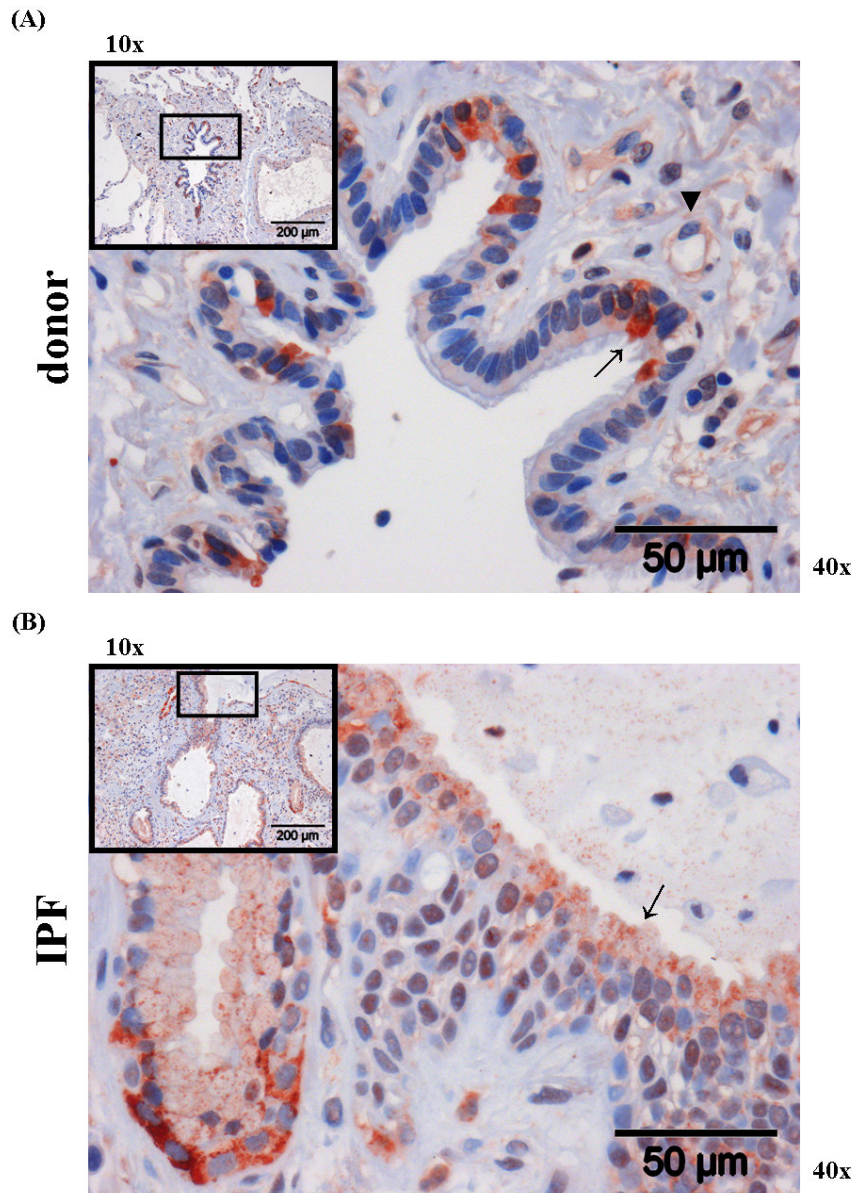
WNT1

figure 4.2.1: Localisation of WNT1 in idiopathic pulmonary fibrosis (IPF). Immunohistochemistry (IHC) was performed on tissue sections of **(A)** healthy transplant donor and **(B)** IPF lungs. IHC pictures focused on the bronchial epithelium. WNT1 staining were representative of two independent sets of three different healthy transplant donor (upper panel) and IPF (lower panel) lung tissue sections, respectively (magnification as indicated). In **(A)**, the arrow representatively indicates cytoplasmic and sporadic nuclear staining. The arrowhead indicates positive endothelial cells. As depicted in **(B)**, the arrow representatively indicates strong apical staining. The arrowhead indicates positive endothelial cells.



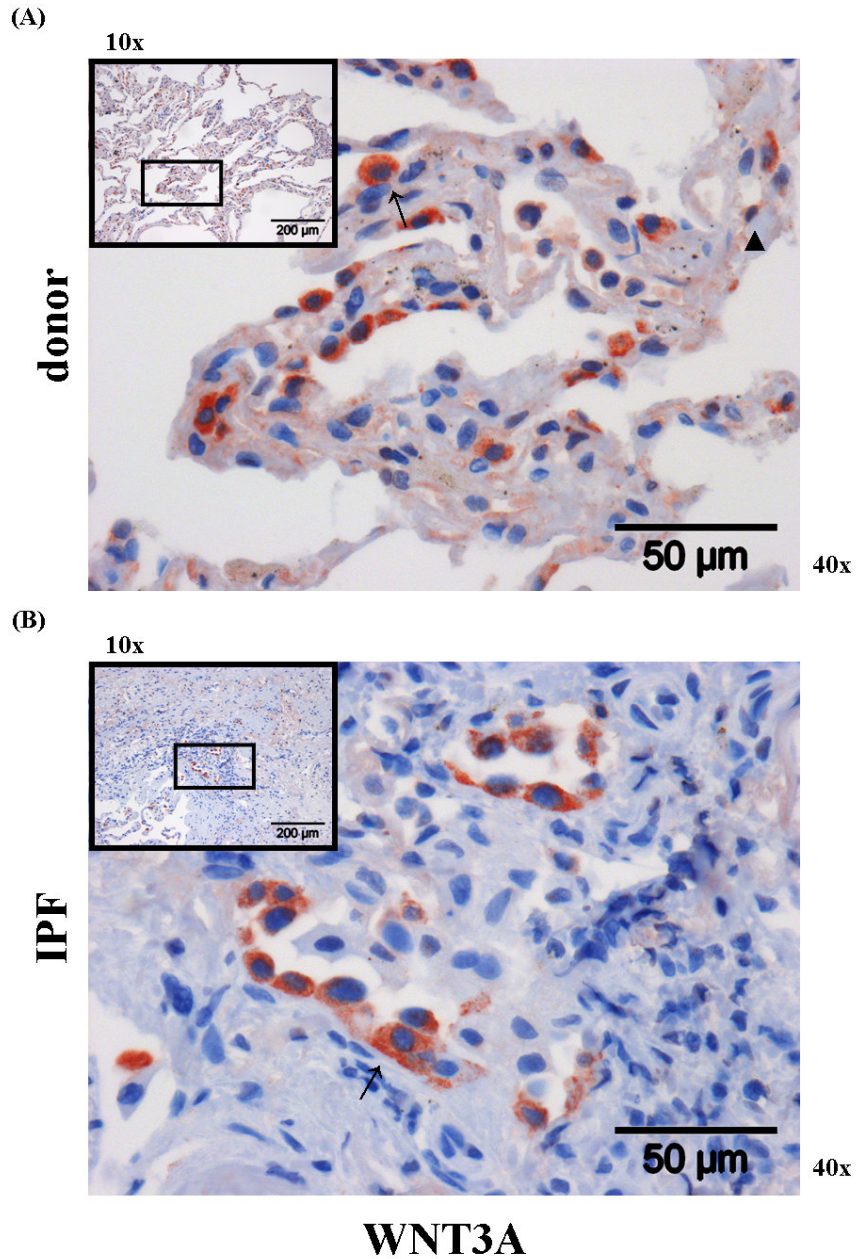
WNT1

figure 4.2.2: Localisation of WNT1 in idiopathic pulmonary fibrosis (IPF). Immunohistochemistry (IHC) was performed on tissue sections of (A) healthy transplant donor and (B) IPF lungs. IHC pictures focused on the alveolar epithelium. WNT1 staining were representative of two independent sets of three different healthy transplant donor (upper panel) and IPF (lower panel) lung tissue sections, respectively (magnification as indicated). In (A), the arrow representatively indicates cytoplasmic and sporadic nuclear staining. The arrowhead indicates positive endothelial cells. As depicted in (B), the arrow representatively indicates strong apical staining.



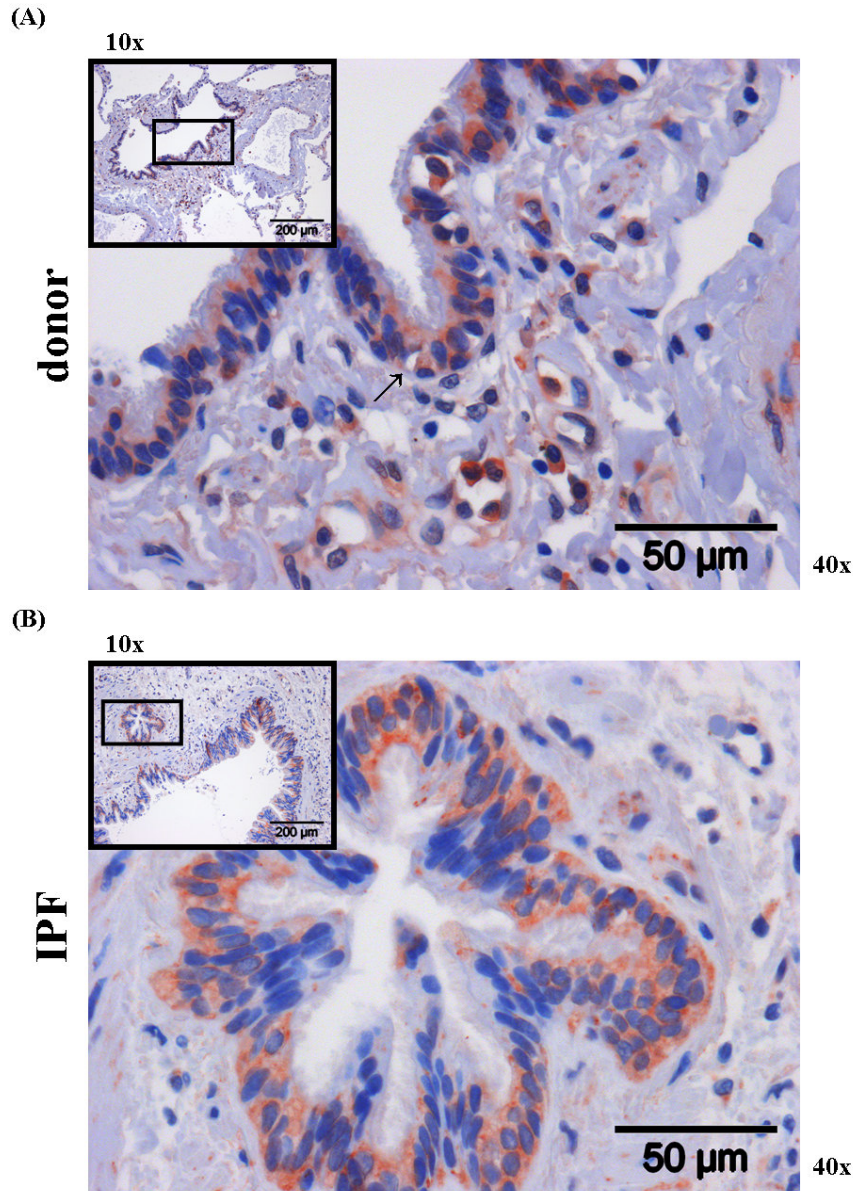
WNT3A

figure 4.3.1: Localisation of WNT3A in idiopathic pulmonary fibrosis (IPF). Immunohistochemistry (IHC) was performed on tissue sections of **(A)** healthy transplant donor and **(B)** IPF lungs. IHC pictures focused on the bronchial epithelium. WNT3A staining were representative of two independent sets of three different healthy transplant donor (upper panel) and IPF (lower panel) lung tissue sections, respectively (magnification as indicated). In **(A)**, the arrow representatively indicates cytoplasmic staining. The arrowhead indicates positive endothelial cells. As depicted in **(B)**, the arrow representatively indicates strong apical staining.



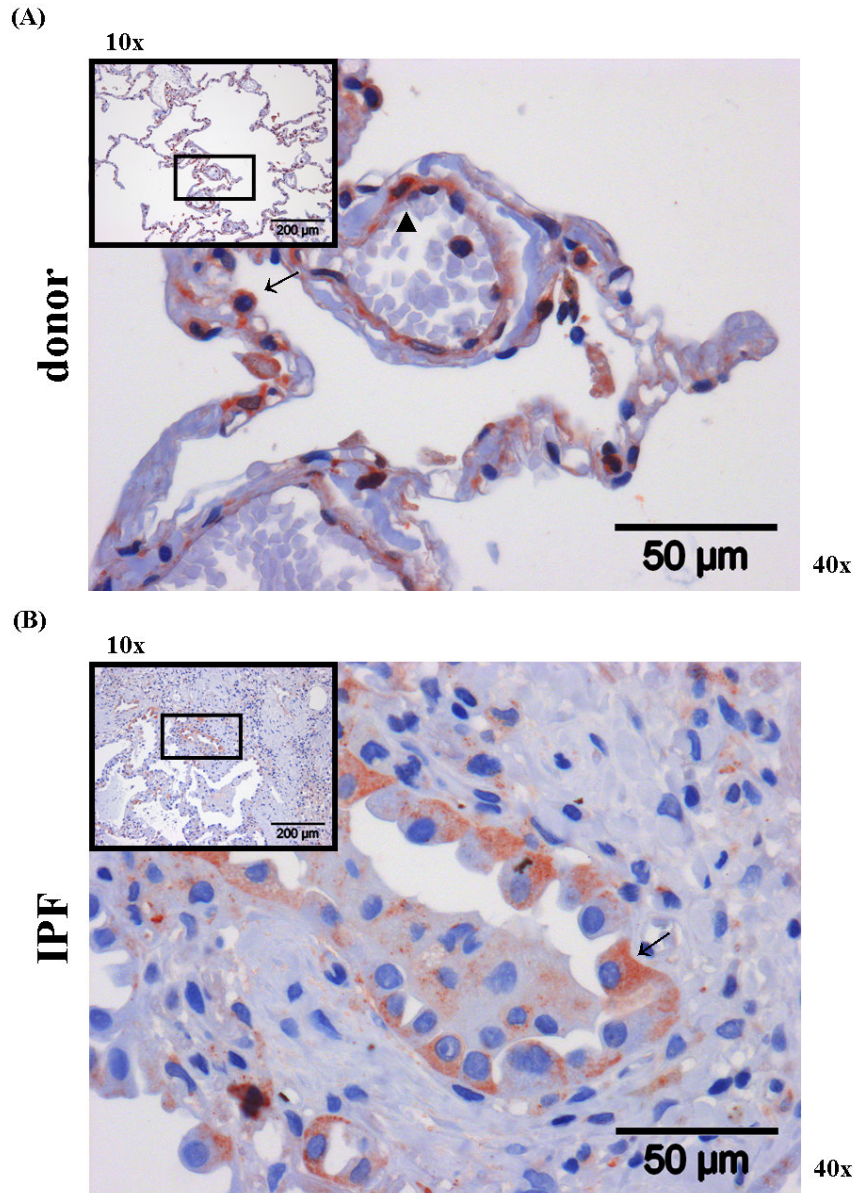
WNT3A

figure 4.3.2: Localisation of WNT3A in idiopathic pulmonary fibrosis (IPF). Immunohistochemistry (IHC) was performed on tissue sections of **(A)** healthy transplant donor and **(B)** IPF lungs. IHC pictures focused on the alveolar epithelium. WNT3A staining were representative of two independent sets of three different healthy transplant donor (upper panel) and IPF (lower panel) lung tissue sections, respectively (magnification as indicated). In **(A)**, the arrow representatively indicates cytoplasmic staining. The arrowhead indicates positive endothelial cells. As depicted in **(B)**, the arrow representatively indicates strong apical staining.



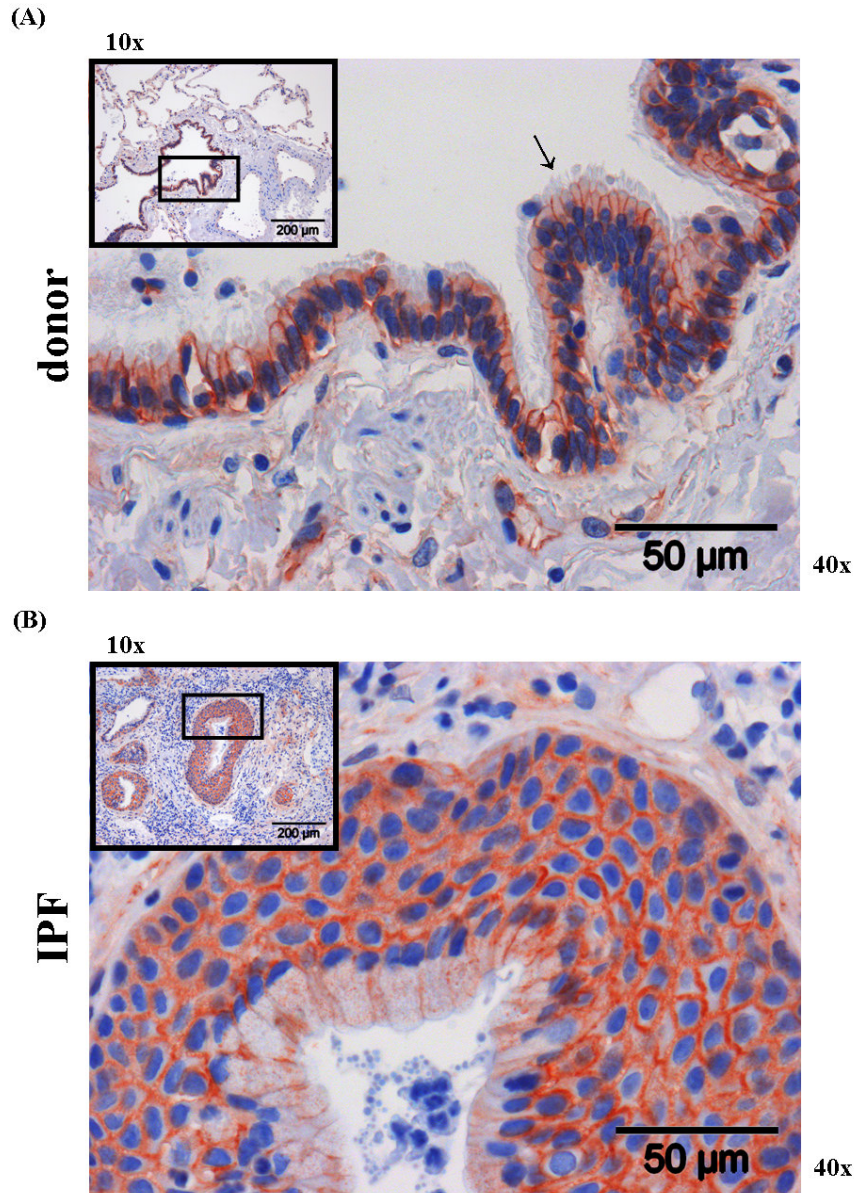
GSK3β

figure 4.4.1: Localisation of glycogen synthase kinase 3β (GSK3β) in idiopathic pulmonary fibrosis (IPF). Immunohistochemistry (IHC) was performed on tissue sections of (A) healthy transplant donor and (B) IPF lungs. IHC pictures focused on the bronchial epithelium. GSK3β staining were representative of two independent sets of three different healthy transplant donor (upper panel) and IPF (lower panel) lung tissue sections, respectively (magnification as indicated). In (A), the arrow representatively indicates cytoplasmic staining. As depicted in (B), GSK3β staining was generally localised at the basal bronchial cell membrane.



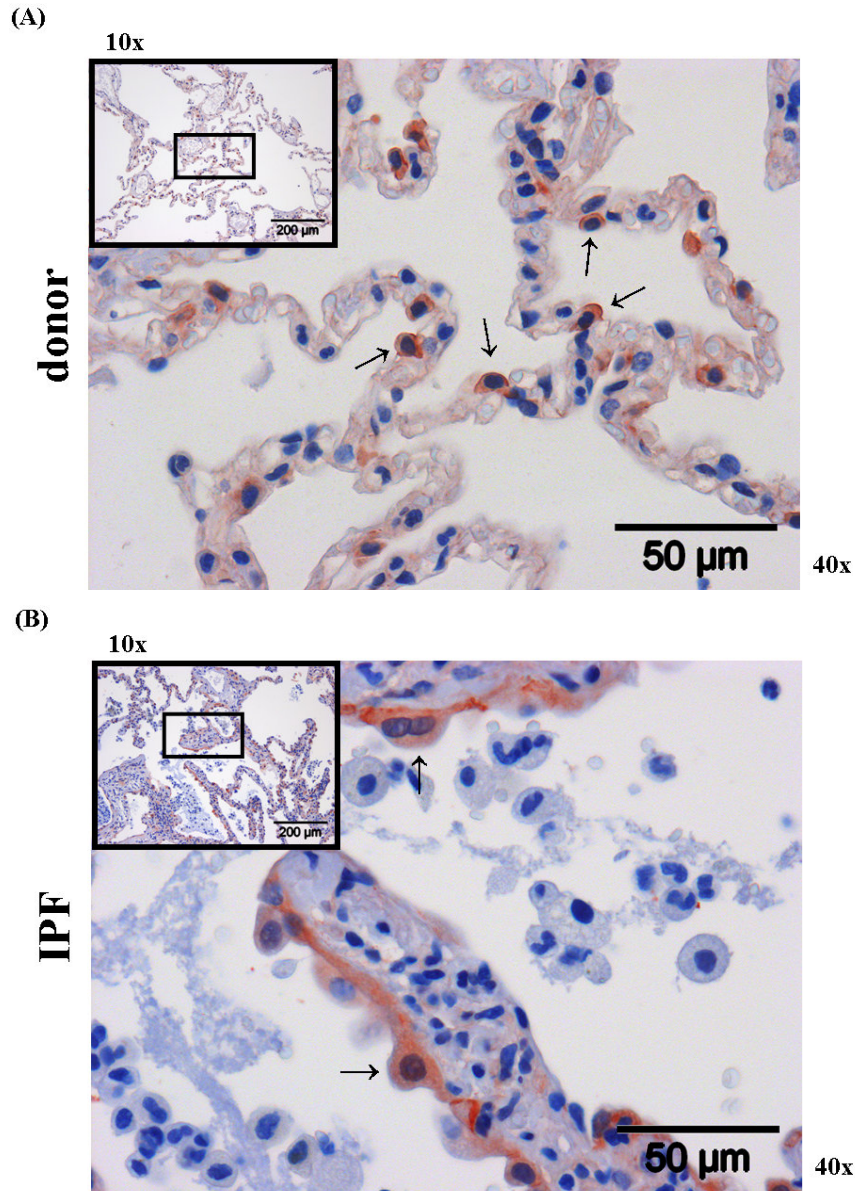
GSK3β

figure 4.4.2: Localisation of glycogen synthase kinase 3β (GSK3β) in idiopathic pulmonary fibrosis (IPF). Immunohistochemistry (IHC) was performed on tissue sections of (A) healthy transplant donor and (B) IPF lungs. IHC pictures focused on the alveolar epithelium. GSK3β staining were representative of two independent sets of three different healthy transplant donor (upper panel) and IPF (lower panel) lung tissue sections, respectively (magnification as indicated). In (A), the arrow representatively indicates cytoplasmic staining. The arrowhead indicates positive endothelial cells. As depicted in (B), the arrow representatively indicates strong basal staining.



CTNNB1

figure 4.5.1: Localisation of β -catenin (CTNNB1) in idiopathic pulmonary fibrosis (IPF). Immunohistochemistry (IHC) was performed on tissue sections of (A) healthy transplant donor and (B) IPF lungs. IHC pictures focused on the bronchial epithelium. CTNNB1 staining were representative of two independent sets of three different healthy transplant donor (upper panel) and IPF (lower panel) lung tissue sections, respectively (magnification as indicated). In (A), the arrow representatively indicates strong membranous staining in ciliated cells. As depicted in (B), CTNNB1 staining was generally localised more cytoplasmic.



CTNNB1

figure 4.5.2: Localisation of β -catenin (CTNNB1) in idiopathic pulmonary fibrosis (IPF). Immunohistochemistry (IHC) was performed on tissue sections of (A) healthy transplant donor and (B) IPF lungs, with focus on the alveolar epithelium. CTNNB1 staining were representative of two independent sets of three different healthy transplant donor (upper panel) and IPF (lower panel) lung tissue sections, respectively (magnification as indicated). In (A), the arrows representatively indicate strong membranous staining in alveolar type II (ATII) cells. As depicted in (B), the arrows representatively indicate strong nuclear staining in single ATII cells.

As depicted in figure 4.5.1 (A) and 4.5.2 (A), strong membranous and cytoplasmic CTNNB1 expression was observed in bronchial epithelial and ATII cells, as well as in endothelial cells of healthy transplant donor lungs. Importantly, in IPF lungs (see figure 4.5.1 (B) and 4.5.2 (B)), CTNNB1 showed less membranous staining. An enhanced expression was detected in the cytoplasm. Additionally, clear nuclear staining was observed in single cells. Especially in bronchial areas and in alveolar type II (ATII) cells a strong CTNNB1 staining was noticed.

In summary, the canonical WNT/ β -catenin signalling pathway components in general were largely expressed in the bronchial and alveolar epithelium of healthy transplant donor and IPF lung tissue.

4.1.3 Activity of the canonical WNT/ β -Catenin signalling pathway in idiopathic pulmonary fibrosis

To determine, whether the canonical WNT/ β -catenin signalling pathway was activated at the protein level in IPF, Western blot (WB) analysis was performed. Therefore, total lung homogenates were obtained from five donor and IPF patients, respectively.

As presented in figure 4.6, increased phosphorylation of GSK3 β and LRP6 in IPF patients was observed compared with transplant donors (=control). This is consistent with elevated protein levels of total CTNNB1, indicating activated canonical WNT/ β -catenin signalling. The analysis revealed upregulated protein levels of cyclinD1, a known target gene of the canonical WNT/ β -catenin signalling pathway. An increased level of alpha-smooth muscle actin (ACTA2 = α -SMA) was detected in IPF lung homogenates compared with donor lung homogenates. Total GSK3 β , total LRP6 and lamin A/C served as loading controls.

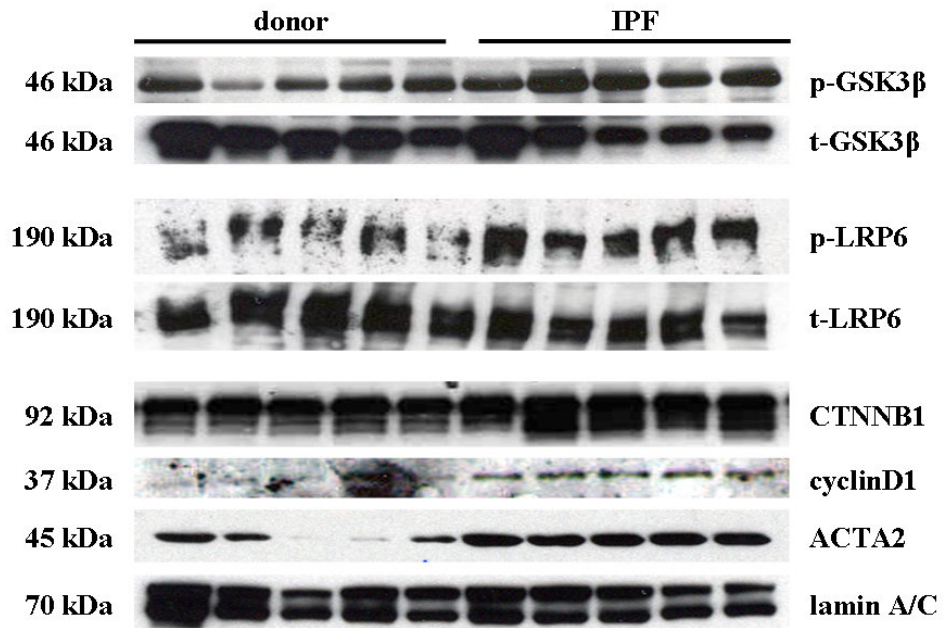


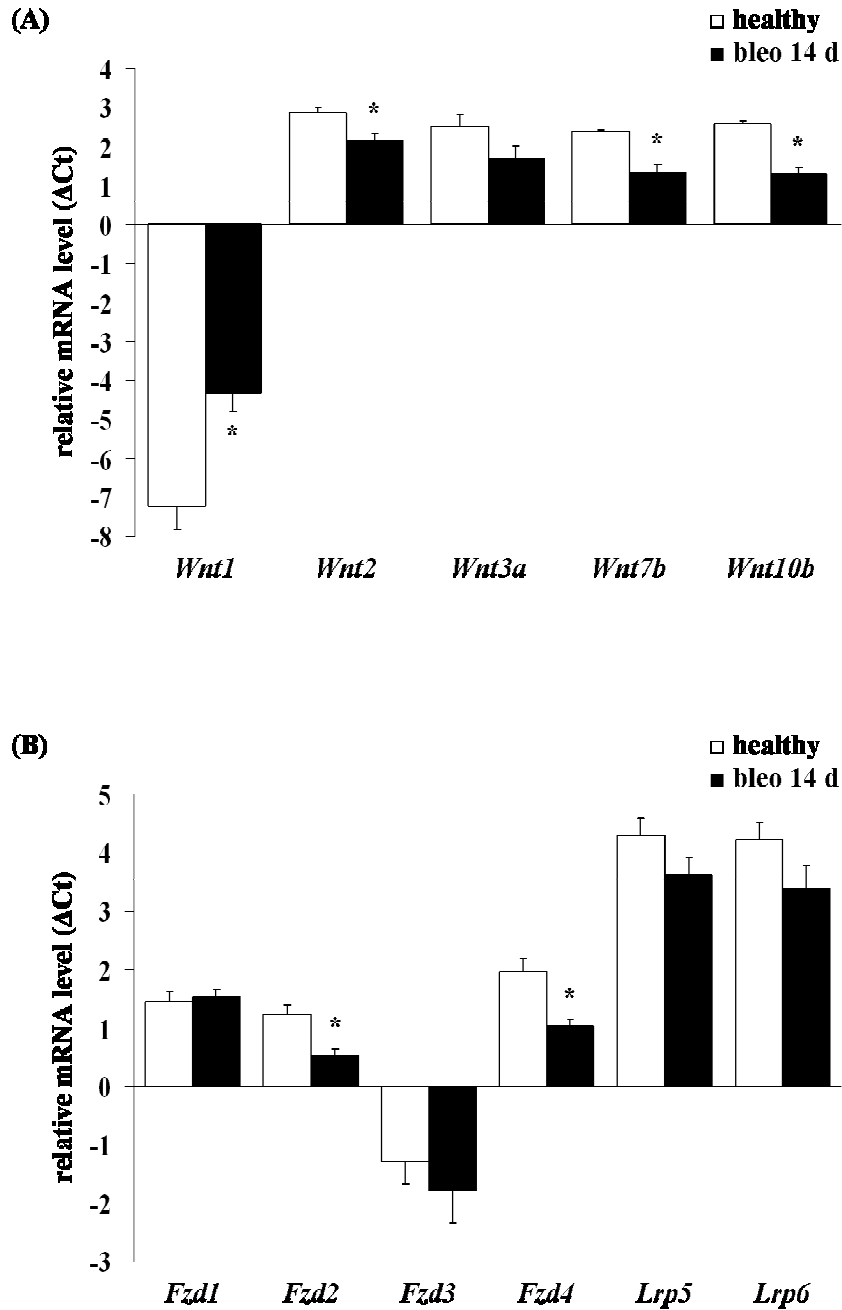
figure 4.6: Protein expression of canonical WNT signalling components in idiopathic pulmonary fibrosis (IPF). The expression of active WNT components in total lung homogenates of transplant donor and IPF patients was analyzed by Western blot. The protein levels of phosphorylated GSK3 β (p-GSK3 β) and LRP6 (p-LRP6), total β -catenin (CNTTB1), the WNT target gene cyclinD1 and ACTA2 were observed. Total GSK3 β (t-GSK3 β), total LRP6 (t-LRP6) and lamin A/C served as loading controls. Results are derived from five donor and IPF patients, respectively. This western blot was performed and the resulting data were kindly provided by Dr. Izabella Chrobak.

4.2 Analysis of the canonical WNT/ β -catenin signalling pathway in experimental pulmonary fibrosis

4.2.1 Expression of the canonical WNT/ β -catenin signalling pathway in experimental pulmonary fibrosis

The mouse model of bleomycin-induced pulmonary fibrosis was used to determine whether the expression of canonical WNT/ β -catenin signalling components was regulated and activated during this process. To induce an experimental model of pulmonary fibrosis, mice were subjected to saline (= control) and to bleomycin treatment for 14 days, respectively. Initially, qRT-PCR was performed to quantify the mRNA expression of canonical WNT/ β -catenin signalling components in lung tissue samples of saline- and bleomycin-treated mice. The total lung homogenates were obtained from six saline- and bleomycin-treated lungs, respectively.

As depicted in figure 4.7 (A), the WNT ligands Wnt2, 3a, 7b and 10b were detected at similar levels in the mouse lung, whereas Wnt1 was much lower expressed in lung tissue from saline-treated mice. In bleomycin-treated lung tissue however, a significant increase of Wnt1 expression was observed (log fold change: 2.90 ± 0.75). Whereas, Wnt2, 7b and 10b showed a marked decrease of mRNA levels in bleomycin-treated total lung homogenates as compared with control lung homogenates (log fold change: -0.71 ± 0.22 , -1.07 ± 0.22 and -1.28 ± 0.18 , respectively). Next, the expression profile of the common WNT receptors, Fzd1, 2, 3 and 4; and the WNT co-receptors, Lrp5 and 6 was determined. As seen in figure 4.7 (B), the co-receptors Lrp5 and 6 were expressed at similar high mRNA levels in saline- and bleomycin-treated lungs. Interestingly, 14 days after bleomycin treatment, there was a significant downregulation of Fzd2 and 4 (log fold change: -0.69 ± 0.20 and -0.94 ± 0.25 , respectively). Figure 4.7 (C) shows the expression of the WNT cytoplasmic factors, Axin1 and 2, as well as Dvl1, 2 and 3, and Gsk3 β . High expression levels of all these components were detected in saline- and bleomycin-treated lungs. Thereby, Axin2 was significantly decreased at 14 days after bleomycin treatment as compared to saline treatment (log fold change: -1.04 ± 0.21).



In figure 4.7 (D), the expression of the WNT transcription factors, Lef1, Tcf3 and 4, as well as the main intracellular canonical WNT signal transducer Ctnnb1 was investigated. Ctnnb1 expression was observed at a notable high abundance in saline- and bleomycin-treated lung homogenates, with no evident changes in expression. All members of the Tcf/Lef family of transcription factors, except for Tcf1 were expressed in mouse lung tissue. Interestingly, Tcf3 and 4 showed a significant

decrease at 14 days after bleomycin treatment (log fold change: -0.61 ± 0.06 and -1.06 ± 0.14 , respectively).

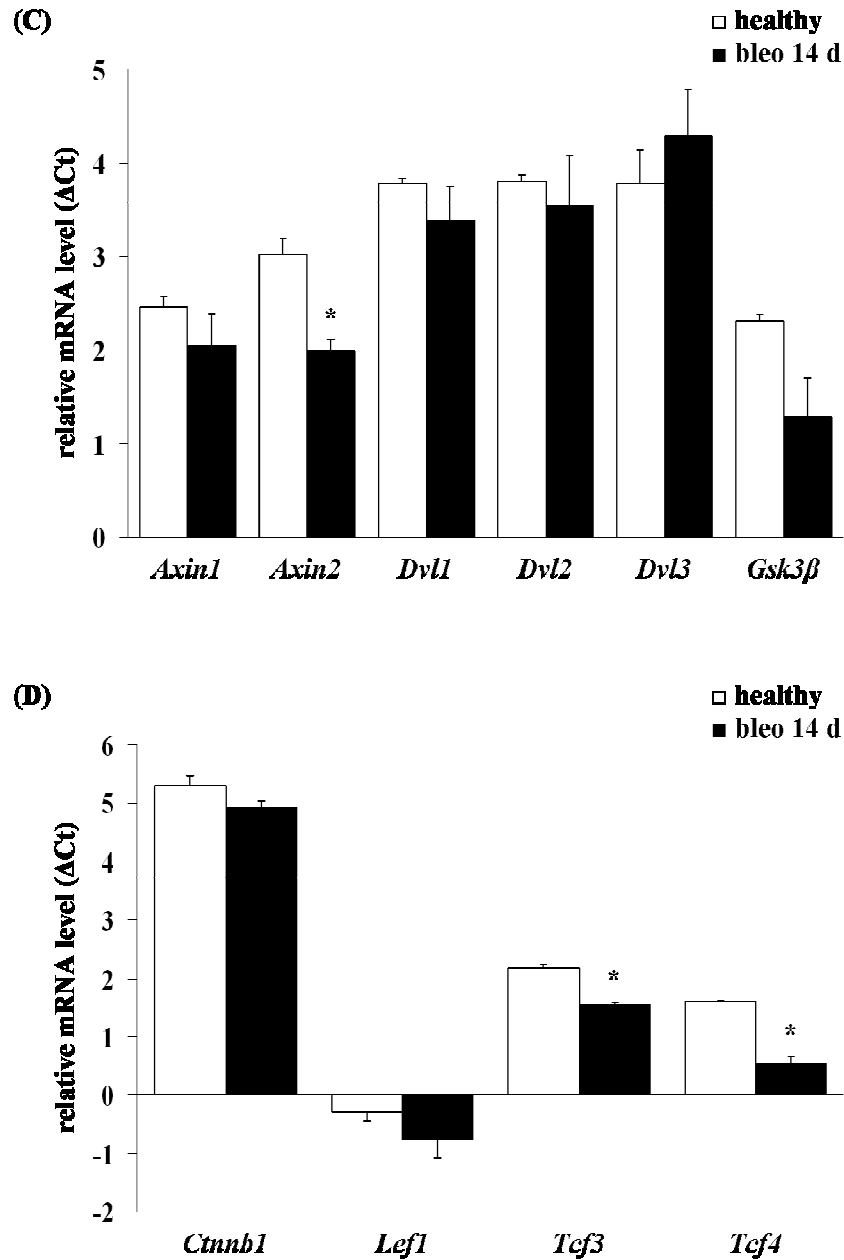


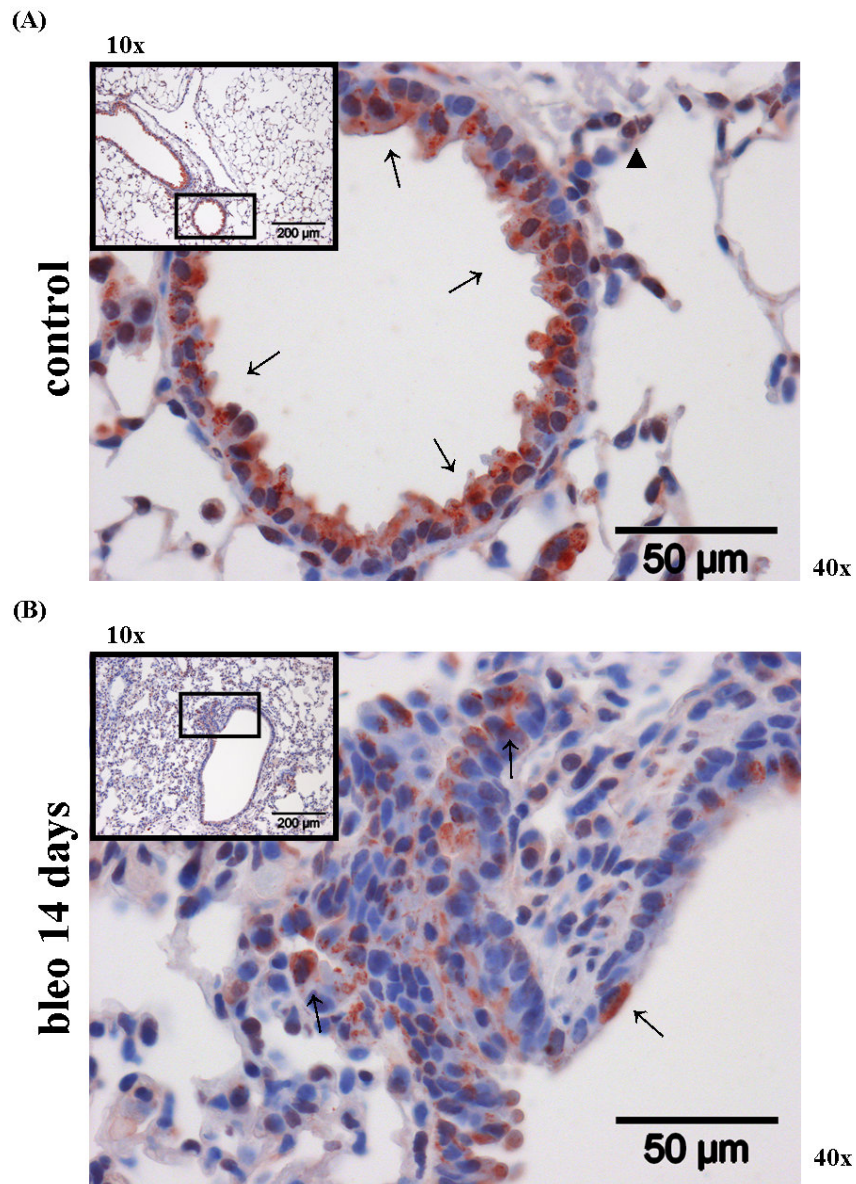
figure 4.7: Gene expression profile of canonical WNT signalling components in experimental pulmonary fibrosis. The relative messenger ribonucleic acid (mRNA) levels of (A) the WNT ligands *Wnt1*, *2*, *3a*, *7b* and *10b*, (B) the receptors frizzled *Fzd1* - *4*, low density lipoprotein-related protein *Lrp5* and *6*, (C) the cytoplasmic factors axis inhibition protein *Axin1*, *2*, dishevelled *Dvl1* - *3*, and intracellular signal

transducer glycogen synthase kinase *Gsk3β*, and **(D)** the intracellular signal transducer *Ctnnb1*, lymphoid enhancer-binding factor *Lef1* and T-cell-specific transcription factor *Tcf3* and 4 were assessed in total lung homogenates of saline- and bleomycin-treated mice 14 days after application by quantitative real time polymerase chain reaction ((q)RT-PCR). Data were presented in a bar graph; plotting the results as ΔC_t ($\Delta C_t = C_t$ reference gene - C_t target gene); statistical significance (p/p-value) was presented as * (* = $p < 0.05$), samples of six individual sets of isolations were used (n = 6).

4.2.2 Localisation of the WNT/ β -catenin signalling pathway in experimental pulmonary fibrosis

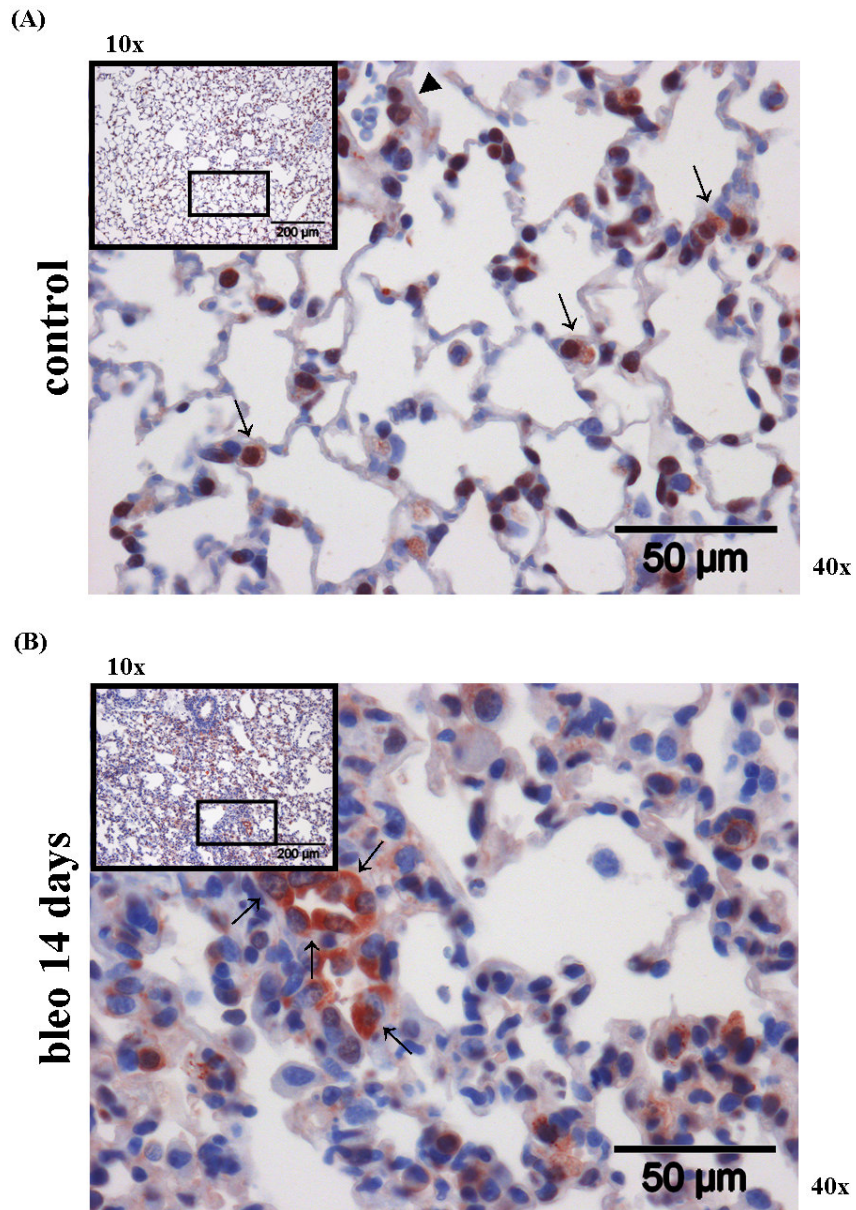
In order to confirm cell-specific expression of the canonical Wnt/ β -catenin signalling pathway components, immunohistochemistry (IHC) was performed. The Wnt ligands Wnt1 and 3a and the main canonical intracellular WNT signal transducers *Ctnnb1* and *Gsk3β* were assessed in lung tissue sections from saline- (= control) and bleomycin-treated mice. The whole lung sections were obtained from three saline- and bleomycin-treated lungs, 14 days after application, respectively.

As shown in figure 4.9 (A), Wnt1 was mainly expressed in bronchial and alveolar epithelium in saline-treated lungs. In figure 4.9 (B), strong staining in alveolar epithelial type II (ATII) cells from bleomycin-treated lungs was observed. Figure 4.10 (A) shows, that Wnt3a protein expression was detected in bronchial epithelial cells in saline- as well as in bleomycin-treated lung tissue. However, in figure 4.10 (B), a strong staining of Wnt3a was revealed in ATII cells from bleomycin-treated lungs compared with control lungs. As depicted in figure 4.11 (A and B), *Gsk3β* was expressed in bronchial epithelial and ATII cells in saline- and bleomycin-treated lung tissues. Figure 4.12 (A) shows a strong membranous and cytoplasmic *Ctnnb1* expression in bronchial epithelial and ATII cells. Additionally, staining was observed in endothelial cells in saline-treated lungs. As seen in figure 4.12 (B), strong *Ctnnb1* staining was observed in bronchial epithelial, ATII and endothelial cells of saline- and bleomycin-treated lungs. The canonical Wnt/ β -catenin signalling pathway components in general were largely expressed in the bronchial and alveolar epithelium of saline- and bleomycin-treated mouse lungs.



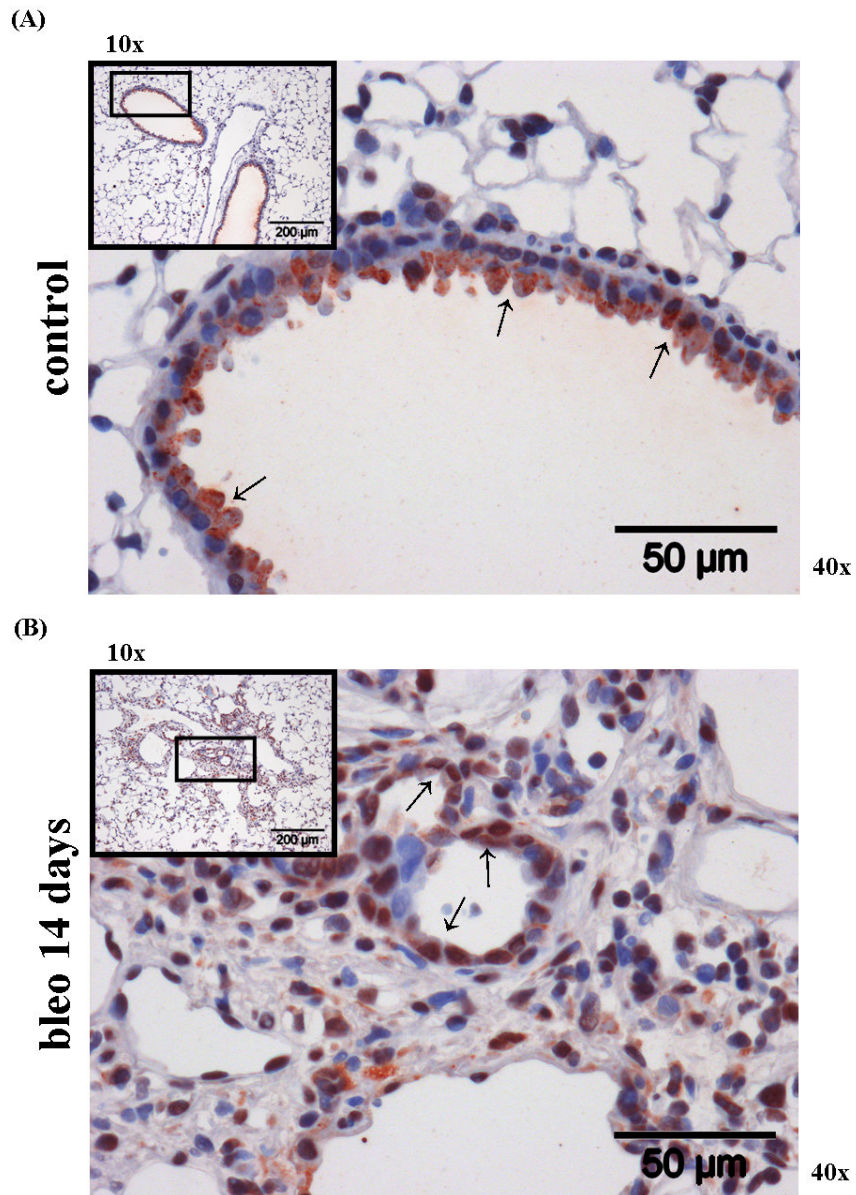
Wnt1

figure 4.8.1: Localisation of Wnt1 in experimental pulmonary fibrosis. Immunohistochemistry (IHC) was performed on tissue sections of (A) saline- and (B) bleomycin-treated mouse lungs 14 days after application, with focus on the bronchial epithelium. Wnt1 staining were representative of two independent sets of three different saline- (upper panel) and bleomycin-treated (lower panel) lung tissue sections, respectively (magnification as indicated). In (A), the arrows representatively indicate cytoplasmic, and sporadic nuclear staining. The arrowhead indicates positive endothelial cells. As depicted in (B), the arrows representatively indicate strong apical staining.



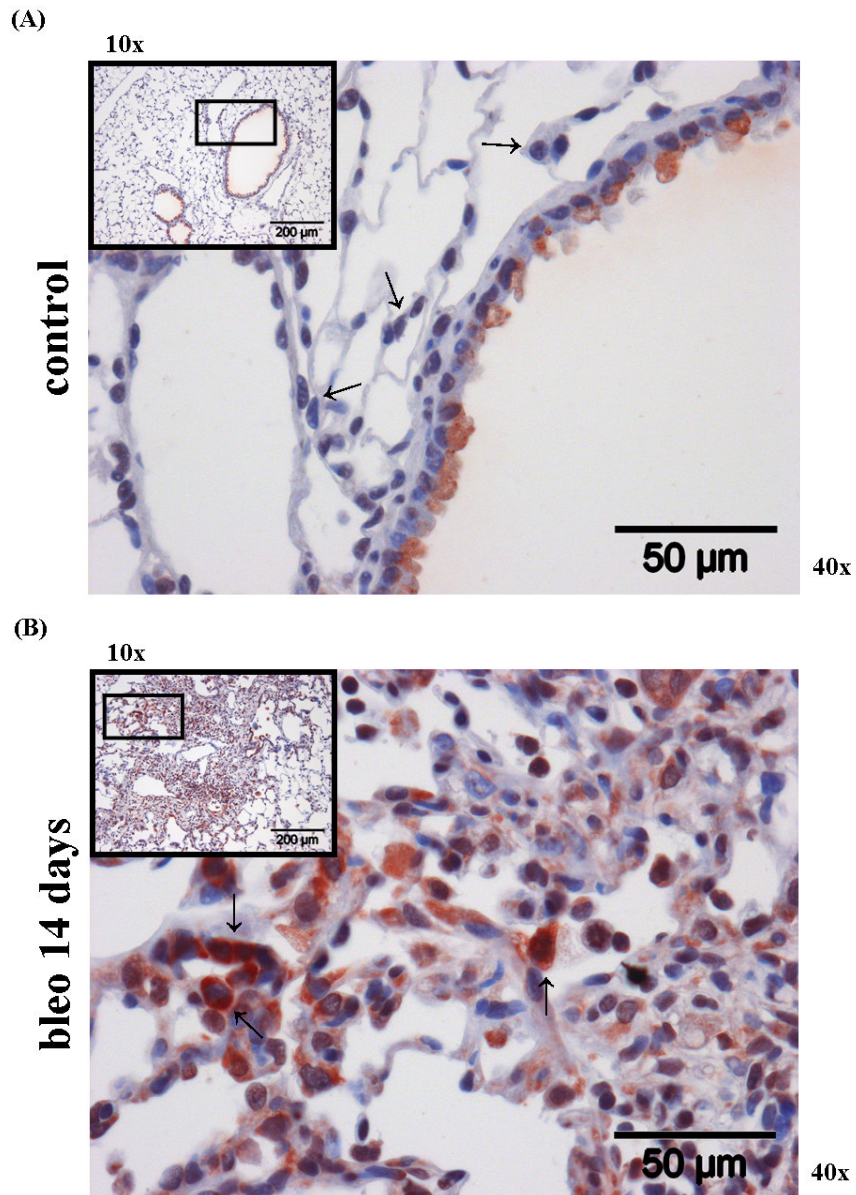
Wnt1

figure 4.8.2: Localisation of Wnt1 in experimental pulmonary fibrosis. Immunohistochemistry (IHC) was performed on tissue sections of (A) saline- and (B) bleomycin-treated mouse lungs 14 days after application, with focus on the alveolar epithelium. Wnt1 staining were representative of two independent sets of three different saline- (upper panel) and bleomycin-treated (lower panel) lung tissue sections, respectively (magnification as indicated). In (A), the arrows representatively indicate nuclear staining. The arrowhead indicates positive endothelial cells. As depicted in (B), the arrows representatively indicate strong staining in ATII cells.



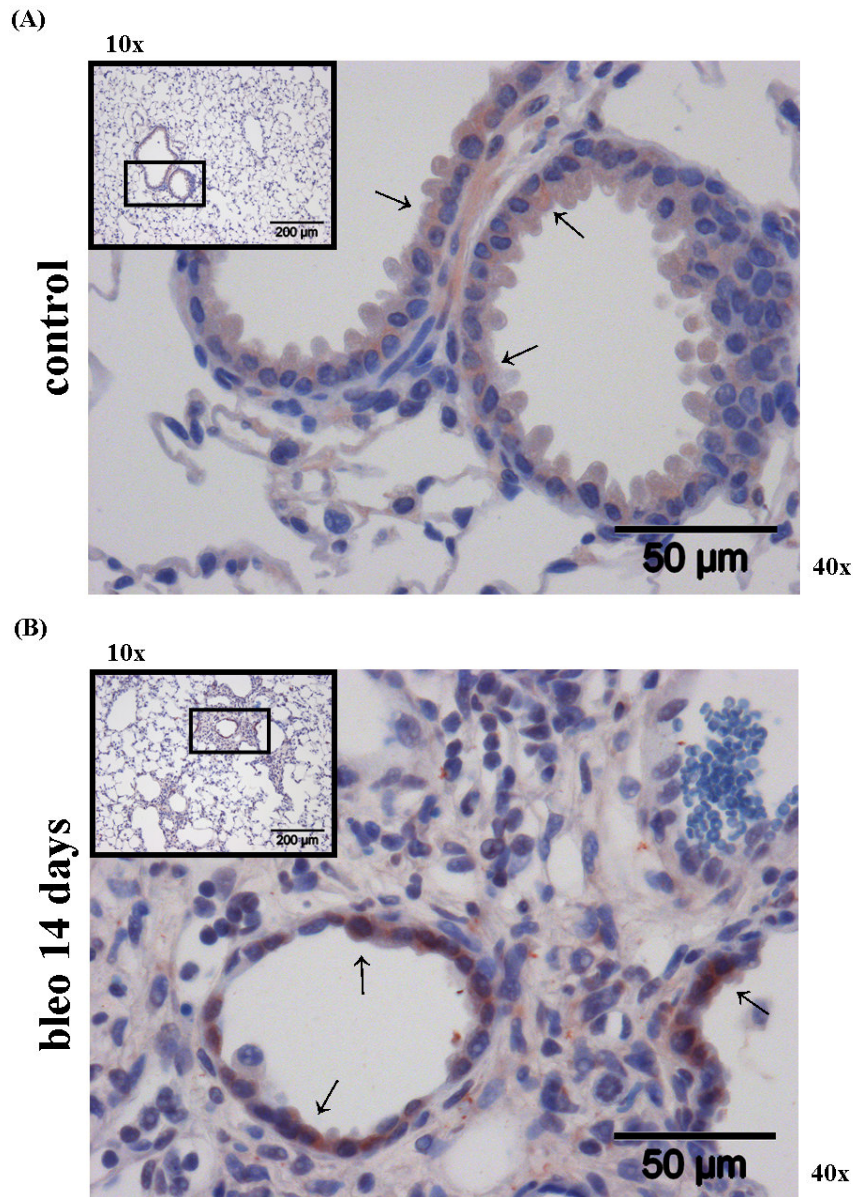
Wnt3a

figure 4.9.1: Localisation of Wnt3a in experimental pulmonary fibrosis. Immunohistochemistry (IHC) was performed on tissue sections of (A) saline- and (B) bleomycin-treated mouse lungs 14 days after application, with focus on the bronchial epithelium. Wnt3a staining were representative of two independent sets of three different saline- (upper panel) and bleomycin-treated (lower panel) lung tissue sections, respectively (magnification as indicated). In (A), the arrows representatively indicate cytoplasmic, and sporadic nuclear staining. As depicted in (B), the arrows representatively indicate strong apical staining.



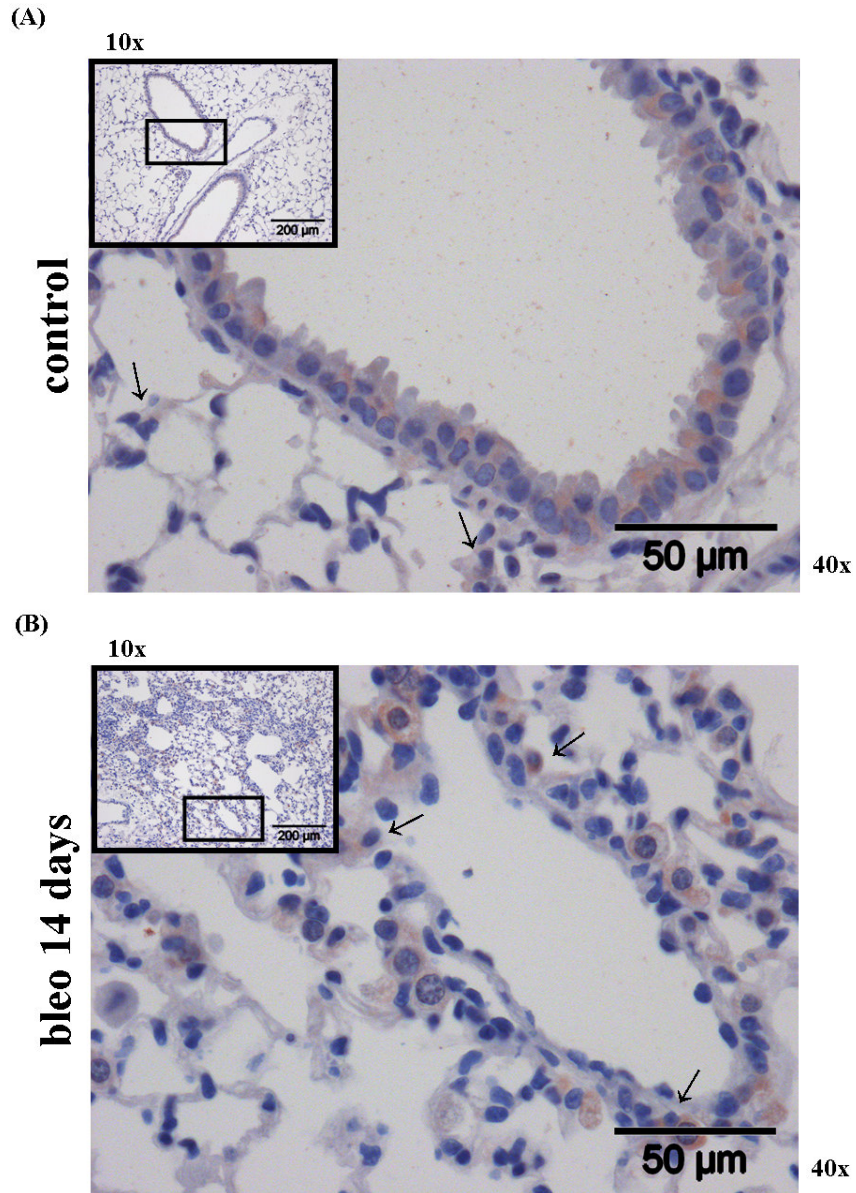
Wnt3a

figure 4.9.2: Localisation of Wnt3a in experimental pulmonary fibrosis. Immunohistochemistry (IHC) was performed on tissue sections of (A) saline- and (B) bleomycin-treated mouse lungs 14 days after application, with focus on the alveolar epithelium. Wnt3a staining were representative of two independent sets of three different saline- (upper panel) and bleomycin-treated (lower panel) lung tissue sections, respectively (magnification as indicated). In (A), the arrows representatively indicate sporadic apical staining. As depicted in (B), the arrows representatively indicate strong cytoplasmic and partly nuclear staining.



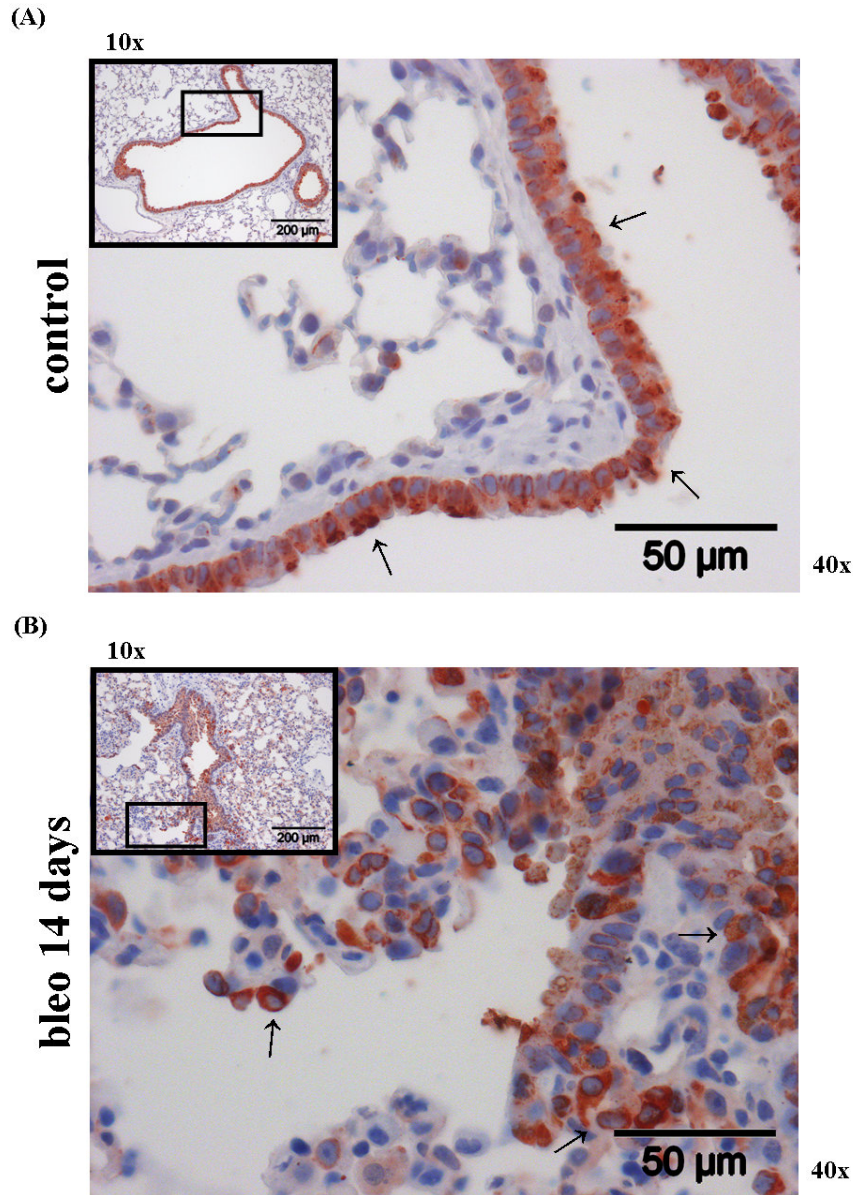
Gsk3β

figure 4.10.1: Localisation of Gsk3β in experimental pulmonary fibrosis. Immunohistochemistry (IHC) was performed on tissue sections of (A) saline- and (B) bleomycin-treated mouse lungs 14 days after application, with focus on the bronchial epithelium. Gsk3β staining were representative of two independent sets of three different saline- (upper panel) and bleomycin-treated (lower panel) lung tissue sections, respectively (magnification as indicated). In (A), the arrows representatively indicate sporadic apical staining. As depicted in (B), the arrows representatively indicate strong cytoplasmic and partly nuclear staining.



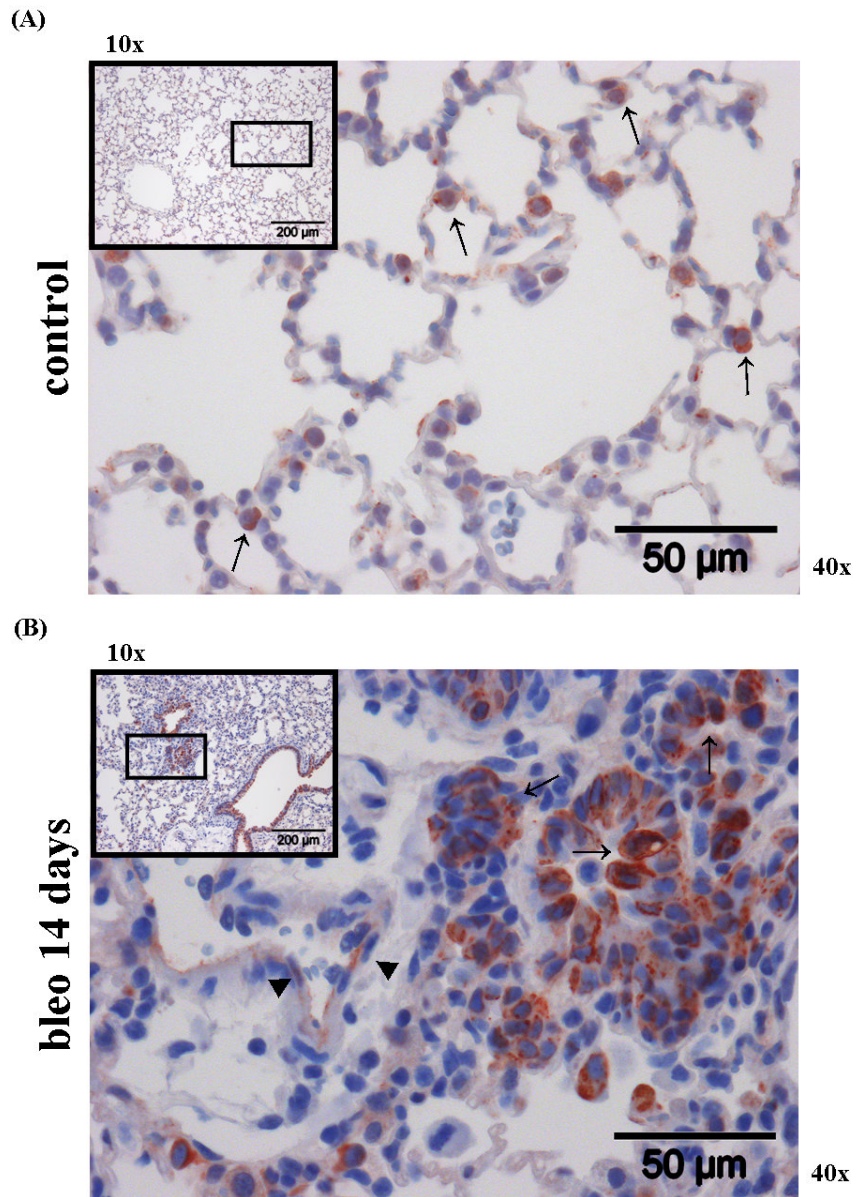
Gsk3β

figure 4.10.2: Localisation of Gsk3β in experimental pulmonary fibrosis. Immunohistochemistry (IHC) was performed on tissue sections of (A) saline- and (B) bleomycin-treated mouse lungs 14 days after application, with focus on the alveolar epithelium. Gsk3β staining were representative of two independent sets of three different saline- (upper panel) and bleomycin-treated (lower panel) lung tissue sections, respectively (magnification as indicated). In (A), the arrows representatively indicate sporadic apical staining. As depicted in (B), the arrows representatively indicate strong cytoplasmic and partly nuclear staining.



Ctnnb1

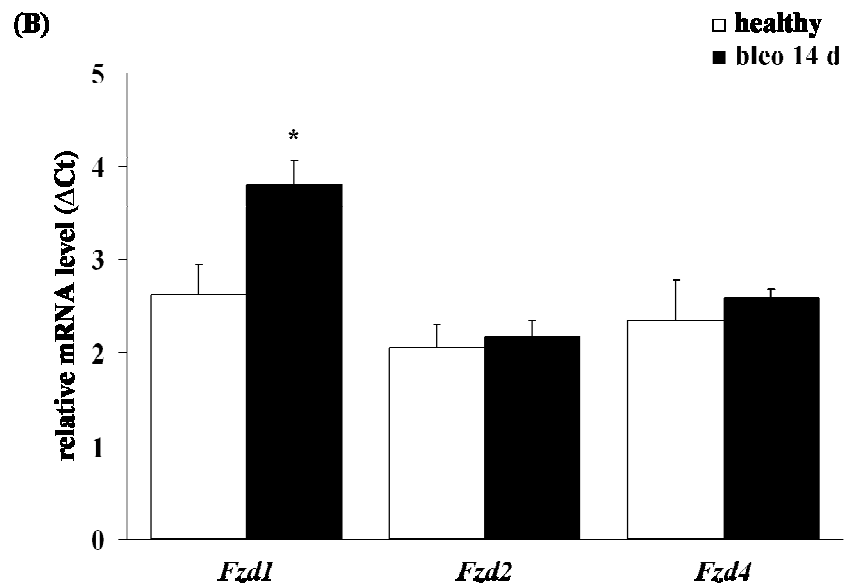
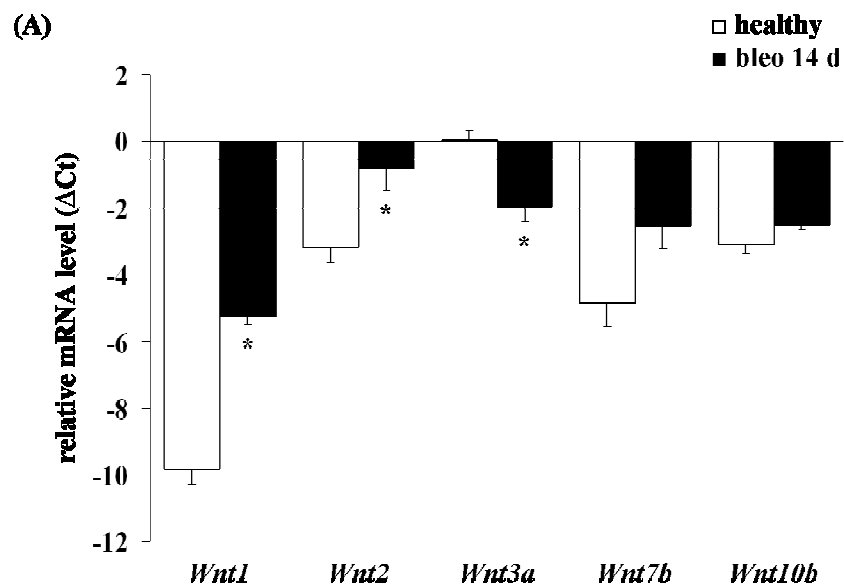
figure 4.11.1: Localisation of Ctnnb1 in experimental pulmonary fibrosis. Immunohistochemistry (IHC) was performed on tissue sections of (A) saline- and (B) bleomycin-treated mouse lungs 14 days after application, with focus on the bronchial epithelium. Ctnnb1 staining were representative of two independent sets of three different saline- (upper panel) and bleomycin-treated (lower panel) lung tissue sections, respectively (magnification as indicated). In (A), the arrows representatively indicate sporadic apical staining. As depicted in (B), the arrows representatively indicate strong cytoplasmic and partly nuclear staining.



CTNNB1

figure 4.11.2: Localisation of Ctnnb1 in experimental pulmonary fibrosis. Immunohistochemistry (IHC) was performed on tissue sections of (A) saline- and (B) bleomycin-treated mouse lungs 14 days after application, with focus on the alveolar epithelium. Ctnnb1 staining were representative of two independent sets of three different saline- (upper panel) and bleomycin-treated (lower panel) lung tissue sections, respectively (magnification as indicated). In (A), the arrows representatively indicated sporadic apical staining. As depicted in (B), the arrows representatively indicated strong cytoplasmic and partly nuclear staining. The arrowheads indicate positive endothelial cells.

To further confirm the epithelial cell-specific localisation, the mRNA expression of canonical WNT/ β -catenin signalling components in ATII cells, isolated from lungs of saline- and bleomycin-treated mice, was investigated. Therefore, ATII cells were obtained from six saline- and bleomycin-treated mice 14 days after application, respectively. In summary, the analysis further confirmed the expression of canonical WNT signalling components in alveolar epithelial cells. More interestingly, in contrast to the data derived from the lung homogenates, an increased expression of most WNT ligands, WNT receptors and intracellular transducers were observed in primary mouse ATII cells isolated from bleomycin-treated lungs.



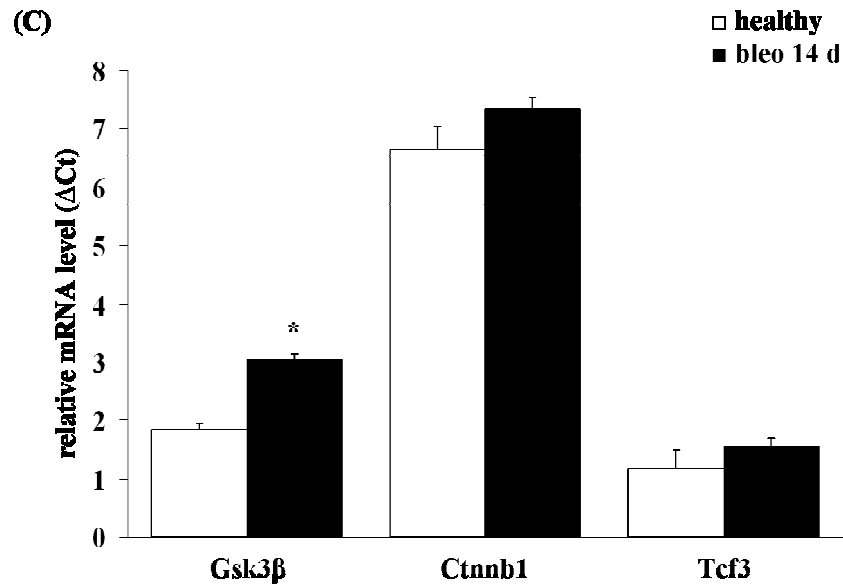


figure 4.12: Gene expression profile of canonical Wnt signalling components in murine alveolar epithelial type II (ATII) cells. The relative messenger ribonucleic acid (mRNA) levels of (A) the Wnt ligands *Wnt1*, *2*, *3a*, *7b* and *10b*, (B) the receptors frizzled *Fzd1*, *2* and *4*, (C) the intracellular signal transducers glycogen synthase kinase *Gsk3β* and β -Catenin (*Ctnb1*), and T-cell-specific transcription factor *Tcf4* were assessed in total lung homogenates of saline- and bleomycin-treated mice 14 days after application by quantitative real time polymerase chain reaction ((q)RT-PCR). Data were presented in a bar graph; plotting the results as ΔC_t ($\Delta C_t = C_t$ reference gene - C_t target gene); statistical significance (p/p-value) was presented as * (* = $p < 0.05$), samples of 6 individual sets of isolations were used ($n = 6$). These data were kindly provided by Dr. Melanie Königshoff.

4.3 Functional analysis of the WNT/ β -catenin signalling pathway

The WNT/ β -catenin signalling pathway was shown to be activated in idiopathic and experimental pulmonary fibrosis; it appeared to be predominantly expressed and localised in alveolar epithelial type II (ATII) cells. In order to investigate the functional relevance of the canonical WNT signalling pathway, potential effects of Wnt3a, a canonical Wnt activator, on gene expression, cell proliferation and protein

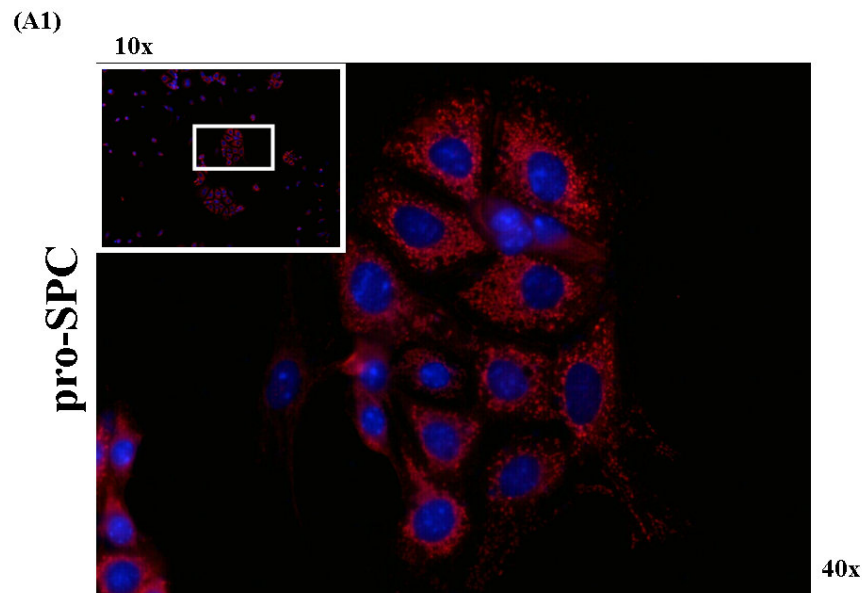
expression, were analysed in isolated primary mouse alveolar epithelial type II (ATII) cells.

4.3.1 Purity and phenotype of primary mouse alveolar epithelial type II (ATII) cells

In order to ensure the availability of exclusively primary mouse alveolar epithelial type II (ATII) cells after the isolation procedure, immunocytochemistry (ICC) was used to analyse the purity and the phenotype of the cells.

Therefore, freshly isolated ATII cells were fixed after attachment for 24 hours and incubated with specific cell marker antibodies (see appendix; table 6.4). As depicted in figure 4.13 (A1 and A2), freshly isolated primary mouse ATII cells showed a purity of greater than 95 %, as most of the cells were immuno-positive for the ATII cell marker pro-surfactant protein C (pro-SPC = red staining), whereas only very few cells stained immuno-positive for the fibroblast cell marker α -smooth muscle actin (Acta2 = green staining).

To investigate the morphology of epithelial cells, immunocytochemistry was performed with specific epithelial cell marker proteins. In figure 4.13 (B) the expression of the specific epithelial marker proteins e-cadherin (Cdh1), zonula occludence protein 1 (Tjp1), and pan-cytokeratin (pan-CK) in these cells was indicative of an epithelial phenotype.



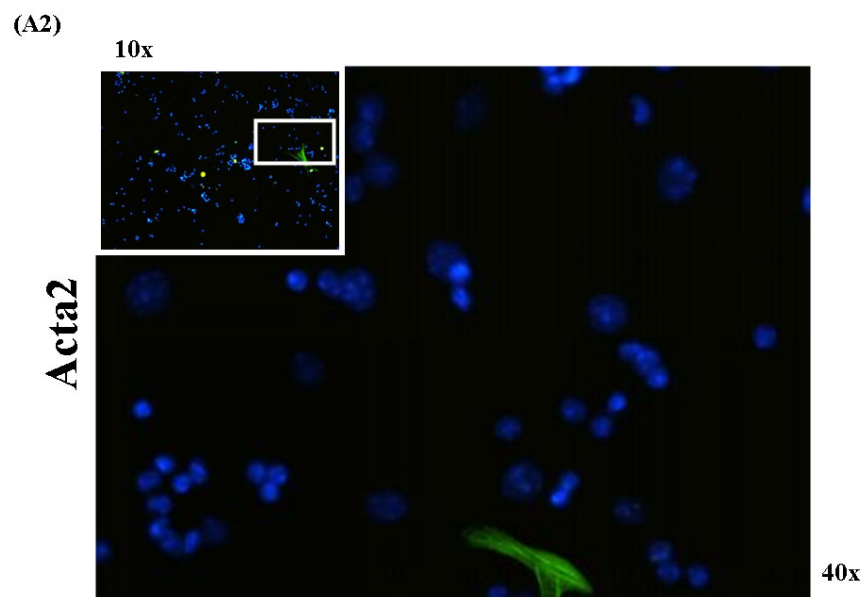
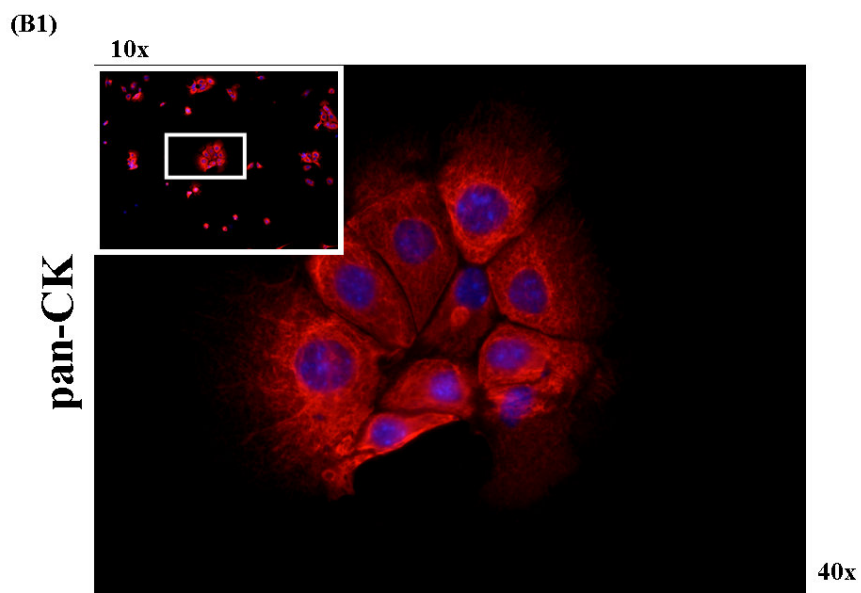


figure 4.13 (A): Purity of primary mouse alveolar epithelial type II (ATII) cells.

Freshly isolated primary mouse alveolar epithelial type II (ATII) cells were fixed after 24 hours of attachment. The expression and localisation of (A1) pro-surfactant protein C (pro-SPC = red staining) and (A2) α -smooth muscle actin (Acta2 = green staining), as evidence for purity, was determined by immunocytochemistry (ICC). Nuclei were visualized by 4'6-diamidino-2-phenylindole (DAPI = blue staining) staining. All stainings were representative of 6 independent sets of freshly isolated primary mouse ATII cells (magnification as indicated).



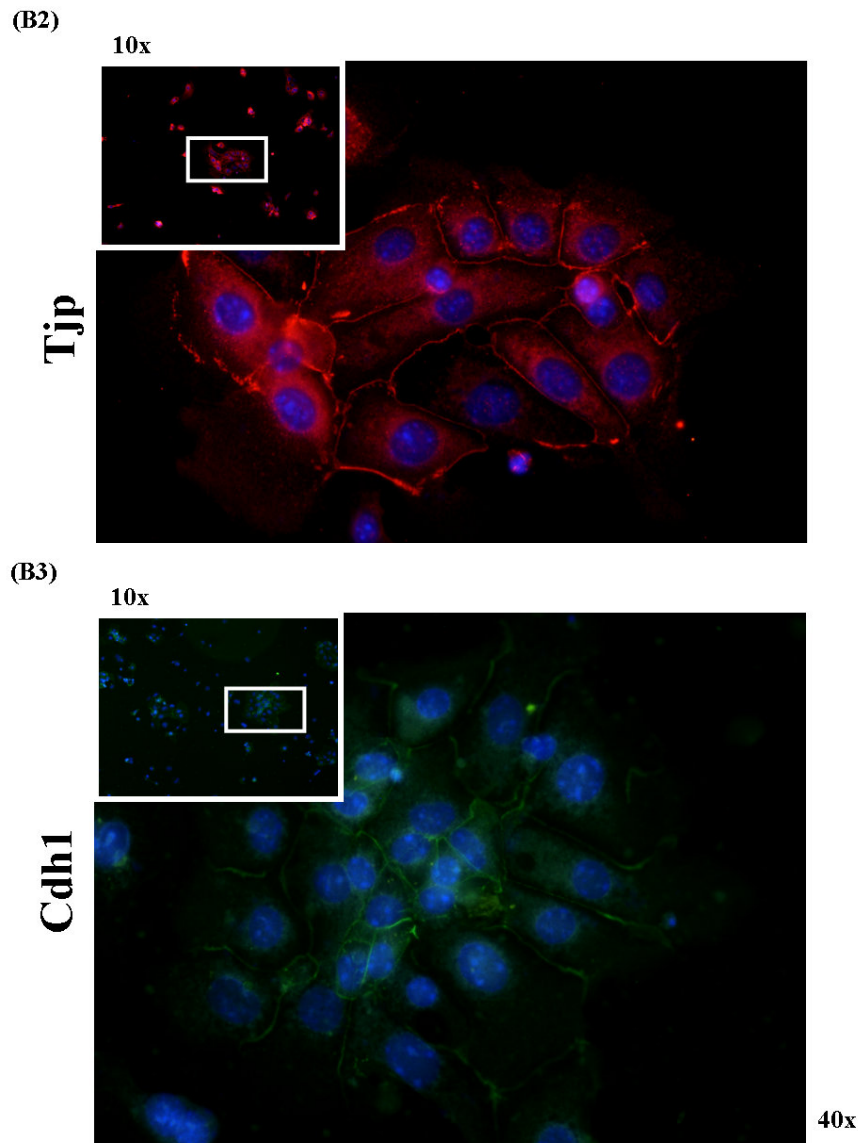


figure 4.13(B): Phenotype of primary mouse alveolar epithelial type II (ATII) cells. Freshly isolated primary mouse alveolar epithelial type II (ATII) cells were fixed after 24 hours of attachment. The expression and localisation of **(B1)** pan-cytokeratin (panCK = red staining), **(B2)** zonula occludence protein 1 (Tjp1 = red staining), and **(B3)** e-cadherin (Cdh1 = green staining), as evidence for an epithelial cellular phenotype, was determined by immunocytochemistry. Nuclei were visualized by 4'6-diamidino-2-phenylindole (DAPI = blue staining) staining. All stainings were representative of 6 independent sets of freshly isolated primary mouse ATII cells (magnification as indicated).

4.3.2 Expression of Wnt3a-induced target genes in primary mouse alveolar epithelial type II (ATII) cells

The expression of the known Wnt target genes *cyclinD1* and *Wisp1* was assessed by (q)RT-PCR. Primary mouse ATII cells were stimulated with Wnt3a (100 ng/ml) for 8 and 24 hours, and unstimulated primary mouse ATII cells at the indicated time-points served as controls. As shown in figure 4.14, Wnt3a treatment led to a significant increase of *cyclinD1* expression after 8 hours as compared to unstimulated cells. Interestingly, *Wisp1* was significantly upregulated only 24 hours after Wnt3a stimulation as compared to unstimulated controls.

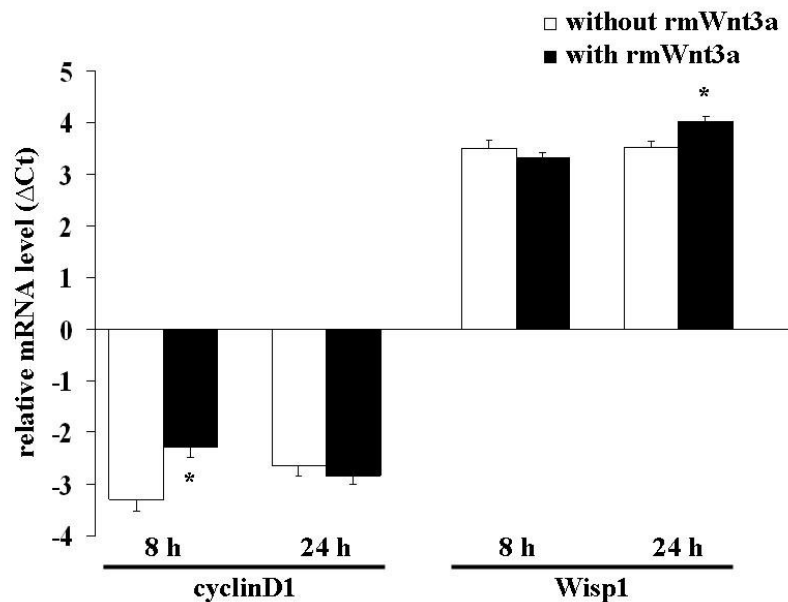
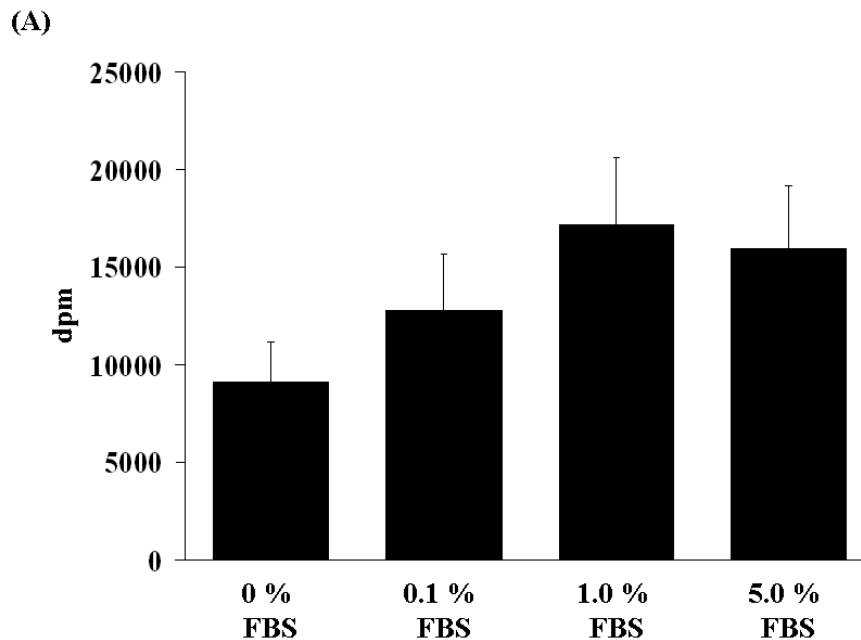


figure 4.14: Messenger RNA (mRNA) expression of Wnt3a-induced target genes of the canonical Wnt/β-catenin signalling pathway in primary mouse alveolar epithelial type II (ATII) cells. The mRNA levels of *cyclinD1* and *Wisp1* were assessed in primary mouse ATII cells by (q)RT-PCR. The cells were stimulated with recombinant mouse Wnt3a protein (rmWnt3a; 100 ng/ml) for 8 and 24 hours; unstimulated cells at the indicated time-points were used as controls. Data were presented in a bar graph; plotting the results as log-fold change (ΔΔCt) of mRNA levels; statistical significance (p/p-value) was presented as * (= p < 0.05), samples of 6 individual sets of isolations were used (n = 6).

4.3.3 Proliferative effects of Wnt3a stimulation on primary mouse alveolar epithelial type II (ATII) cells

An earlier study investigated that Wnt3a stimulation significantly increased proliferation of A549 cells, an epithelial cell line. In contrast, Wnt3a did not affect fibroblast proliferation, clarifying that Wnt ligands have a cell-specific effect on resident lung cells. In order to analyse, whether Wnt3a treatment has an equal effect on primary mouse ATII cell proliferation, the [³H] thymidine proliferation assay was performed. To assess the minimal proliferation rate, without any further stimulation, as well as the adequate survival and growth conditions for primary mouse ATII cells, different fetal bovine serum (FBS) concentrations were used, as shown in figure 4.15 (A). After [³H] thymidine incorporation, results revealed that optimal growth response was present at a minimum serum concentration of 0.1%. Even though growth response was equally present at a serum concentration of 1.0%, the higher serum concentration is inappropriate, as the additional stimulatory effects cannot be excluded.



Subsequently, the effect of recombinant mouse protein Wnt3a on primary mouse ATII cell proliferation was assessed. The cells were stimulated for 21 h with two different concentrations of recombinant mouse protein Wnt3a, namely 50 and 100ng/ml. As depicted in figure 4.15 (B), primary mouse ATII cells demonstrated a significant increase in cell proliferation by WNT3A (both, 50 and 100 ng/ml) treatment as compared to cells in medium supplied with 0.1% FCS, exclusively.

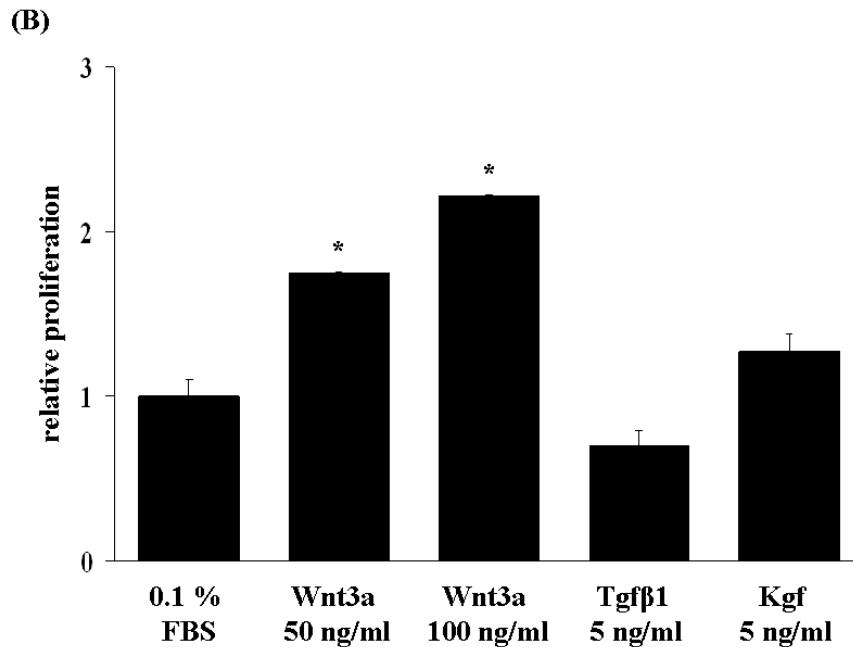


figure 4.15: Proliferative effect induced by Wnt3a in primary mouse alveolar epithelial type II (ATII) cells. (A) To determine the sufficient conditions for optimal proliferation, freshly isolated primary mouse ATII cells were cultured after attachment and synchronisation in the presence of 0%, 0.1%, 1.0% and 5.0% fetal bovine serum (FBS). Data were presented in a scatter diagram in absolute proliferation (dpm) as means \pm standard error of the mean (s.e.m.); statistical significance (p/p-value) was presented as * (= $p < 0.05$), samples of 5 individual sets of isolations were used ($n = 5$). **(B)** Freshly isolated mouse ATII cells were stimulated after attachment and synchronisation with Wnt3a (50 and 100 ng/ml), Tgfβ1 (5 ng/ml) and Kgf (5 ng/ml) in medium supplied with 0.1% FBS. Cells in medium supplied with 0.1% FBS, but without any further stimulation were used as controls. ATII cell proliferation was analysed by [3 H] thymidine incorporation. Data were presented in a

scatter diagram in relative proliferation as means \pm standard error of the mean (s.e.m.); statistical significance (p/p-value) was presented as * (= $p < 0.05$). All experiments were performed three times, each condition in quadruplicates.

The pro-proliferative effect was even more pronounced, than that of the keratinocyte growth factor (Kgf; 5 ng/ml), which was used as a positive control. The transforming growth factor beta 1 (Tgf β 1; 5 ng/ml) had an anti-proliferative effect and was used as a negative control.

4.3.4 Whole genome microarray analysis on Wnt3a-induced primary mouse alveolar epithelial type II (ATII) cells

In order to identify further potential target genes of the canonical Wnt/ β -catenin signalling pathway, whole genome microarray analysis was performed. Therefore, freshly isolated primary mouse ATII cells were cultured according to the protocol and stimulated with recombinant mouse protein Wnt3a for 8 and 24 hours. Time-matched unstimulated cells were used as controls. The expression profile was investigated, comparing mRNA of unstimulated and Wnt3a-stimulated cells at indicated time-points. As shown in figure 4.16 (A and B; left panels), several genes were differentially regulated in Wnt3a-stimulated primary mouse ATII cells at 8 and 24 hours. The volcano plots served as an overview of up- and downregulated genes. The X - axis indicates the log fold change, the Y - axis indicates the ratio. In figure 4.16 (A and B; right panels), red and green indicated increased and decreased gene expression levels, respectively, in Wnt3a-stimulated *versus* unstimulated ATII cells. The heatmaps consisted of columns, representing individual samples, and rows, showing the selected genes. Here, a group of upregulated genes were shown, among the top 50 regulated genes. Amongst other proteins, the ATII cell gene expression profile indicated an enrichment of the mRNAs encoding pro-inflammatory cytokines, especially *IL1 β* and *IL6*, in primary mouse ATII cells. Interestingly, also the upregulation of *Axin2*, *Dkk2* and *Tcf7* specific mRNAs coding, components of the canonical Wnt/ β -catenin signalling pathway, were observed. Differentially expressed transcripts also included genes that have previously been reported to be upregulated in bleomycin-induced lung fibrosis and IPF, including *Spp1* and *Timp1*. A selection of 26 target genes, which are already suggested to play a role in lung fibrosis or which

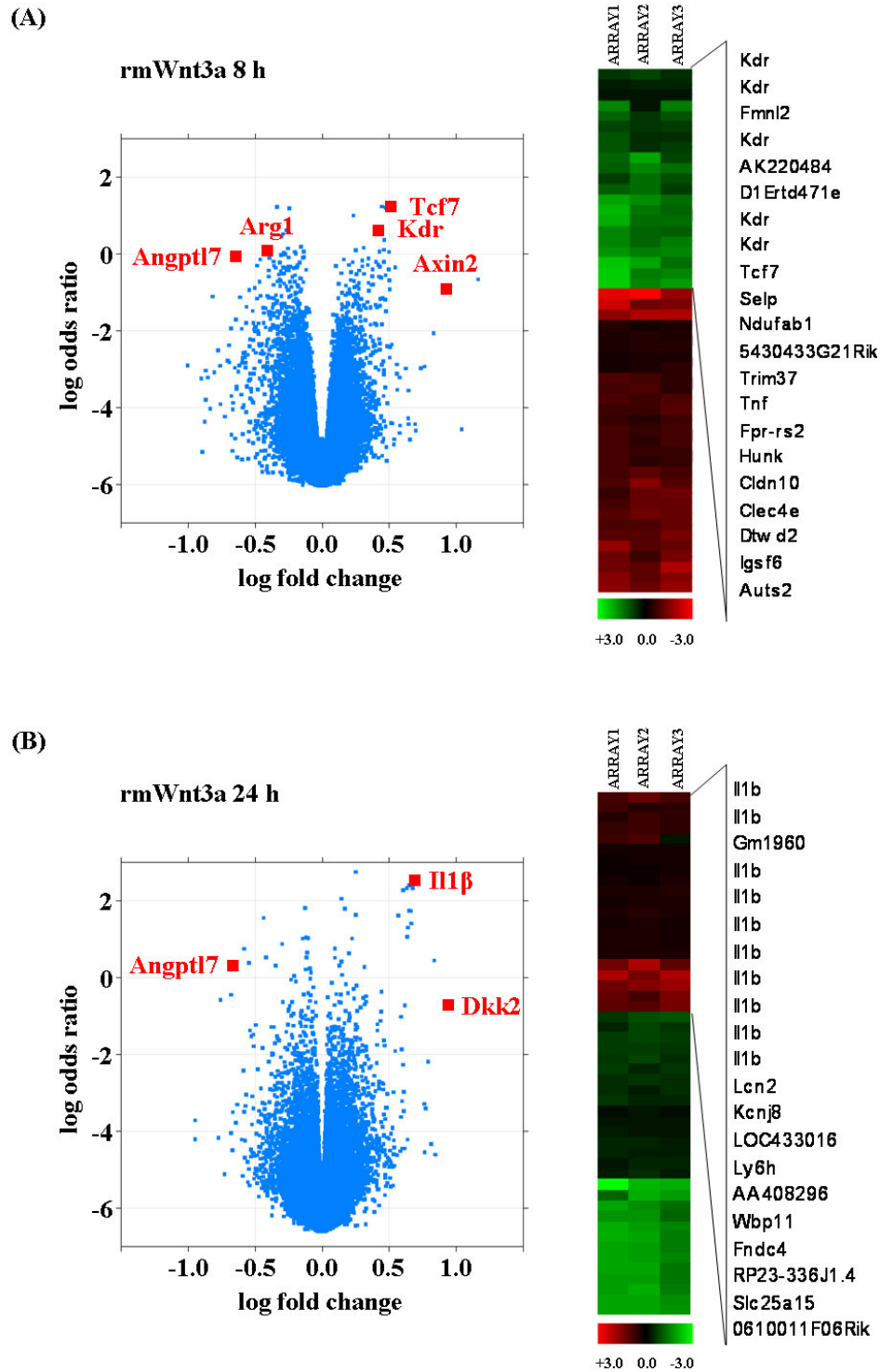
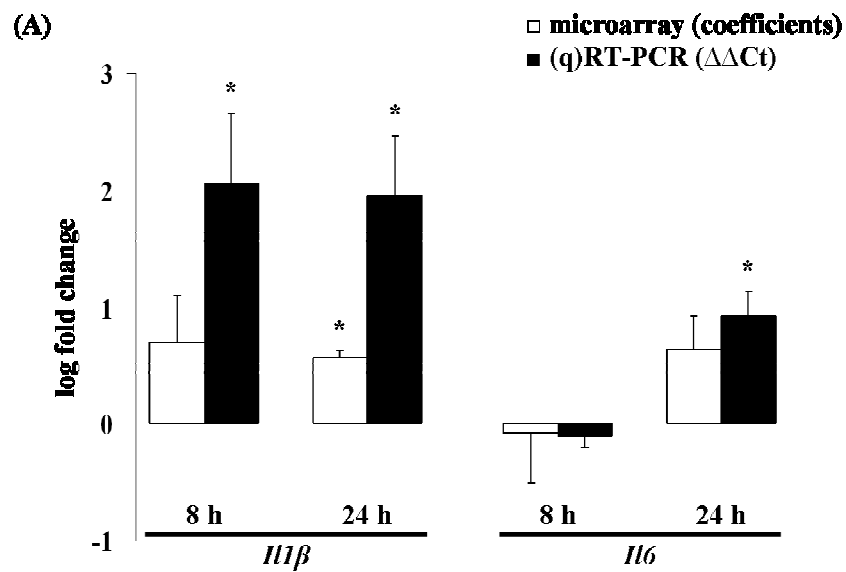


figure 4.16: Whole genome expression analysis on Wnt3a-induced primary mouse alveolar epithelial type II (ATII) cells. Primary mouse alveolar epithelial type II (ATII) cell gene expression profiles were analyzed by whole genome expression analysis using ribonucleic acid (RNA) from isolated ATII cells, upon 8

and 24 hour stimulation with recombinant mouse Wnt3a protein. Volcano plots and heatmaps indicated increased and decreased gene expression levels, respectively, in Wnt3a-stimulated versus unstimulated ATII cells after (A) 8 hours and (B) 24 hours of stimulation. The whole genome microarray was performed and the appropriate data were kindly provided by Marlene Stein and Jochen Wilhelm.

could be of great interest, as they are involved in the canonical WNT signalling pathway, were investigated in more detail (see appendix, table 6.5). To confirm the results of the microarray, the gene expression profiles were further investigated by (q)RT-PCR, using six independent sets of freshly isolated ATII cells, stimulated for 8 and 24 hours.



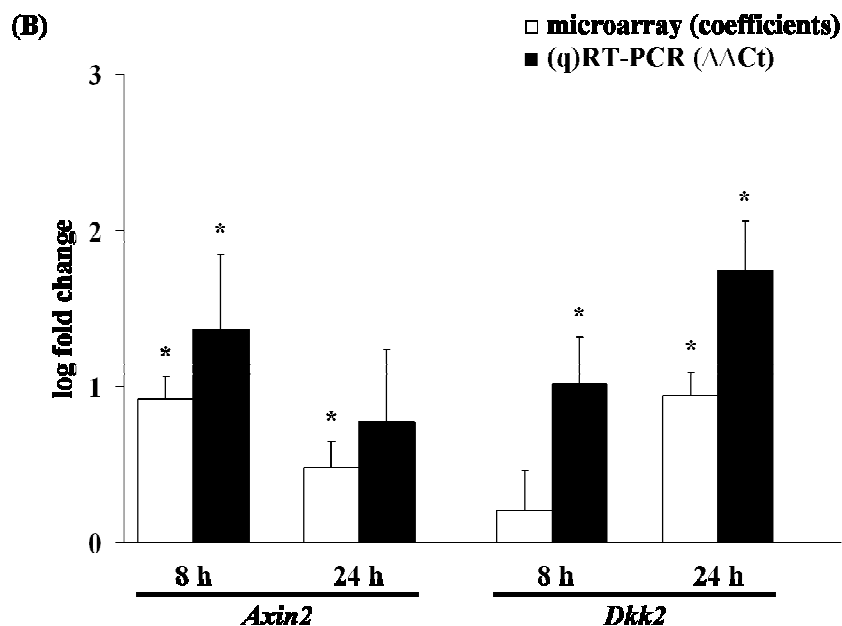


figure 4.17: Messenger RNA (mRNA) expression of potential Wnt3a-induced target genes in primary mouse alveolar epithelial type II (ATII) cells. The confirmation of the microarray results for special selected genes was performed by quantitative real time polymerase chain reaction (q)RT-PCR, using isolated primary mouse alveolar epithelial type II (ATII) cells, stimulated with recombinant mouse protein Wnt3a protein for 8 and 24 hours. The mRNA levels of **(A)** the cytokines, interleukin 1 β (*IL1 β*) and interleukin 6 (*IL6*), as well as of **(B)** axis inhibition protein 2 (*Axin2*) and dickkopf-related protein 2 (*Dkk2*), inhibitors of the canonical Wnt/ β -catenin signalling pathway were assessed. Data were presented in a bar graph; plotting the results as log-fold change ($\Delta\Delta Ct$) of mRNA levels, comparing the microarray results with the (q)RT-PCR results; statistical significance (p/p-value) was presented as * (= p < 0.05), samples of 6 individual isolations were used (n = 6).

Out of 26 selected genes, 20 genes were finally confirmed. In turn, out of these genes, significantly upregulated expression of the cytokines *IL1 β* and *IL6* in Wnt3a-stimulated primary mouse ATII cells were of special interest, as they are known to be relevant in lung fibrosis. As shown in figure 4.17 (A), *IL1 β* mRNA expression level was significantly increased after stimulation with recombinant mouse protein Wnt3a protein for 8 and 24 hours, while *IL6* mRNA expression level was detectable and increased only after 24 hours of stimulation. Equally interesting, as depicted in figure

4.17 (B), the expression of *Axin2*, a cytoplasmic factor of the canonical Wnt/ β -catenin signalling pathway, was significantly upregulated, as well as *Dkk2*, an inhibitor of the canonical Wnt/ β -catenin signalling pathway. The results were plotted as log-fold change ($\Delta\Delta\text{Ct}$) of mRNA levels to compare the results from microarray with the results from (q)RT-PCR.

4.4 Analysis of the novel WNT target genes IL1 β and IL6 *in vitro* and *in vivo*

4.4.1 ELISA analysis for quantification of IL1 β and IL6

The aim was to quantify the secreted protein levels of interleukin 1 β (IL1 β) and interleukin 6 (IL6) in different sample types (supernatants of Wnt3a-stimulated and unstimulated primary mouse ATII cells, conditioned media of primary mouse ATII cells and bronchoalveolar lavage fluids (BALFs), obtained from saline- and bleomycin-treated mice, as well as Wnt3a-treated TOPGAL mice. In addition, BALFs from human transplant donors and IPF patients were also analysed by enzyme-linked immunosorbent assay (ELISA). Interestingly, as shown in figure 4.18 (A) and (B), IL1 β and IL6 were secreted into the supernatants of both, Wnt3a-stimulated and unstimulated (= control) primary mouse ATII cells, respectively. In general, the secreted IL6 protein level in supernatants of primary mouse ATII cells was higher as compared to the secreted IL1 β protein level. However, both interleukins showed similar and significantly enhanced release by primary mouse ATII cells, after stimulation with recombinant mouse protein Wnt3a protein for 24 hours as compared to stimulation for 8 hours.

In figure 4.19, IL1 β and IL6 were present in the conditioned media of primary mouse ATII cells, isolated from saline- and bleomycin-treated mouse lungs after 14 days of application, respectively. In general, the secreted IL6 protein level in conditioned media of primary mouse ATII cells was higher as compared to the secreted IL1 β protein level. However, both interleukins showed significantly enhanced release in conditioned media of primary mouse ATII cells, due to bleomycin treatment.

As depicted in figure 4.20 (A and B), the quantity of IL1 β and IL6 was also determined in bronchoalveolar lavage fluid (BALF) obtained from saline- (= control)

and bleomycin-treated mice, 14 and 21 days after application, and from Wnt reporter mice (TOPGAL), orotracheally treated with Wnt3a. Interestingly, a strong heterogeneity was observed. In figure 4.20 (A), IL1 β protein expression levels were significantly increased in BALFs obtained from bleomycin-treated mice, 14 and 21 days after application, as well as in BALFs obtained from Wnt3a-treated TOPGAL mice as compared to control mice.

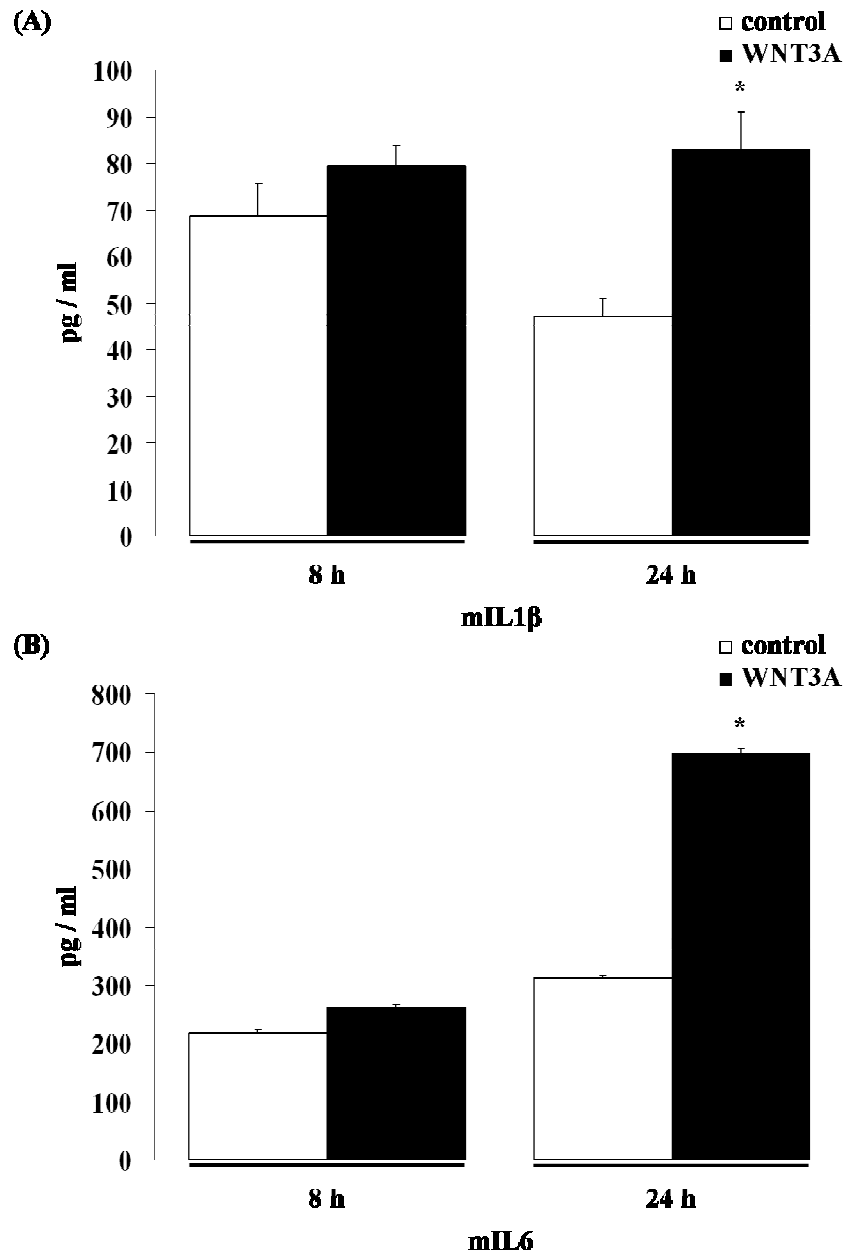


figure 4.18: Protein quantification in supernatants of Wnt3a-stimulated primary mouse alveolar epithelial type II (ATII) cells. The protein levels of (A) interleukin

1 β (IL1 β) and (B) interleukin 6 (IL6), assessed in supernatants of freshly isolated primary mouse alveolar epithelial type II (ATII) cells, stimulated with recombinant mouse protein Wnt3a for 8 and 24 hours (= Wnt3a), as well as unstimulated (= control), were quantified by a mouse-specific IL1 β and IL6 enzyme-linked immunosorbent assay (ELISA), respectively. Data were presented in a scatter diagram in picogramme per millilitre (pg/ml) as means \pm standard error of the mean (s.e.m.); statistical significance (p/p-value) was presented as * (= p < 0.05), 6 individual samples each, were used (n = 6).

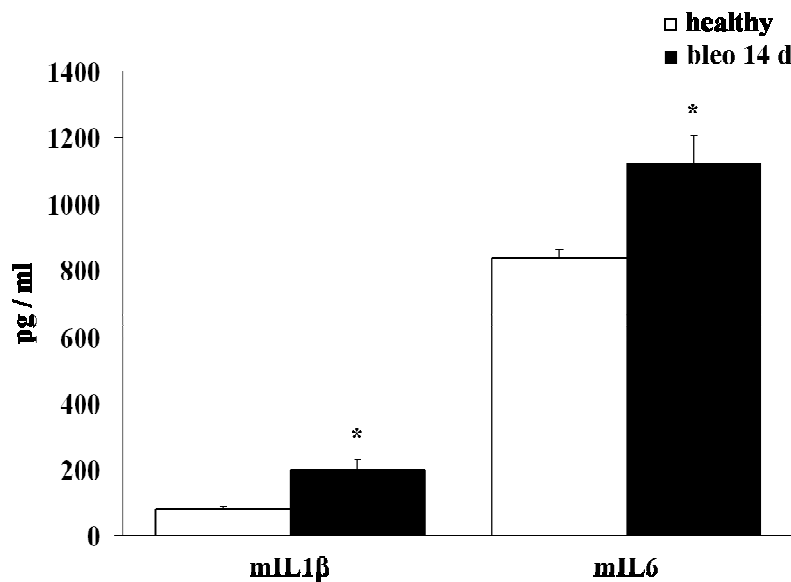


figure 4.19: Protein quantification in the conditioned media from bleomycin-treated primary mouse alveolar epithelial type II (ATII) cells. The protein levels of mouse interleukin 1 β (IL1 β) and interleukin 6 (IL6), assessed in the conditioned media of primary mouse alveolar epithelial type II (ATII) cells, isolated from saline- (= healthy) and bleomycin-treated mouse lungs, 14 days (= bleo 14 d) after application, were quantified by a mouse-specific IL1 β and IL6 enzyme-linked immunosorbent assay (ELISA), respectively. Data were presented in a bar graph in picogramme per millilitre (pg/ml) as means \pm standard error of the mean (s.e.m.); statistical significance (p/p-value) was presented as * (= p < 0.05), 6 individual samples each, were used (n = 6).

Generally, IL6 was detected at lower protein quantity levels than IL1 β in mouse BALFs. In contrast, as depicted in figure 4.20 (B), IL6 showed a significant upregulation in BALFs obtained from Wnt3a-treated TOPGAL mice compared with BALFs obtained from control mice.

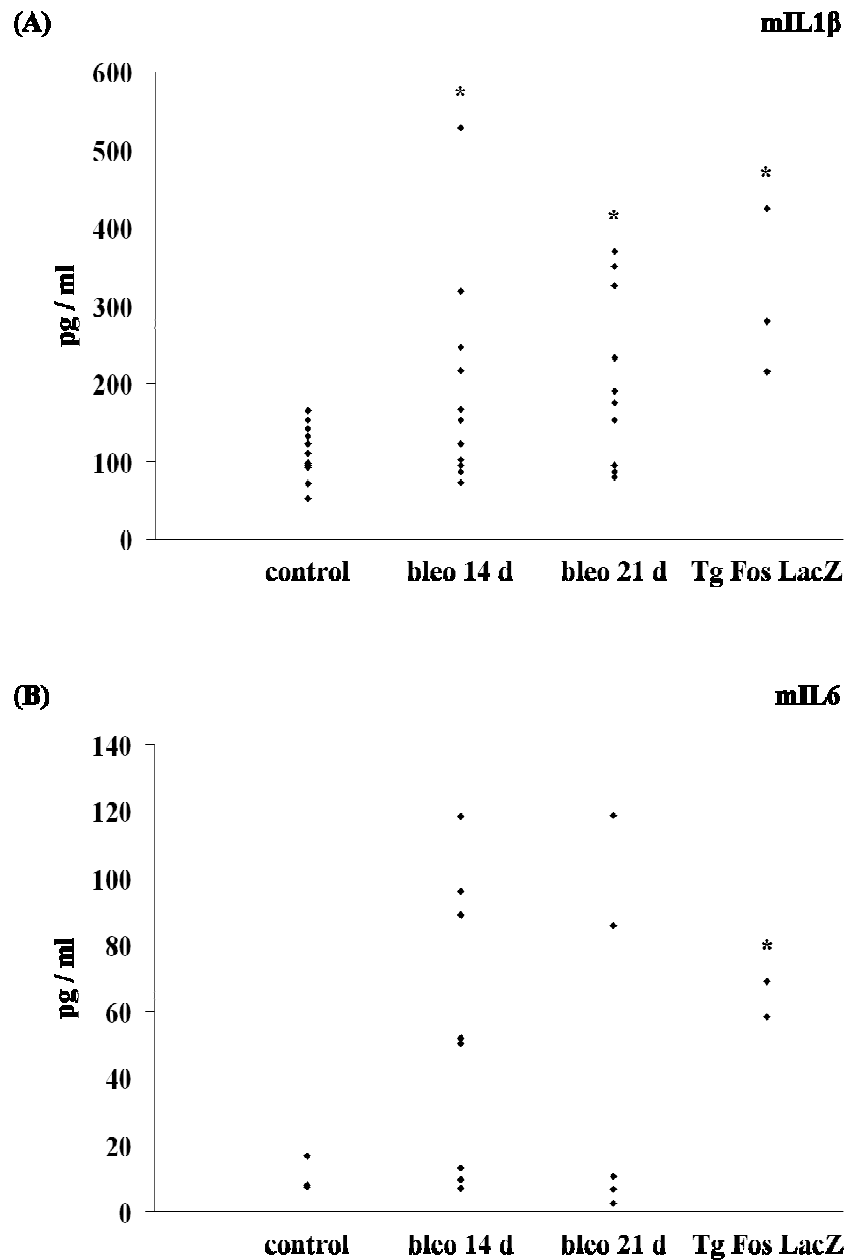


figure 4.20: Protein quantification in mouse bronchoalveolar lavage fluids (BALFs). The protein levels of (A) mouse interleukin 1 β (IL1 β) and (B) mouse

interleukin 6 (IL6), assessed in bronchoalveolar lavage fluids (BALFs) obtained from saline- (= control) and bleomycin-treated mice, 14 and 21 days (= bleo 14 d and 21 d) after application, and transgenic Wnt reporter/Wnt3a-treated TOPGAL (Tg Fos LacZ) mice were quantified by a mouse-specific IL1 β and IL6 enzyme-linked immunosorbent assay (ELISA), respectively. Data were presented in a scatter diagram in picogramme per millilitre (pg/ml) as means \pm standard error of the mean (s.e.m.); statistical significance (p/p-value) was presented as * (= p < 0.05), 12 individual samples each, were used (n = 12).

In figure 4.21, the protein expression level of IL1 β was measured in human samples. Similar protein expression levels of IL1 β were detected in BALFs from transplant donors and IPF patients.

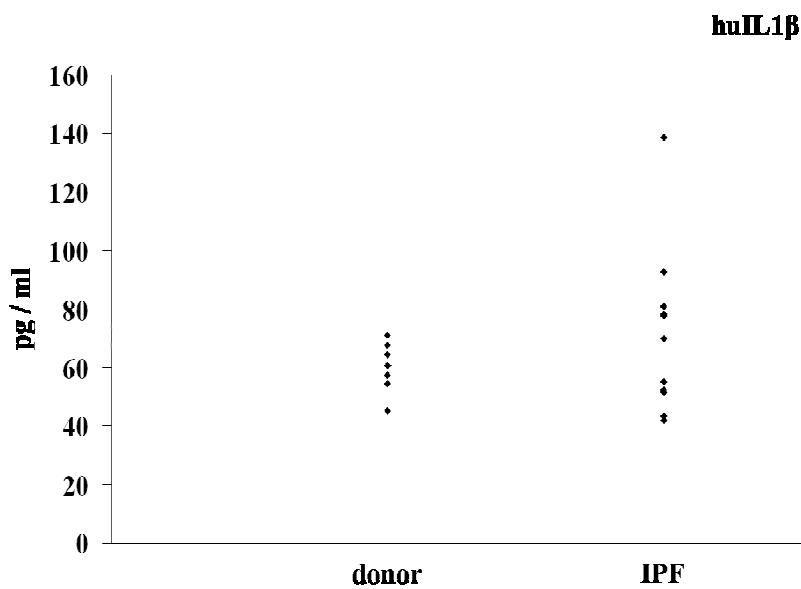


figure 4.21: **Protein quantification in human bronchoalveolar lavage fluids (BALFs).** The protein levels of interleukin 1 β (IL1 β), assessed in bronchoalveolar lavage fluids (BALFs) obtained from transplant donor (= control) and idiopathic pulmonary fibrosis (IPF) patients were quantified by a human interleukin 1 β (huIL1 β) enzyme-linked immunosorbent assay (ELISA). Data were presented in a scatter diagram in picogramme per millilitre (pg/ml) as means \pm standard error of the mean (s.e.m.); 12 individual samples were used (n = 12).

5 DISCUSSION

The current study revealed that the canonical WNT/ β -catenin signalling pathway might at least partially be involved in the pathogenesis of lung fibrosis. It was demonstrated that functional components of WNT/ β -catenin signalling were present in both, experimental murine and human idiopathic pulmonary fibrosis (IPF). The expression and activity of the WNT signalling pathway was mainly detected in bronchial and alveolar epithelium of the lung. In particular, this study identified alveolar epithelial type II (ATII) cells as a major source and target of WNT signalling and demonstrated putative autocrine effects of WNT ligands on cell proliferation and WNT target gene expression in ATII cells. Additionally, it was identified that active WNT/ β -catenin signalling led to an increased expression of proinflammatory cytokines, such as interleukin 1 β (IL1 β) and interleukin 6 (IL6), in ATII cells. The interaction of WNT signalling and IL1 β /IL6 is suggested to possibly play a crucial role in the progression of IPF.

IPF, the most common form of the idiopathic interstitial pneumonias (IIP) in humans, is a progressive and fatal lung disease, which is characterized by distorted lung architecture and severe loss of respiratory function. IPF exhibits a poor prognosis due to unresponsiveness to currently available therapies [24, 36]. Known to be active during developmental processes, the canonical WNT/ β -catenin signalling pathway has been suggested to be reactivated in chronic diseases, which are characterised by pathologic tissue remodelling [82]. In 2006, Douglas and colleagues showed that active WNT/ β -catenin signalling occurs in the fibro-proliferative phase after acute lung inflammation, using a mouse model of oxidant-induced injury. Thus, the WNT signalling pathway is suggested to be involved in lung regeneration after injury [85]. In this respect, the WNT signalling pathway is of special interest.

In recent studies, unbiased microarray screens revealed increased expression levels of several WNT signalling genes, including WNT2 and 5A, FZD6, 7 and 10, and LEF1, in IPF lungs as compared to transplant donor lungs [82, 86]. Most recently, it was demonstrated that canonical WNT signalling induces skin fibrosis. Thus, transgenic mice overexpressing Wnt10b proved to be an activator for the development of dermal

fibrosis, increased collagen deposition, fibroblast activation and myofibroblast accumulation. These new transgenic mice represent a novel animal model, useful for further studies of WNT signalling in fibrosis [87]. In 2003, Chilosì and colleagues reported increased nuclear localisation of β -catenin (CTNNB1) in ATII cells and in interstitial fibroblasts in IPF lungs [78], indicative of active WNT signalling in IPF [79].

In the current study, a comprehensive analysis of the mRNA expression of canonical WNT/ β -catenin signalling components was performed in total lung homogenates from IPF patients and transplant donors, demonstrating different expression of WNT signalling components in IPF lung epithelium. An immunohistochemical analysis revealed particularly bronchial and alveolar epithelium as specific cell types capable of WNT signalling. Several WNT signal pathway components were largely expressed in donor and IPF lung tissue, with increased immunohistochemical staining in bronchial epithelial and hyperplastic ATII cells at sites of bronchiolisation under conditions of IPF. Interestingly, also DKK1, a WNT regulator, was predominantly localised in basal bronchial epithelial cells and in hyperplastic alveolar epithelial cells in IPF, which may be a suitable therapeutic target for IPF [88].

Normally, β -catenin levels are tightly regulated in the developing and healthy adult lung, with low cytoplasmic/nuclear β -catenin [89]. Several studies investigated WNT signalling in lung morphogenesis demonstrating, that a deletion of β -catenin in epithelial cells impairs lung morphogenesis, arrests the differentiation of alveolar epithelial cells and leaves the lung containing mainly conducting airways. Consistently, aberrant activation of β -catenin in epithelial cells of the developing lung causes enlarged air space, atypical expression of ATII cells and goblet cell hyperplasia [61, 90]. In this study only rare nuclear staining of β -catenin was observed; however, Chilosì and colleagues identified nuclear localisation of β -catenin by immunohistochemistry [78]. Recent investigations have provided evidence supporting the sparse nuclear localisation of β -catenin, as it plays a key role in canonical WNT signalling and only a minority of the intracellular β -catenin content in epithelial cells is responsible for WNT signalling, while the majority of β -catenin molecules is present at the localisation of cell-cell contacts [91, 92]. Although nuclear β -catenin expression is difficult to determine in general, different tissue preparation techniques or antibodies used for IHC could also be responsible for the observed

differences. It was shown that *in vivo* constitutive β -catenin signalling is not exhibited in adult and healthy ATII cells, but rather, this pathway is activated during lung injury, known to promote alveolar epithelial cell survival, migration, and differentiation towards an ATI-like cell phenotype. Accordingly, these results suggested that ATII cells may function as facultative progenitor cells [93].

In general, it was evident that β -catenin-mediated WNT signalling is central to mechanisms of lung healing in stem cell maintenance, as well as in several diseases like fibrosis and cancer. In detail, β -catenin signalling is known to stimulate cell fate, migration, differentiation, wound closure and tissue remodelling, as well as tissue destruction through several downstream mediators like MMPs, IL1 β , IL6 or TGF- β . Furthermore, β -catenin, an essential mediator of the canonical WNT signalling pathway, promotes the expression of cyclinD1, which additionally indicates cell proliferation [94]. Most recently, Kim and colleagues [95] observed that the use of β -catenin siRNA was able to block the WNT/ β -catenin pathway. While Henderson and his working group [96] inhibited the WNT pathway at the nuclear transcription level, in this study the effector molecule was inhibited at the cytoplasm level. Thereby, intratracheal instillation of β -catenin siRNA was utilised, which selectively and effectively inhibited β -catenin and reduced TGF- β expression. Bleomycin-induced pulmonary fibrosis was attenuated as an outcome of this. These findings reconfirmed that using specific siRNA to target WNT/ β -catenin signalling, may be a safe and effective therapeutic approach in the treatment of IPF. However, a noninvasive procedure for intrapulmonary delivery of aerosolized siRNA poses a major challenge [95]. It was shown in former studies that the use of siRNA to block specific key molecules by gene silencing has significant effects. There have been several preclinical and clinical trials for siRNA treatment in various lung diseases [97].

In this study, functional WNT signalling in IPF was further assessed at the protein level. Increased phosphorylation of LRP6 and GSK3 β , combined with increased expression of total β -catenin in total lung homogenates of IPF patients as compared to transplant donors, indicates activation of the WNT/ β -catenin signalling pathway. Recently it was demonstrated that increased phosphorylation of LRP6 and GSK3 β are the most sensitive indicators of WNT activity in tissue sections [98, 99]. Additionally, an earlier study showed that gene expression analysis of WNT signalling components in primary human ATII cells from IPF patients further corroborated the results [100].

WNT1, however was not regulated in the freshly isolated primary ATII cells, but in the lung homogenates from IPF patients. Therefore, other cell types, such as endothelial cells or bronchial smooth muscle cells may serve as possible sources of WNT1 expression in IPF.

Subsequently, the WNT expression and activity were assessed in an experimental model of lung fibrosis. Different models of pulmonary fibrosis have been developed over the years. However, it is not possible to display all features of IPF, especially the progressive and irreversible nature of this disease [101]. The bleomycin-induced mouse model of experimental lung fibrosis, a well-studied model of IPF, is generally used to study the pathogenetic mechanisms of this disease. As a single intratracheal administration of bleomycin, an anti-neoplastic agent, induces peribronchial fibrosis in the mouse, this condition comparatively reproduces the histological features of IPF in humans [102]. The instillation of bleomycin is easy to handle, reproducible and easily available. Overall, the model of bleomycin-induced pulmonary fibrosis is widely accepted to investigate the molecular mechanisms *in vivo* and to identify new targets for medication. However, this model has its limits, as bleomycin-induced fibrosis is reversible, and as such, has to be carefully compared with IPF [101].

To further elucidate whether WNT/ β -catenin activation is also present in experimental lung fibrosis, a comprehensive analysis was performed by qRT-PCR. The current study shows the occurrence of essential WNT/ β -catenin signalling components in the mouse lung, and regulation thereof in ATII cells. These findings are in agreement with the results observed in IPF and donor transplant tissue, suggesting ATII cells as target cells for expression of canonical WNT signalling components. A recent study has demonstrated that mice treated with freshly isolated primary ATII cells, by intratracheal instillation, show reduced manifestations of bleomycin-induced pulmonary fibrosis [103]. Immunohistochemical analysis confirmed these results, showing enhanced staining of alveolar epithelial cells in bleomycin-treated mouse lungs compared with saline-treated mouse lungs. Additionally, in 2009, Liu and colleagues reported increased nuclear localisation of β -catenin in epithelial cells of remodelled and fibrotic lung areas, indicating active WNT signalling in bleomycin-induced pulmonary fibrosis [104]. Importantly, a recent study used TOPGAL reporter mice to localise the activation of the WNT/ β -catenin pathway *in vivo* in experimental

lung fibrosis. Accordingly, mice were treated orotracheally with either recombinant Wnt3a to demonstrate the capability of the lung to activate WNT/ β -catenin signalling or with bleomycin to induce lung fibrosis. It has been shown that bronchial and alveolar epithelial cells stained for β -galactosidase (β -GAL), in response to Wnt3a or bleomycin treatment [39]. WNT ligands are mainly secreted by lung epithelial cells, indicating that WNT signalling in the adult lung initiates from the epithelium and may act mainly in an autocrine fashion on epithelial cells in the early phase of lung fibrosis development. Liu and colleagues observed that WNT/ β -catenin signalling is activated in murine bleomycin-induced lung fibrosis. Accordingly, target genes like cyclinD1, Mmp7, and Tgf β were expressed and localised in bleomycin-treated transgenic Wnt reporter mice [104]. Recently, another study reconfirmed that bleomycin exposure induces aberrant activation of Wnt/ β -catenin signalling. Additionally, it was demonstrated that administration of ICG-001, a small molecule, which inhibits T-cell factor/ β -catenin transcription, selectively blocks the β -catenin/CBP interaction and with it reduces the expression of WNT target genes. The administration of ICG-001 concurrent with bleomycin not only prevented, but attenuated and reversed established pulmonary fibrosis, enhanced tissue repair and significantly improved survival. As canonical WNT signalling is known to be of particular importance in the pathogenesis of IPF, the selective blockade of the pathway displays a further potential therapeutic approach [96].

In sum, increased WNT/ β -catenin signalling occurs at sites of alveolar epithelial cell injury and hyperplasia in response to bleomycin, underlining the impact of this pathway on impaired alveolar repair in the progress of the disease. Thus, activation of WNT signalling may be important in the course of IPF.

In the present study, the autocrine effects of WNT signalling, particularly the role of WNT signalling on ATII cell proliferation, was analysed. The importance of ATII cell proliferation in lung fibrosis has been demonstrated in experimental as well as human idiopathic fibrosis. ATII cells from bleomycin-treated mice reveal a significant increase in cell proliferation compared with ATII cells from saline-treated control mice. These findings point out that initial lung injury may lead to ATII cell proliferation, which represents an important pathomechanism in experimental lung fibrosis [39]. Interestingly, a recent study showed that higher concentrations of DKK1 led to a reduction of WNT3A-induced effects, while no significant effect on epithelial

cell proliferation was observed after stimulation of human bronchial and epithelial cell lines with DKK1 alone [88]. The dose-dependent exertion of DKK1 can attenuate WNT signalling effects, and therefore may act as a potential therapeutic agent.

Epithelial restitution involves acute inflammatory response, survival, apoptosis, proliferation and migration of cells to restore cell numbers and differentiation to recover function. But regional differences within the lung when coupled with persistent injury may contribute to the pathology of several diseases. Abnormalities in these epithelial cell functions contribute to the pathogenesis of IPF [36, 94]. Active WNT signalling is known to cause epithelial cell hyperplasia in non-pulmonary epithelia. Therefore, WNT signalling may be a mediator for ATII cell hyperplasia and increased bronchial epithelial cell proliferation in IPF [44].

WNT3A was used in this study to assess the functional effects of canonical WNT signalling in epithelial cells. Although WNT3A was the only ligand, which was not upregulated in IPF, several in vitro studies reported WNT3A as a potent inducer of WNT/ β -catenin signalling [105], which is also recognized as the prototypic WNT ligand for in vitro stimulations [42]. It was demonstrated, using a TCF/LEF-driven reporter gene assay that WNT3A, but not WNT7A, initiates a potent canonical WNT/ β -catenin response [100]. A recent study revealed that WNT3A increased levels of N-cadherin, α -catenin and β -catenin in primary cultured chondrocytes. In addition, WNT3A caused a significant translocation of β -catenin to the nucleus and increased the transcriptional activity of the β -catenin-TCF/LEF complex [106]. Importantly, WNT3A belongs to one of the few WNT ligands, which is available in active and recombinant form. Other WNT ligands used in in vitro studies, such as WNT1, are commonly either overexpressed by viral transduction, or supplied in the form of conditioned media harvested from WNT1 overexpressing cell lines [107, 108]. The current study demonstrates that stimulation with the canonical murine WNT ligand Wnt3a leads to a significant increase in ATII cell proliferation. ATII cells are generally considered to be the facultative progenitor cells for the recovery of the pneumocyte pools, with the capability to differentiate into ATI cells following lung injury. However, it should be pointed out that the evidence in support of the role of ATII cells as progenitors is based in part on earlier studies showing increased ATII cell proliferation following injury and the incorporation of [³H]-thymidine in ATII cells [94]. In the lung, the two most abundant epithelial cell types are responsible for

forming the lung air barrier. The ATI cell is distinguished by its flattened shape and large surface area, which presumably facilitates the diffusion of oxygen and carbon dioxide. The ATII cell produces surfactants, which reduce surface tension, among other functions; given the number of alveoli and their extensive surface area [109-111]. These data are in accordance with studies, reporting induction of proliferation in neural progenitor cells in response to WNT3A [112]. In addition, these results have been confirmed in A549 lung epithelial cells, showing a strong increase of cell count, upon WNT3A stimulation [100]. This study focused on canonical WNT signalling. Interestingly, a recent study showed increased expression of WNT5A on mRNA and protein levels in fibroblasts isolated from UIP lung tissue compared with normal fibroblasts, pointing to a difference in canonical and non-canonical WNT signalling pathway. WNT5A was identified as a regulator of fibroblast proliferation [86]. These observations suggest that the secretion and function of WNT ligands occur in a cell-specific manner.

Additionally, potential target genes of the WNT/ β -catenin signalling pathway in ATII cells were identified in this study using whole genome microarray analysis. Several other study groups have observed active Wnt/ β -catenin signalling and increased expression of pathway components by placing primary ATII cells in culture [113, 114]. Initially, it was investigated that primary mouse ATII cells were responsive to Wnt3a stimulation as they expressed known WNT target genes, such as cyclinD1 and Wnt1-inducible signalling protein 1 (Wisp1). WISP1, which belongs to the CCN family of growth factors, was identified as a direct target gene of the WNT/ β -catenin signalling pathway, having anti-apoptotic and proliferative effects on epithelial and mesenchymal cells [115, 116]. Interestingly, WISP1 has been recently identified to play a crucial role in experimental and human pulmonary fibrosis. Increased mRNA and protein expression levels of WISP1 were observed in ATII cells from IPF lungs compared with ATII cells from transplant donor lungs. Furthermore, autocrine effects of WISP1 were reported, leading to ATII cell hyperplasia and expression of profibrotic cytokines [39]. In addition, MMP7, a known key mediator of pulmonary fibrosis and found on the surface of lung epithelial cells, is one of several MMPs that activate TGF- β . To come full circle, TGF- β has been identified as a “master switch” in the induction of EMT in several tissues including the lung, and, specifically, together with β -catenin, in ATII cells, which reconfirms the crucial role of WNT/ β -

catenin signalling in IPF. This activation directly or indirectly stimulates many of the proinflammatory cytokines, like IL1 β , that participate in inflammation-mediated tissue destruction and elaboration of ECM [94]. In spite of these facts, the MMP expression levels in this study were unchanged.

Normally, the WNT signalling system is tightly controlled in a spatiotemporal manner by different secreted WNT regulators. The unbiased microarray revealed increased expression levels of the WNT regulators Axin2 and dickkopf2 (Dkk2) have been observed in Wnt3a-stimulated ATII cells. Axin2, which is the human homologue of mouse conductin and rat axil, is known to be a component of WNT signalling, which directly interacts with β -catenin, GSK3 β and APC to regulate phosphorylation and stability of β -catenin and is implicated in downregulation of WNT signalling. Overexpression of Axin destabilises β -catenin, induced by active WNT signalling and therefore acts in a negative feedback loop [117, 118]. Recent studies indicated that isolated and cultured ATII cells may recapitulate key aspects of an *in vivo* response to alveolar lung injury. Interestingly, Axin2 expression was detected in ATII cells of saline- treated control mice, raising suspicion that a low level of WNT/ β -catenin signalling is present in a distinct cell population [93]. Among the dickkopf (Dkk) family, four different Dkk proteins (Dkk1-4) have been discovered, which share conserved cysteine-rich domains. Dkk2, an extracellular protein, belongs to the group of WNT regulators, which modulates WNT signalling by binding to the WNT binding domain of LRP6. Dkk2 can function either as an activator or inhibitor of WNT signalling, depending on its cellular context and the availability of WNT and co-receptors. Additionally, Dkk proteins are expressed in response to active WNT/ β -catenin signalling and bind with high affinity to a second class of receptors, termed Kremen (Krm). The complex formation of DKK, KRM, and LRP6 is thought to lead to endocytosis of the whole receptor complex, which ultimately potentiates the ability of DKK to regulate and block WNT signalling [119-121]. Most recently, a study demonstrated altered expression of WNT regulators in IPF. In whole lung homogenates from IPF patients increased expression of DKK1, DKK4 and KRM1 was detected. In addition, DKK1 was expressed with a significantly increased amount in BALF of IPF patients.

These observations suggested that DKK proteins may be crucial for lung epithelial cell injury and repair mechanisms in IPF. Further studies are needed to elucidate the effects of DKK proteins on different cell types to reveal the potential therapeutic

capability in IPF [88]. Recent studies demonstrated that the blockade of the WNT signalling pathway, using recombinant DKK proteins, inhibited renal and liver fibrosis [77, 122].

In this context, recent studies showed that aberrant WNT/ β -catenin signalling is also linked to the pathogenesis of renal fibrosis and that blockage of the signal transduction leads to intervention of disease progression. Certain qualities of some currently available drugs have modulating effects on the signalling pathway [123]. One aim would be to develop orally active WNT inhibitors, providing a potentially important pharmacological resource for further investigation of the WNT/ β -catenin signalling, as well as offering a possible novel therapeutic target in pulmonary fibrosis.

Soluble factors, like growth factors (TGF- β , KGF), cytokines (IL1 β , IL6, IL8, IL-13), chemokines (MCP-1), prostaglandins (PGE2) and matrix components participate in epithelial repair [94]. In addition, the microarray screen in this study identified interleukin1 β (IL1 β) and interleukin (IL6) 6 as novel WNT target genes. Of all genes differentially expressed in Wnt3a-stimulated murine ATII cells, this study focused on the cytokines IL1 β and IL6, for the following reasons: First, a study from Kolb and colleagues showed that IL1 β plays a crucial role in the development of experimental pulmonary fibrosis [37]. A recombinant replication-deficient adenovirus vector was used to transfer and overexpress the gene for human IL1 β in epithelial cells of rodent lungs. The extended expression of IL1 β leads to acute alveolar injury, subsequently inducing TGF- β expression and severe progressive lung fibrosis. Matrix deposition and fibroblast foci appeared similar to those seen in human pulmonary fibrosis. Additionally, a significant accumulation of extracellular collagen and fibronectin was observed. IL1 β is known to directly induce acute and chronic inflammation, enlargement of distal airspaces, and airway fibrosis in the adult mouse [124] and is suggested to be a therapeutic target in diseases associated with fibrosis and tissue remodelling, such as IPF. Second, it has been reported that IL1 β is produced in injured and apoptotic lung epithelial cells upon bleomycin administration. For optimal IL1 β production, autocrine or paracrine mechanisms are discussed that amplify the response. IL1 β is known to stimulate the induction of other pro-inflammatory cytokines. Accordingly, significantly increased concentrations of IL6 and TNF α were observed in bronchoalveolar lavage fluid (BALF) from treated rodents [37, 125].

Third, IL6 is known to be involved in the pathogenesis of various inflammatory diseases. Lung pathology after bleomycin exposure showed significant fibrotic changes with increased collagen content in IL6-deficient mice compared with wild-type mice. These results indicate that IL6 may play an important role in the pathogenesis of bleomycin-induced lung injury and subsequent fibrotic changes [126]. Forth, several studies observed that IL1 β in general is able to regulate WNT signalling. One group tested the expression of various WNT molecules, using IL1 β in primary culture chondrocytes obtained from rabbits. IL1 β led to upregulated β -catenin levels, finally resulting in a significant increase of Wnt5a and 7a expression levels in primary culture chondrocytes [127]. Newest studies demonstrated that fibrotic tissue remodelling is induced by distinct cytokine-dependent mechanisms. Thereby, the effector cytokines IL13 and IL17A played central roles. Moreover, these findings suggested that TGF- β and proinflammatory mediators like IL1 β promote fibrosis by regulating and increasing the production of IL17A [128]. Hence, the question arises, whether IL1 β and / or IL6 accordingly mediate the fibrotic effects of WNT signalling.

ATII cells, one of the effector cells in IPF have been shown to be a major source of cytokines and growth factors, including interleukins (ILs) [129-131]. ILs also termed as cytokines, are non-structural, highly active proteins. IL1 family members alter the host response to an inflammatory, infectious or immunological challenge and are involved in various disorders of the lung. IL1 α and IL1 β are inflammatory cytokines, which bind with similar affinity to the IL1 receptor (IL1R) and the IL1R accessory protein (IL1RA). The IL1RA acts as a natural antagonist of IL1 α /IL1 β by trapping IL1R1 molecules. IL1 β is synthesized as an inactive cytoplasmic precursor (pro-IL1 β), which essentially lacks biological effects. The active, mature IL1 β is produced upon cleavage of pro-IL1 β by a specific IL1 β converting enzyme (ICE or caspase-1) or by proteases [132]. IL1 β is a pro-inflammatory cytokine primarily produced by activated macrophages and monocytes; as well as by fibroblasts, neutrophils, bronchial and alveolar epithelial cells. As a central cytokine it is involved in the initiation and persistence of inflammation [133]. IL1 β induces the production of IL6 or TNF α , thereby leading to neutrophil recruitment and fibroblast proliferation, which may elicits potent fibrotic responses. These findings suggest that IL1 β may be a potent inducer and mediator of several other members of the cytokine family. Analyses of bleomycin-treated whole mouse lung homogenates revealed significantly

increased levels of several IL17A-promoting cytokines, most strikingly the mediators IL1 β and IL6. IL1 β mRNA expression and cytokine production correlated with the degree of fibrosis after intratracheal administration of bleomycin [128]. This observation has been confirmed in several recent studies, suggesting an important role for IL1 β in the development of bleomycin-induced pulmonary fibrosis [125, 134-136]. In primary rat ATII cells, as well as in A549 cells, as a model of human ATII cells, IL1 β stimulation induced a significant increase of IL6 [137]. Recent studies reported that ATII cells secreted several cytokines, such as monocyte chemotactic protein (MCP)-1, macrophage inflammatory proteins (MIP)-1 α and -2, interleukin (IL) 8, and chemokine (C-C motif) ligand (CCL) 5 in response to IL1 β [129, 131]. A number of human and animal studies have revealed the presence of IL1 β in tissues undergoing fibrogenesis with accumulation of myofibroblasts and matrix deposition, such as chronic fibrotic lung diseases [132, 138, 139].

The family of IL6-type cytokines, including IL6, activates target genes, which are involved in differentiation, survival, apoptosis and proliferation. IL6 binds to plasma membrane receptor complexes containing the common signal transducing receptor chain glycoprotein 130 (gp 130) [140]. IL6 is released by a variety of cell types including monocytes, macrophages, fibroblasts, endothelial and epithelial cells, induced by inflammatory and profibrotic mediators, such as IL1 β , TNF α , PDGF and TGF β . Accordingly, it is suggested that IL6 contributes to the onset and maintenance of several ILDs [141, 142]. Moreover it has been shown that IL1 β induced IL6, IL8 and MCP1 expression in bronchial epithelial cells or fibroblasts [128].

Both, IL1 β and IL6 were upregulated upon WNT3A stimulation in vitro as well as in vivo. Importantly, IL1 β and IL6 were increased in the supernatants of ATII cells isolated from fibrotic mouse lungs, as well as in the BALF from these mice. These results conform to the investigation that IL1 β was also increased in the BALF of IPF patients. Additionally, IL17A expression levels were increased, indicating that these cytokines may be involved in the development of IPF [128]. In accordance, a recent study showed activated WNT/ β -catenin signalling, with increased WNT7B expression levels, in rheumatoid arthritis and osteoarthritis. Interestingly, synovium from rheumatoid arthritis patients and WNT7B-transfected normal synovial cells showed increased levels of IL1 β , IL6 and TNF α compared with normal samples [143].

Most recently, studies investigated the correlation of several cytokine levels with cellular characteristics in BALFs and lung function parameters in different ILDs. Interestingly, increased IL1 receptor antagonist (IL1RA) expression was observed in IPF. Additionally, increased interleukin (IL)8 expression is suggested to correlate with prominent fibrosis and strong lung function decline [144, 145]. In addition, significantly increased levels of IL6 have been detected in BALFs of different pathologic conditions, including IPF [146]. Interestingly, in this study, no IL6 expression levels were detectable in BALFs from IPF patients. Possible reasons may be discrepancies in the BALF extraction methods or preparation techniques. Several studies investigated different animal models of acute lung injury and pulmonary fibrosis, by application of bleomycin, silica or irradiation, leading to increased cytokine expression [138, 139]. It has been shown that the expression of IL1 β and IL6 in bleomycin-induced pulmonary fibrosis is influencing fibroblast activation, proliferation and collagen deposition [147]. In addition, it was shown that exogenous rmIL1 β recapitulates acute inflammation induced by bleomycin with alveolar tissue destruction and remodelling, resulting in progressive interstitial fibrosis, confirming the proinflammatory and profibrotic effects of IL1 β [37, 125]. These observations were confirmed and amplified by showing that IL1 β -mediated inflammation and fibrosis is dependent on IL17A, a critical downstream mediator. IL17A deficiency significantly reduced bleomycin-induced fibrosis in wildtype mice, as shown by analysis of collagen expression in the BALF and collagen deposition in the lung. In bleomycin-treated IL17A^{-/-} mice compared with wildtype animals reduced inflammation and fibrosis, associated with decreased IL1 β expression was observed. In vitro experiments with cultured fibroblasts demonstrated that IL17A promotes IL1 β production and vice versa [128, 148, 149].

In sum, it has been suggested that IL17A and IL1 β cross-regulate each other, which explains their additive roles in bleomycin-induced fibrosis.

Furthermore, in IL6-deficient mice attenuated fibrotic changes were observed compared with wild-type mice, upon bleomycin treatment. These results indicate that IL6 may play an important role in the pathogenesis of bleomycin-induced lung fibrosis [126]. These cytokines have been demonstrated to be produced at the sites of active fibrosis where they appear to be expressed by activated inflammatory cells, such as macrophages. More interestingly, other non-inflammatory lung cells,

including myofibroblasts and epithelial cells, have been found to be significant sources as well. The regulation of diverse functions of lung inflammatory and epithelial cells can further influence the fibrotic process by autocrine and paracrine mechanisms [150]. Latest findings assign IL13 an impact with fibrotic activity; suggesting a role in bleomycin-induced pulmonary fibrosis. It has been indicated that IL13 triggers fibrosis by inducing and activating TGF- β signalling. Of special interest is a recently described IL1 β -driven model of experimental fibrosis, which mimics bleomycin-induced pulmonary fibrosis. Therefore, IL1 β is suggested to be a critical mediator of pulmonary fibrosis, highly dependent on IL17A by stimulating the production [128].

In summary, the WNT/ β -catenin signaling pathway is one of the core signal transduction pathways. This study demonstrates that WNT/ β -catenin signalling is expressed in human and mouse lung epithelium. These results provided evidence that WNT signalling pathway components are mainly increased and active in the bronchial and alveolar epithelium in IPF and experimental lung fibrosis, and may influence alveolar epithelial cell injury and hyperplasia due to significant dysregulation of the tightly controlled WNT/ β -catenin pathway. Therefore it is strongly suggested that especially WNT3A, which is aberrantly secreted by ATII cells in IPF, takes a crucial role in the development of the disease and modification of WNT signalling may represent a therapeutic option in IPF.

IL17A was identified as a critical mediator of pulmonary fibrosis after bleomycin administration, a blockade of IL17A could act as a potential treatment of pulmonary fibrosis [128]. It will be important to translate those approaches, identified from studies of cultured cells, into studies of human cells. There is a significant need for understanding how these varied and sometimes disparate signals are integrated into a coordinated response. This will require increased understanding of the source of the mediators, the pathways that become activated, the timing of their activation, their spatial targeting, and the factors that regulate their responsiveness.

Anti-inflammatory therapies including corticosteroids have limited efficacy in this ultimately fatal disorder; an important unmet need is to identify new agents that interact with key molecular pathways involved in the pathogenesis of pulmonary fibrosis to prevent progression or reverse fibrosis in these patients. Because no effective treatment for IPF exists, selective regulation of WNT/ β -catenin-dependent transcription suggests a potential previously unexplored therapeutic approach for IPF.

Alveolar cell death is one of the chief causes, which impairs lung diseases, like fibrosis. Therefore, several studies suggested that the use of pharmacological activators of the canonical WNT pathway possibly stimulates tissue reconstruction, and especially alveolar epithelial cell repair [151, 152]. Flozak and colleagues used adenoviral vectors to express proteins in ATII cultures that would constitutively activate or inhibit β -catenin signalling. Activation of this pathway can be achieved by expressing a point mutant version of β -catenin, resistant to degradation. Conversely, inhibition of this pathway can be achieved through expression of ICAT, a polypeptide that specifically antagonizes β -catenin transcription through binding β -catenin and competing for its interactions with both TCF/p300 [93]. Interestingly, a recent study observed reduced expression of the WNT/ β -catenin signalling pathway in two different mouse models of experimental chronic obstructive pulmonary disease (COPD) and emphysema, using cigarette smoke exposure and elastase instillation in wildtype and TOPGAL reporter mice, respectively. In general, COPD is characterised by parenchymal tissue destruction and impaired repair capacity, resulting from an imbalance between lung injury and repair processes. Furthermore, LiCl, a well-known activator of WNT/ β -catenin signalling, was used and demonstrated enhanced activation of the signal pathway in lung epithelial cells, which led to a significant reduction of experimental emphysema with restored alveolar epithelial structure and function. These results not only suggest that reduced activity of WNT/ β -catenin signalling is a common and relevant feature of COPD and emphysema development, but also that activation may be a preventive and effective therapeutic approach [153].

5.1 Conclusions and future perspectives

Among all idiopathic interstitial pneumonias (IIP), idiopathic pulmonary fibrosis (IPF) is the most common and most severe form. As of now, the pathomechanisms are not completely understood, which leads to the fact that appropriate therapies do not yet exist. In this study, evidence for the reactivation of WNT/ β -catenin signalling, including several WNT target molecules, which contribute to the development and progression of fibrosis, is provided. The key finding of the present study is that canonical WNT signalling/WNT pathway components are expressed and operative in adult lung epithelium of experimental and idiopathic pulmonary fibrosis. In addition,

the interleukins, IL1 β and IL6 were identified as novel WNT target genes expressed by the alveolar epithelium in lung fibrosis, likewise presumed to be involved in the pathogenesis of the disease. Future studies analyzing the autocrine and paracrine effects of IL1 β /IL6 and crosstalk with WNT/ β -Catenin pathway, in particular WNT3A in alveolar epithelial cells, are required to reveal the functional effects. Detailed in vivo and in vitro will shed more light into the relevance of this proposed signalling pathway.

In light of recent research regarding IPF and WNT signalling this detection strongly suggests WNT/ β -catenin signalling and its effectors to be activated and expressed in ATII cells during the pathogenesis of IPF. Inhibiting WNT/ β -catenin signal transduction more specifically or antagonizing its downstream effectors, using novel small molecules, could possibly prevent the progression of the disease. In summary, the aim of further investigation is to elucidate the downstream mechanisms and the effects of WNT in more detail. Thus, modification of WNT signalling and better understanding of the cytokines and the cytokine networks involved in IPF leads to the possibility of new therapeutic approaches.

6 APPENDIX

6.1 List of human (q)RT-PCR primers

table 6.1: Human primer sequences and amplicon sizes. All primer sets worked under identical (q)RT-PCR cycling conditions with similar efficiencies to obtain simultaneous amplification in the same run. Sequences were taken from GeneBank, all accession numbers are given.

Gene	Accession		sequences (5' → 3')	length	Amplicon
AXIN1	NM_003502	for	GAGGATGCGGAGAAGAACCA	20bp	115bp
		rev	GACAAGGGTCTGGAGTTCTCATG	23bp	
AXIN2	NM_004655	for	AGAAATGCATCGCAGTGTGAAG	22bp	65bp
		rev	GGTGGGTTCTCGGGAAATG	19bp	
β-catenin/ CTNNB1	NM_001904	for	AAGTGGGTGGTATAGAGGCTCTTG	24bp	77bp
		rev	GATGGCAGGCTCAGTGATGTC	21bp	
DVL1	NM_004421	for	TGACGGCCGCATCGA	15bp	82bp
		rev	TGTTCTCAAAGTTCACGTCATTCAC	25bp	
DVL2	NM_004422	for	CAGTCACGCTAAACATGGAGAAGT	24bp	65bp
		rev	CTCATTGCTCTGGCCAACAA	20bp	
DVL3	NM_004423	for	ACCCAGCTATAAGTTCTTCTTCAAGTCT	28bp	80bp
		rev	TGGCATTGTCATCCGAGATCT	21bp	
FZD1	NM_003505	for	AGCGCCGTGGAGTTCGT	17bp	64bp
		rev	CGAAAGAGAGTTGTCTAGTGAGGAAAC	27bp	

FZD2	NM_001466	for	CACGCCGCGCATGTC	15bp	63bp
		rev	ACGATGAGCGTCATGAGGTATTT	23bp	
FZD3	NM_017412	for	GGTGTTCCTTGGCCTGAAGA	20bp	72bp
		rev	CACAAGTCGAGGATATGGCTCAT	23bp	
FZD4	NM_012193	for	GACAACTTTCACACCGCTCATC	22bp	164bp
		rev	CCTTCAGGACGGGTTTCCACA	19bp	
GSK3 β	NM_002093	for	CTCATGCTCGGATTCAAGCA	20bp	86bp
		rev	GGTCTGTCCACGGTCTCCAGTA	22bp	
HPRT1	NM_000194	for	AAGGACCCACGAAGTGTTG	20bp	157bp
		rev	GGCTTTGTATTTTGCTTTTCCA	22bp	
LEF1	NM_016269	for	CATCAGGTACAGGTCCAAGAATGA	24bp	93bp
		rev	GTCGCTGCCTTGGCTTTG	18bp	
LRP5	NM_002335	for	GCTGTACCCGCCGATCCT	18bp	138bp
		rev	GGCGCCATTCTCGAAT	18bp	
LRP6	NM_002336	for	GATTCAGATCTCCGGCGAATT	21bp	83bp
		rev	GGCTGCAAGATATTGGAGTCTTCT	24bp	
TCF3	NM_031283	for	ACCATCTCCAGCACACTTGTCTAATA	26bp	71bp
		rev	GAGTCAGCGGATGCATGTGA	20bp	
TCF4	NM_030756	for	GCGCGGGATAACTATGGAAAG	21bp	89bp
		rev	GGATTTAGGAAACATTCGCTGTGT	24bp	
WNT1	NM_005430	for	CTCATGAACCTTCACAACAACGA	23bp	80bp
		rev	ATCCCGTGGCACTTGCA	17bp	

WNT2	NM_003391	for	CCTGATGAATCTTCACAACAACAGA	25bp	78bp
		rev	CCGTGGCACTTGCCTCTT	19bp	
WNT3A	NM_033131	for	GCCCCACTCGGATACTTCTACT	23bp	98bp
		rev	GAGGAATACTGTGGCCCAACA	21bp	
WNT7B	NM_058238	for	GCAAGTGGATTTTCTACGTGTTTCT	25bp	65bp
		rev	TGACAGTGCTCCGAGCTTCA	20bp	
WNT10B	NM_003394	for	GCGCCAGGTGGTAACTGAA	19bp	59bp
		rev	TGCCTGATGTGCCATGACA	19bp	

6.2 List of mouse (q)RT-PCR primers

table 6.2: Mouse primer sequences and amplicon sizes. All primer sets worked under identical (q)RT-PCR cycling conditions with similar efficiencies to obtain simultaneous amplification in the same run. Sequences were taken from GeneBank, all accession numbers are given.

Gene	Accession		sequences (5' → 3')	length	amplicon
Axin1	NM_009733	for	CGAAGGGAGATGCAGGAGAGTA	22bp	67bp
		rev	AAGTGCAGGAATGTGAGGTAGA	23bp	
Axin2	NM_015732	for	AGCAGAGGGACAGGAACCA	19bp	108bp
		rev	CACTTGCCAGTTTCTTTGGCT	21bp	
β-catenin/ Ctnnb1	NM_007614	for	TCAAGAGAGCAAGCTCATCATTCT	24bp	115bp
		rev	CACCTTCAGCACTCTGCTTGTG	22bp	
CyclinD1	NM_007631	for	ATGCCAGAGGCGGATGAGA	19bp	98bp
		rev	ATGGAGGGTGGGTTGGAAAT	20bp	
Dkk2	NM_020265	for	GAGATCGCAACCATGGTCACT	21bp	102bp
		rev	GGGTCTCCTTCATGTCCCTTTATATG	26bp	
Dvl1	NM_010091	for	CAGCGCTGAGGCAGACA	18bp	63bp
		rev	GGACATGGTGGAGTCTGTGATG	22bp	
Dvl2	NM_007888	for	CGAGCCTGGAGACATGCTTT	20bp	62bp
		rev	CGTCGTTGCTCATGTTCTCAA	21bp	
Dvl3	NM_007889	for	GATTGAGCGGTCCTCGTCTTT	21bp	136bp
		rev	CATCACCTCGCTCATTGCTTT	21bp	

Fzd1	NM_021457	for	AAACAGCACAGGTTCTGCAAAA	22bp	58bp
		rev	TGGGCCCTCTCGTTCCTT	18bp	
Fzd2	NM_020510	for	TCCATCTGGTGGGTGATTCTG	21bp	66bp
		rev	CTCGTGGCCCCACTTCATT	19bp	
Fzd3	NM_021458	for	GCCTATAGCGAGTGTTCAAAACCTCA	25bp	78bp
		rev	TGGAAACCTACTGCACTCCATATCT	25bp	
Fzd4	NM_008055	for	GCCCCAGAACGACCACAA	18bp	64bp
		rev	GGGCAAGGGAACCTCTTCAT	20bp	
Gsk3 β	NM_019827	for	TTTGAGCTGGTACCCTAGGATGA	23bp	75bp
		rev	TTCTTCGCTTTCGATGCA	19bp	
Il1 β	NM_008361	for	AGTTGACGGACCCCAAAAGAT	21bp	57bp
		rev	GGACAGCCCAGGTCAAAGG	19bp	
Il6	NM_031168	for	TCGGAGGCTTAATTACACATGTTCT	25bp	67bp
		rev	TTGCCATTGCACAACTCTTTTC	22bp	
Lef1	NM_010703	for	GGCGGCGTTGGACAGAT	17bp	67bp
		rev	CACCCGTGATGGGATAAACAG	21bp	
Lrp5	NM_008513	for	CAACGTGGACGTGTTTTATTCTTC	24bp	138bp
		rev	CAGCGACTGGTGCTGTAGTCA	21bp	
Lrp6	NM_008514	for	CCATTCCTCTCACTGGTGTCAA	22bp	146bp
		rev	GCCAAACTCTACCACATGTTCCA	23bp	
Pbgd	NM_007392	for	ATGTCCGGTAACGGCGGC	18bp	139bp
		rev	GGTACAAGGCTTTCAGCATCGC	22bp	

Tcf3	NM_009332	for	TCCAGCACACTTGTCCAACAA	21bp	61bp
		rev	CAGCGGGTGCATGTGATG	18bp	
Tcf4	NM_009333	for	GTGGGAACTGCCCCGTTT	18bp	59bp
		rev	GTTCTAAGAGCACAGGGCAGTTG	23bp	
Wisp1	NM_018865	for	GTCCTGAGGGTGGGCAACAT	20bp	97bp
		rev	GGGCGTGTAGTCGTTTCCTCT	21bp	
Wnt1	NM_021279	for	CAAATGGCAATTCCGAAACC	20bp	112bp
		rev	GATTGCGAAGATGAACGCTG	20bp	
Wnt2	NM_023653	for	AGCCCTGATGAACCTTCACAAC	22bp	78bp
		rev	TGACACTTGCATTCTTGTTC AAG	24bp	
Wnt3a	NM_009522	for	GCACCACCGTCAGCAACA	18bp	57bp
		rev	GGGTGGCTTTGTCCAGAACA	20bp	
Wnt7b	NM_009528	for	TCGAAAGTGGATCTTTTACGTGTTT	25bp	67bp
		rev	TGACAATGCTCCGAGCTTCA	20bp	
Wnt10b	NM_011718	for	TGGGACGCCAGGTGGTAA	18bp	60bp
		rev	CTGACGTTCCATGGCATTG	20bp	

6.3 Characteristics of IPF patients

table 6.3: Characteristics of IPF patients with UIP pattern. VC = vital capacity, DL_{CO}/VA = diffusing capacity of the lung for carbon monoxide (CO) per unit of alveolar volume (all in % predicted), TLC = total lung capacity, PaO₂ = partial pressure of oxygen (O₂) in the arterial blood, PaCO₂ = partial pressure of carbon dioxide (CO₂) in the arterial blood.

no.	Diagnosis	gender	age (yr.)	VC (%)	DLCO/VA (%)	TLC (%)	PaO ₂ (mmHg)	PaCO ₂ (mmHg)
1	IPF (UIP)	female	62	68	63	81	64	41
2	IPF (UIP)	female	54	45	44	53	72	42
3	IPF (UIP)	male	66	86	56	78	90	41
4	IPF (UIP)	male	76	41	73	47	79	38
5	IPF (UIP)	male	68	57	37	55	51	34
6	IPF (UIP)	male	60	33	65	42	69	41
7	IPF (UIP)	male	64	69	54	71	70	35
8	IPF (UIP)	male	67	74	57	90	70	41
9	IPF (UIP)	male	79	81	42	75	45	37
10	IPF (UIP)	male	65	60	48	62	61	34
11	IPF (UIP)	male	65	64	75	58	78	35
12	IPF (UIP)	male	69	36	64	41	71	46

6.4 List of antibodies

6.4.1 Primary antibodies

table 6.4.1: Primary antibodies. Antibodies were used for Western blot (WB), immunohistochemical (IHC) and immunocytochemical (ICC) analysis.

Antibody	Host	Dilution			company
		WB	IHC	ICC	
WB					
α -smooth muscle actin (Acta2 = α -SMA)	Mouse	1 : 100	-	-	Sigma-Aldrich
β -catenin	Rabbit	1 : 3000	-	-	Cell Signaling Technology
CyclinD1 (CCND1)	Rabbit	1 : 3000	-	-	Millipore
GSK3 β	Rabbit	1 : 1000	-	-	Cell Signaling Technology
phospho-GSK3 β	Rabbit	1 : 1000	-	-	Cell Signaling Technology
Lamin A/C	Rabbit	1 : 3000	-	-	Santa Cruz Biotechnology
LRP6	Rabbit	1 : 1000	-	-	Cell Signaling Technology
Phosphor-LRP6	Rabbit	1 : 1000	-	-	Cell Signaling Technology
IHC					
β -catenin	Rabbit	-	1 : 50	-	Cell Signaling Technology
GSK3 β	Rabbit	-	1 : 25	-	Cell Signaling Technology
WNT1	Rabbit	-	1 : 50	-	Abcam
WNT3A	Rabbit	-	1 : 50	-	Invitrogen
ICC					

α -smooth muscle actin (Acta2 = α -SMA)	Mouse	-	-	1 : 400	Sigma-Aldrich
Cdh1	mouse	-	-	1 : 50	BD Bioscience
panCK	rabbit	-	-	1 : 1000	Dako
pro-SPC	rabbit	-	-	1 : 100	Chemicon
ZO-1	rabbit	-	-	1 : 1000	Zymed

6.4.2 Secondary antibodies

table 6.4.2: Secondary antibodies. Antibodies were used for Western blot (WB), immunohistochemical (IHC) and immunocytochemical (ICC) analysis.

Antibody	Host	dilution			company
		WB	IHC	ICC	
WB					
HRP-conjugated anti-mouse IgG	Rabbit	1 : 1000	-	-	Pierce
HRP-conjugated anti-rabbit IgG	Goat	1 : 1000	-	-	Pierce
HRP-conjugated anti-rat IgG	Rabbit	1 : 1000	-	-	Pierce
IHC					
Biotinylated anti-mouse IgG	Goat	-	ready to use	-	Invitrogen
Biotinylated anti-rabbit IgG	Goat	-	ready to use	-	Invitrogen
ICC					
Alexa Fluor 555 anti-mouse IgG	Goat	-	-	1 : 1000	Invitrogen
Alexa Fluor 555 anti-rabbit IgG	Goat	-	-	1 : 1000	Invitrogen
Alexa Fluor 555 anti-rat IgG	Goat	-	-	1 : 1000	Invitrogen
FITC-conjugated anti-mouse IgG	Goat	-	-	1 : 100	Dako

6.5 Microarray gene list

table 6.5: List of selected target genes found in the microarray. Genes were partly confirmed by (q)RT-PCR

Symbol	accession no.		Wnt3a (8 h)	Wnt3a (24 h)
Angptl4	NM_020581	coefficient	0,58	0,49
		ddCT	0,18	0,64
Angptl7	NM_001039554	coefficient	-0,65	-0,67
		ddCT	-1,21	-1,25
Aqp1	NM_007472	coefficient	-0,33	-0,48
		ddCT	-0,04	-0,34
Arg1	NM_007482	coefficient	-0,40	0,13
		ddCT	-0,80	-0,42
Axin2	NM_015732	coefficient	0,92	0,49
		ddCT	1,31	0,83
Col5a2	NM_007737	coefficient	-0,50	-0,13
		ddCT	-0,19	-0,27
Col7a1	NM_007738	coefficient	-0,43	0,22
		ddCT	-0,32	-0,95
Dcn	NM_007833	coefficient	-0,16	-0,46
		ddCT	-0,17	-0,10
Dkk2	NM_020265	coefficient	0,21	0,94
		ddCT	0,91	1,87
Fn1	NM_010233	coefficient	-0,56	-0,21
		ddCT	-0,42	0,29
Grem2	NM_011825	coefficient	-0,20	0,49
		ddCT	-0,09	0,30
Has2	NM_008216	coefficient	0,42	0,52
		ddCT	0,37	0,48
Il1 β	NM_008361	coefficient	0,70	0,57
		ddCT	1,91	2,19
Il6	NM_031168	coefficient	-0,08	0,64
		ddCT	0,21	0,63
Kdr	NM_010612	coefficient	0,50	-0,15
		ddCT	0,54	-0,07

Lcn2	NM_008491	coefficient	0,07	0,65
		ddCT	2,41	1,45
Magoh	NM_010760	coefficient	-0,34	-0,52
		ddCT	0,56	0,21
Nkd1	NM_027280	coefficient	0,77	0,28
		ddCT	1,15	0,42
Prickle1	NM_001033217	coefficient	0,41	0,34
		ddCT	0,56	0,41
Rock1	NM_009071	coefficient	0,36	-0,47
		ddCT	0,40	-0,31
Spp1	NM_009263	coefficient	-0,48	0,00
		ddCT	-0,20	-0,26
Tcf7	NM_009331	coefficient	0,48	0,08
		ddCT	0,94	0,71
Timp1	NM_011593	coefficient	0,01	0,46
		ddCT	-0,45	0,25
Tagln	NM_011526	coefficient	-0,19	0,41
		ddCT	0,10	0,18
Zyx	NM_011772	coefficient	-0,23	0,49
		ddCT	0,05	0,22

7 REFERENCES

1. American Thoracic Society/European Respiratory Society International Multidisciplinary Consensus Classification of the Idiopathic Interstitial Pneumonias. This joint statement of the American Thoracic Society (ATS), and the European Respiratory Society (ERS) was adopted by the ATS board of directors, June 2001 and by the ERS Executive Committee, June 2001. *Am J Respir Crit Care Med* 2002; 165(2): 277-304.
2. Bourke SJ. Interstitial lung disease: progress and problems. *Postgrad Med J* 2006; 82(970): 494-499.
3. King TE, Jr. Clinical advances in the diagnosis and therapy of the interstitial lung diseases. *Am J Respir Crit Care Med* 2005; 172(3): 268-279.
4. Meltzer EB, Noble PW. Idiopathic pulmonary fibrosis. *Orphanet J Rare Dis* 2008; 3: 8.
5. Raghu G, Weycker D, Edelsberg J, Bradford WZ, Oster G. Incidence and prevalence of idiopathic pulmonary fibrosis. *Am J Respir Crit Care Med* 2006; 174(7): 810-816.
6. American Thoracic Society. Idiopathic pulmonary fibrosis: diagnosis and treatment. International consensus statement. American Thoracic Society (ATS), and the European Respiratory Society (ERS). *Am J Respir Crit Care Med* 2000; 161(2 Pt 1): 646-664.
7. Baumgartner KB, Samet JM, Stidley CA, Colby TV, Waldron JA. Cigarette smoking: a risk factor for idiopathic pulmonary fibrosis. *Am J Respir Crit Care Med* 1997; 155(1): 242-248.
8. Dempsey OJ. Clinical review: idiopathic pulmonary fibrosis--past, present and future. *Respir Med* 2006; 100(11): 1871-1885.
9. Collard HR, King TE, Jr., Bartelson BB, Vourlekis JS, Schwarz MI, Brown KK. Changes in clinical and physiologic variables predict survival in idiopathic pulmonary fibrosis. *Am J Respir Crit Care Med* 2003; 168(5): 538-542.
10. Selman M, King TE, Pardo A. Idiopathic pulmonary fibrosis: prevailing and evolving hypotheses about its pathogenesis and implications for therapy. *Ann Intern Med* 2001; 134(2): 136-151.
11. Kim DS, Collard HR, King TE, Jr. Classification and natural history of the idiopathic interstitial pneumonias. *Proc Am Thorac Soc* 2006; 3(4): 285-292.
12. Martinez FJ, Safrin S, Weycker D, Starko KM, Bradford WZ, King TE, Jr., Flaherty KR, Schwartz DA, Noble PW, Raghu G, Brown KK. The clinical course of patients with idiopathic pulmonary fibrosis. *Ann Intern Med* 2005; 142(12 Pt 1): 963-967.
13. Hunninghake GW, Lynch DA, Galvin JR, Gross BH, Muller N, Schwartz DA, King TE, Jr., Lynch JP, 3rd, Hegele R, Waldron J, Colby TV, Hogg JC. Radiologic findings are strongly associated with a pathologic diagnosis of usual interstitial pneumonia. *Chest* 2003; 124(4): 1215-1223.
14. Lynch DA, Godwin JD, Safrin S, Starko KM, Hormel P, Brown KK, Raghu G, King TE, Jr., Bradford WZ, Schwartz DA, Richard Webb W. High-resolution computed tomography in idiopathic pulmonary fibrosis: diagnosis and prognosis. *Am J Respir Crit Care Med* 2005; 172(4): 488-493.
15. Raghu G, Brown KK, Costabel U, Cottin V, du Bois RM, Lasky JA, Thomeer M, Utz JP, Khandker RK, McDermott L, Fatenejad S. Treatment of idiopathic

- pulmonary fibrosis with etanercept: an exploratory, placebo-controlled trial. *Am J Respir Crit Care Med* 2008; 178(9): 948-955.
16. Maher TM, Wells AU, Laurent GJ. Idiopathic pulmonary fibrosis: multiple causes and multiple mechanisms? *Eur Respir J* 2007; 30(5): 835-839.
 17. Daniels CE, Ryu JH. Treatment of idiopathic pulmonary fibrosis. *Semin Respir Crit Care Med* 2006; 27(6): 668-676.
 18. Walter N, Collard HR, King TE, Jr. Current perspectives on the treatment of idiopathic pulmonary fibrosis. *Proc Am Thorac Soc* 2006; 3(4): 330-338.
 19. Nathan SD. Lung transplantation: disease-specific considerations for referral. *Chest* 2005; 127(3): 1006-1016.
 20. Rinaldi M, Sansone F, Boffini M, El Qarra S, Solidoro P, Cavallo N, Ruffini E, Baldi S. Single versus double lung transplantation in pulmonary fibrosis: a debated topic. *Transplant Proc* 2008; 40(6): 2010-2012.
 21. Thabut G, Mal H, Castier Y, Groussard O, Brugiere O, Marrash-Chahla R, Leseche G, Fournier M. Survival benefit of lung transplantation for patients with idiopathic pulmonary fibrosis. *J Thorac Cardiovasc Surg* 2003; 126(2): 469-475.
 22. Williams TJ, Wilson JW. Challenges in pulmonary fibrosis: 7--Novel therapies and lung transplantation. *Thorax* 2008; 63(3): 277-284.
 23. Katzenstein AL, Myers JL. Idiopathic pulmonary fibrosis: clinical relevance of pathologic classification. *Am J Respir Crit Care Med* 1998; 157(4 Pt 1): 1301-1315.
 24. Visscher DW, Myers JL. Histologic spectrum of idiopathic interstitial pneumonias. *Proc Am Thorac Soc* 2006; 3(4): 322-329.
 25. King TE, Jr., Schwarz MI, Brown K, Tooze JA, Colby TV, Waldron JA, Jr., Flint A, Thurlbeck W, Cherniack RM. Idiopathic pulmonary fibrosis: relationship between histopathologic features and mortality. *Am J Respir Crit Care Med* 2001; 164(6): 1025-1032.
 26. Nicholson AG, Fulford LG, Colby TV, du Bois RM, Hansell DM, Wells AU. The relationship between individual histologic features and disease progression in idiopathic pulmonary fibrosis. *Am J Respir Crit Care Med* 2002; 166(2): 173-177.
 27. Hinz B, Phan SH, Thannickal VJ, Galli A, Bochaton-Piallat ML, Gabbiani G. The myofibroblast: one function, multiple origins. *Am J Pathol* 2007; 170(6): 1807-1816.
 28. Phan SH. The myofibroblast in pulmonary fibrosis. *Chest* 2002; 122(6 Suppl): 286S-289S.
 29. Scotton CJ, Chambers RC. Molecular targets in pulmonary fibrosis: the myofibroblast in focus. *Chest* 2007; 132(4): 1311-1321.
 30. Willis BC, duBois RM, Borok Z. Epithelial origin of myofibroblasts during fibrosis in the lung. *Proc Am Thorac Soc* 2006; 3(4): 377-382.
 31. Gross TJ, Hunninghake GW. Idiopathic pulmonary fibrosis. *N Engl J Med* 2001; 345(7): 517-525.
 32. Strieter RM. Pathogenesis and natural history of usual interstitial pneumonia: the whole story or the last chapter of a long novel. *Chest* 2005; 128(5 Suppl 1): 526S-532S.
 33. Noble PW, Homer RJ. Back to the future: historical perspective on the pathogenesis of idiopathic pulmonary fibrosis. *Am J Respir Cell Mol Biol* 2005; 33(2): 113-120.
 34. Gauldie J, Kolb M, Sime PJ. A new direction in the pathogenesis of idiopathic pulmonary fibrosis? *Respir Res* 2002; 3: 1.

35. Selman M, Pardo A. Idiopathic pulmonary fibrosis: an epithelial/fibroblastic cross-talk disorder. *Respir Res* 2002; 3: 3.
36. Horowitz JC, Thannickal VJ. Epithelial-mesenchymal interactions in pulmonary fibrosis. *Semin Respir Crit Care Med* 2006; 27(6): 600-612.
37. Kolb M, Margetts PJ, Anthony DC, Pitossi F, Gauldie J. Transient expression of IL-1beta induces acute lung injury and chronic repair leading to pulmonary fibrosis. *J Clin Invest* 2001; 107(12): 1529-1536.
38. Konigshoff M, Wilhelm A, Jahn A, Sedding D, Amarie OV, Eul B, Seeger W, Fink L, Gunther A, Eickelberg O, Rose F. The angiotensin II receptor 2 is expressed and mediates angiotensin II signaling in lung fibrosis. *Am J Respir Cell Mol Biol* 2007; 37(6): 640-650.
39. Konigshoff M, Kramer M, Balsara N, Wilhelm J, Amarie OV, Jahn A, Rose F, Fink L, Seeger W, Schaefer L, Gunther A, Eickelberg O. WNT1-inducible signaling protein-1 mediates pulmonary fibrosis in mice and is upregulated in humans with idiopathic pulmonary fibrosis. *J Clin Invest* 2009; 119(4): 772-787.
40. Gordon MD, Nusse R. Wnt signaling: multiple pathways, multiple receptors, and multiple transcription factors. *J Biol Chem* 2006; 281(32): 22429-22433.
41. Mikels AJ, Nusse R. Wnts as ligands: processing, secretion and reception. *Oncogene* 2006; 25(57): 7461-7468.
42. Moon RT, Kohn AD, De Ferrari GV, Kaykas A. WNT and beta-catenin signalling: diseases and therapies. *Nat Rev Genet* 2004; 5(9): 691-701.
43. Nusse R. Wnt signaling in disease and in development. *Cell Res* 2005; 15(1): 28-32.
44. Johnson ML, Rajamannan N. Diseases of Wnt signaling. *Rev Endocr Metab Disord* 2006; 7(1-2): 41-49.
45. Logan CY, Nusse R. The Wnt signaling pathway in development and disease. *Annu Rev Cell Dev Biol* 2004; 20: 781-810.
46. Cadigan KM, Liu YI. Wnt signaling: complexity at the surface. *J Cell Sci* 2006; 119(Pt 3): 395-402.
47. Nusse R, van Ooyen A, Cox D, Fung YK, Varmus H. Mode of proviral activation of a putative mammary oncogene (int-1) on mouse chromosome 15. *Nature* 1984; 307(5947): 131-136.
48. Nusse R, Varmus HE. Many tumors induced by the mouse mammary tumor virus contain a provirus integrated in the same region of the host genome. *Cell* 1982; 31(1): 99-109.
49. Nusslein-Volhard C, Wieschaus E. Mutations affecting segment number and polarity in *Drosophila*. *Nature* 1980; 287(5785): 795-801.
50. Kikuchi A, Yamamoto H, Kishida S. Multiplicity of the interactions of Wnt proteins and their receptors. *Cell Signal* 2007; 19(4): 659-671.
51. MacDonald BT, Yokota C, Tamai K, Zeng X, He X. Wnt signal amplification via activity, cooperativity, and regulation of multiple intracellular PPPSP motifs in the Wnt co-receptor LRP6. *J Biol Chem* 2008; 283(23): 16115-16123.
52. Clevers H. Wnt/beta-catenin signaling in development and disease. *Cell* 2006; 127(3): 469-480.
53. Goss AM, Tian Y, Tsukiyama T, Cohen ED, Zhou D, Lu MM, Yamaguchi TP, Morrissey EE. Wnt2/2b and beta-catenin signaling are necessary and sufficient to specify lung progenitors in the foregut. *Dev Cell* 2009; 17(2): 290-298.
54. Levay-Young BK, Navre M. Growth and developmental regulation of wnt-2 (irp) gene in mesenchymal cells of fetal lung. *Am J Physiol* 1992; 262(6 Pt 1): L672-683.

55. Li L, Mao J, Sun L, Liu W, Wu D. Second cysteine-rich domain of Dickkopf-2 activates canonical Wnt signaling pathway via LRP-6 independently of dishevelled. *J Biol Chem* 2002; 277(8): 5977-5981.
56. Shu W, Jiang YQ, Lu MM, Morrissey EE. Wnt7b regulates mesenchymal proliferation and vascular development in the lung. *Development* 2002; 129(20): 4831-4842.
57. Rajagopal J, Carroll TJ, Guseh JS, Bores SA, Blank LJ, Anderson WJ, Yu J, Zhou Q, McMahon AP, Melton DA. Wnt7b stimulates embryonic lung growth by coordinately increasing the replication of epithelium and mesenchyme. *Development* 2008; 135(9): 1625-1634.
58. Maretto S, Cordenonsi M, Dupont S, Braghetta P, Broccoli V, Hassan AB, Volpin D, Bressan GM, Piccolo S. Mapping Wnt/beta-catenin signaling during mouse development and in colorectal tumors. *Proc Natl Acad Sci U S A* 2003; 100(6): 3299-3304.
59. Okubo T, Hogan BL. Hyperactive Wnt signaling changes the developmental potential of embryonic lung endoderm. *J Biol* 2004; 3(3): 11.
60. Dean CH, Miller LA, Smith AN, Dufort D, Lang RA, Niswander LA. Canonical Wnt signaling negatively regulates branching morphogenesis of the lung and lacrimal gland. *Dev Biol* 2005; 286(1): 270-286.
61. Mucenski ML, Wert SE, Nation JM, Loudy DE, Huelsken J, Birchmeier W, Morrissey EE, Whitsett JA. beta-Catenin is required for specification of proximal/distal cell fate during lung morphogenesis. *J Biol Chem* 2003; 278(41): 40231-40238.
62. Winn RA, Marek L, Han SY, Rodriguez K, Rodriguez N, Hammond M, Van Scoyk M, Acosta H, Mirus J, Barry N, Bren-Mattison Y, Van Raay TJ, Nemenoff RA, Heasley LE. Restoration of Wnt-7a expression reverses non-small cell lung cancer cellular transformation through frizzled-9-mediated growth inhibition and promotion of cell differentiation. *J Biol Chem* 2005; 280(20): 19625-19634.
63. Kikuchi A. Tumor formation by genetic mutations in the components of the Wnt signaling pathway. *Cancer Sci* 2003; 94(3): 225-229.
64. Paul S, Dey A. Wnt signaling and cancer development: therapeutic implication. *Neoplasia* 2008; 55(3): 165-176.
65. Polakis P. Wnt signaling and cancer. *Genes Dev* 2000; 14(15): 1837-1851.
66. Lammi L, Arte S, Somer M, Jarvinen H, Lahermo P, Thesleff I, Pirinen S, Nieminen P. Mutations in AXIN2 cause familial tooth agenesis and predispose to colorectal cancer. *Am J Hum Genet* 2004; 74(5): 1043-1050.
67. Chen S, Guttridge DC, You Z, Zhang Z, Fribley A, Mayo MW, Kitajewski J, Wang CY. Wnt-1 signaling inhibits apoptosis by activating beta-catenin/T cell factor-mediated transcription. *J Cell Biol* 2001; 152(1): 87-96.
68. He B, Jablons DM. Wnt signaling in stem cells and lung cancer. *Ernst Schering Found Symp Proc* 2006(5): 27-58.
69. Mazieres J, He B, You L, Xu Z, Jablons DM. Wnt signaling in lung cancer. *Cancer Lett* 2005; 222(1): 1-10.
70. Uematsu K, He B, You L, Xu Z, McCormick F, Jablons DM. Activation of the Wnt pathway in non small cell lung cancer: evidence of dishevelled overexpression. *Oncogene* 2003; 22(46): 7218-7221.
71. You L, He B, Xu Z, Uematsu K, Mazieres J, Mikami I, Reguart N, Moody TW, Kitajewski J, McCormick F, Jablons DM. Inhibition of Wnt-2-mediated signaling induces programmed cell death in non-small-cell lung cancer cells. *Oncogene* 2004; 23(36): 6170-6174.

72. Huang CL, Liu D, Nakano J, Ishikawa S, Kontani K, Yokomise H, Ueno M. Wnt5a expression is associated with the tumor proliferation and the stromal vascular endothelial growth factor--an expression in non-small-cell lung cancer. *J Clin Oncol* 2005; 23(34): 8765-8773.
73. Pongracz JE, Stockley RA. Wnt signalling in lung development and diseases. *Respir Res* 2006; 7: 15.
74. Kim D, Rath O, Kolch W, Cho KH. A hidden oncogenic positive feedback loop caused by crosstalk between Wnt and ERK pathways. *Oncogene* 2007; 26(31): 4571-4579.
75. Surendran K, McCaul SP, Simon TC. A role for Wnt-4 in renal fibrosis. *Am J Physiol Renal Physiol* 2002; 282(3): F431-441.
76. Surendran K, Schiavi S, Hruska KA. Wnt-dependent beta-catenin signaling is activated after unilateral ureteral obstruction, and recombinant secreted frizzled-related protein 4 alters the progression of renal fibrosis. *J Am Soc Nephrol* 2005; 16(8): 2373-2384.
77. Cheng JH, She H, Han YP, Wang J, Xiong S, Asahina K, Tsukamoto H. Wnt antagonism inhibits hepatic stellate cell activation and liver fibrosis. *Am J Physiol Gastrointest Liver Physiol* 2008; 294(1): G39-49.
78. Chilosi M, Poletti V, Zamo A, Lestani M, Montagna L, Piccoli P, Pedron S, Bertaso M, Scarpa A, Murer B, Cancellieri A, Maestro R, Semenzato G, Doglioni C. Aberrant Wnt/beta-catenin pathway activation in idiopathic pulmonary fibrosis. *Am J Pathol* 2003; 162(5): 1495-1502.
79. Morrissey EE. Wnt signaling and pulmonary fibrosis. *Am J Pathol* 2003; 162(5): 1393-1397.
80. Kaminski N, Rosas IO. Gene expression profiling as a window into idiopathic pulmonary fibrosis pathogenesis: can we identify the right target genes? *Proc Am Thorac Soc* 2006; 3(4): 339-344.
81. Selman M, Pardo A, Barrera L, Estrada A, Watson SR, Wilson K, Aziz N, Kaminski N, Zlotnik A. Gene expression profiles distinguish idiopathic pulmonary fibrosis from hypersensitivity pneumonitis. *Am J Respir Crit Care Med* 2006; 173(2): 188-198.
82. Selman M, Pardo A, Kaminski N. Idiopathic pulmonary fibrosis: aberrant recapitulation of developmental programs? *PLoS Med* 2008; 5(3): e62.
83. Lewis CC, Yang JY, Huang X, Banerjee SK, Blackburn MR, Baluk P, McDonald DM, Blackwell TS, Nagabhushanam V, Peters W, Voehringer D, Erle DJ. Disease-specific gene expression profiling in multiple models of lung disease. *Am J Respir Crit Care Med* 2008; 177(4): 376-387.
84. DasGupta R, Fuchs E. Multiple roles for activated LEF/TCF transcription complexes during hair follicle development and differentiation. *Development* 1999; 126(20): 4557-4568.
85. Douglas IS, Diaz del Valle F, Winn RA, Voelkel NF. Beta-catenin in the fibroproliferative response to acute lung injury. *Am J Respir Cell Mol Biol* 2006; 34(3): 274-285.
86. Vuga LJ, Ben-Yehudah A, Kovkarova-Naumovski E, Oriss T, Gibson KF, Feghali-Bostwick C, Kaminski N. WNT5A is a regulator of fibroblast proliferation and resistance to apoptosis. *Am J Respir Cell Mol Biol* 2009; 41(5): 583-589.
87. Wei J, Melichian D, Komura K, Hinchcliff M, Lam AP, Lafyatis R, Gottardi CJ, Macdougald OA, Varga J. Canonical Wnt signaling induces skin fibrosis and

- subcutaneous lipoatrophy: A novel mouse model for scleroderma? *Arthritis Rheum*: 63(6): 1707-1717.
88. Pfaff EM, Becker S, Gunther A, Konigshoff M. Dickkopf proteins influence lung epithelial cell proliferation in idiopathic pulmonary fibrosis. *Eur Respir J*: 37(1): 79-87.
 89. Zemke AC, Teisanu RM, Giangreco A, Drake JA, Brockway BL, Reynolds SD, Stripp BR. beta-Catenin is not necessary for maintenance or repair of the bronchiolar epithelium. *Am J Respir Cell Mol Biol* 2009: 41(5): 535-543.
 90. Weng T, Liu L. The role of pleiotrophin and beta-catenin in fetal lung development. *Respir Res*: 11: 80.
 91. Brembeck FH, Rosario M, Birchmeier W. Balancing cell adhesion and Wnt signaling, the key role of beta-catenin. *Curr Opin Genet Dev* 2006: 16(1): 51-59.
 92. Perez-Moreno M, Fuchs E. Catenins: keeping cells from getting their signals crossed. *Dev Cell* 2006: 11(5): 601-612.
 93. Flozak AS, Lam AP, Russell S, Jain M, Peled ON, Sheppard KA, Beri R, Mutlu GM, Budinger GR, Gottardi CJ. Beta-catenin/T-cell factor signaling is activated during lung injury and promotes the survival and migration of alveolar epithelial cells. *J Biol Chem*: 285(5): 3157-3167.
 94. Crosby LM, Waters CM. Epithelial repair mechanisms in the lung. *Am J Physiol Lung Cell Mol Physiol*: 298(6): L715-731.
 95. Kim TH, Kim SH, Seo JY, Chung H, Kwak HJ, Lee SK, Yoon HJ, Shin DH, Park SS, Sohn JW. Blockade of the Wnt/beta-catenin pathway attenuates bleomycin-induced pulmonary fibrosis. *Tohoku J Exp Med*: 223(1): 45-54.
 96. Henderson WR, Jr., Chi EY, Ye X, Nguyen C, Tien YT, Zhou B, Borok Z, Knight DA, Kahn M. Inhibition of Wnt/beta-catenin/CREB binding protein (CBP) signaling reverses pulmonary fibrosis. *Proc Natl Acad Sci U S A*: 107(32): 14309-14314.
 97. Shrivastava N, Srivastava A. RNA interference: an emerging generation of biologicals. *Biotechnol J* 2008: 3(3): 339-353.
 98. Bilic J, Huang YL, Davidson G, Zimmermann T, Cruciat CM, Bienz M, Niehrs C. Wnt induces LRP6 signalosomes and promotes dishevelled-dependent LRP6 phosphorylation. *Science* 2007: 316(5831): 1619-1622.
 99. Forde JE, Dale TC. Glycogen synthase kinase 3: a key regulator of cellular fate. *Cell Mol Life Sci* 2007: 64(15): 1930-1944.
 100. Konigshoff M, Balsara N, Pfaff EM, Kramer M, Chrobak I, Seeger W, Eickelberg O. Functional Wnt signaling is increased in idiopathic pulmonary fibrosis. *PLoS One* 2008: 3(5): e2142.
 101. Moeller A, Ask K, Warburton D, Gauldie J, Kolb M. The bleomycin animal model: a useful tool to investigate treatment options for idiopathic pulmonary fibrosis? *Int J Biochem Cell Biol* 2008: 40(3): 362-382.
 102. Adamson IY, Bowden DH. The pathogenesis of bleomycin-induced pulmonary fibrosis in mice. *Am J Pathol* 1974: 77(2): 185-197.
 103. Serrano-Mollar A, Nacher M, Gay-Jordi G, Closa D, Xaubet A, Bulbena O. Intratracheal transplantation of alveolar type II cells reverses bleomycin-induced lung fibrosis. *Am J Respir Crit Care Med* 2007: 176(12): 1261-1268.
 104. Liu L, Carron B, Yee HT, Yie TA, Hajjou M, Rom W. Wnt pathway in pulmonary fibrosis in the bleomycin mouse model. *J Environ Pathol Toxicol Oncol* 2009: 28(2): 99-108.

105. Lu D, Zhao Y, Tawatao R, Cottam HB, Sen M, Leoni LM, Kipps TJ, Corr M, Carson DA. Activation of the Wnt signaling pathway in chronic lymphocytic leukemia. *Proc Natl Acad Sci U S A* 2004; 101(9): 3118-3123.
106. Hwang SG, Yu SS, Lee SW, Chun JS. Wnt-3a regulates chondrocyte differentiation via c-Jun/AP-1 pathway. *FEBS Lett* 2005; 579(21): 4837-4842.
107. Szeto W, Jiang W, Tice DA, Rubinfeld B, Hollingshead PG, Fong SE, Dugger DL, Pham T, Yansura DG, Wong TA, Grimaldi JC, Corpuz RT, Singh JS, Frantz GD, Devaux B, Crowley CW, Schwall RH, Eberhard DA, Rastelli L, Polakis P, Pennica D. Overexpression of the retinoic acid-responsive gene *Stra6* in human cancers and its synergistic induction by Wnt-1 and retinoic acid. *Cancer Res* 2001; 61(10): 4197-4205.
108. Taneyhill L, Pennica D. Identification of Wnt responsive genes using a murine mammary epithelial cell line model system. *BMC Dev Biol* 2004; 4: 6.
109. Daniels CB, Orgeig S. Pulmonary surfactant: the key to the evolution of air breathing. *News Physiol Sci* 2003; 18: 151-157.
110. George CL, Goss KL, Meyerholz DK, Lamb FS, Snyder JM. Surfactant-associated protein A provides critical immunoprotection in neonatal mice. *Infect Immun* 2008; 76(1): 380-390.
111. Wofford JA, Wright JR. Surfactant protein A regulates IgG-mediated phagocytosis in inflammatory neutrophils. *Am J Physiol Lung Cell Mol Physiol* 2007; 293(6): L1437-1443.
112. Lee SM, Tole S, Grove E, McMahon AP. A local Wnt-3a signal is required for development of the mammalian hippocampus. *Development* 2000; 127(3): 457-467.
113. Cheng CW, Yeh JC, Fan TP, Smith SK, Charnock-Jones DS. Wnt5a-mediated non-canonical Wnt signalling regulates human endothelial cell proliferation and migration. *Biochem Biophys Res Commun* 2008; 365(2): 285-290.
114. Goodwin AM, Sullivan KM, D'Amore PA. Cultured endothelial cells display endogenous activation of the canonical Wnt signaling pathway and express multiple ligands, receptors, and secreted modulators of Wnt signaling. *Dev Dyn* 2006; 235(11): 3110-3120.
115. Brigstock DR. The CCN family: a new stimulus package. *J Endocrinol* 2003; 178(2): 169-175.
116. Pennica D, Swanson TA, Welsh JW, Roy MA, Lawrence DA, Lee J, Brush J, Taneyhill LA, Deuel B, Lew M, Watanabe C, Cohen RL, Melhem MF, Finley GG, Quirke P, Goddard AD, Hillan KJ, Gurney AL, Botstein D, Levine AJ. WISP genes are members of the connective tissue growth factor family that are up-regulated in wnt-1-transformed cells and aberrantly expressed in human colon tumors. *Proc Natl Acad Sci U S A* 1998; 95(25): 14717-14722.
117. Behrens J, Jerchow BA, Wurtele M, Grimm J, Asbrand C, Wirtz R, Kuhl M, Wedlich D, Birchmeier W. Functional interaction of an axin homolog, conductin, with beta-catenin, APC, and GSK3beta. *Science* 1998; 280(5363): 596-599.
118. Kikuchi A. Regulation of beta-catenin signaling in the Wnt pathway. *Biochem Biophys Res Commun* 2000; 268(2): 243-248.
119. Mao B, Niehrs C. *Kremen2* modulates *Dickkopf2* activity during Wnt/LRP6 signaling. *Gene* 2003; 302(1-2): 179-183.
120. Niehrs C. Function and biological roles of the *Dickkopf* family of Wnt modulators. *Oncogene* 2006; 25(57): 7469-7481.

121. Wu W, Glinka A, Delius H, Niehrs C. Mutual antagonism between dickkopf1 and dickkopf2 regulates Wnt/beta-catenin signalling. *Curr Biol* 2000; 10(24): 1611-1614.
122. He W, Dai C, Li Y, Zeng G, Monga SP, Liu Y. Wnt/beta-catenin signaling promotes renal interstitial fibrosis. *J Am Soc Nephrol* 2009; 20(4): 765-776.
123. Hwang I, Seo EY, Ha H. Wnt/beta-catenin signaling: a novel target for therapeutic intervention of fibrotic kidney disease. *Arch Pharm Res* 2009; 32(12): 1653-1662.
124. Lappalainen U, Whitsett JA, Wert SE, Tichelaar JW, Bry K. Interleukin-1beta causes pulmonary inflammation, emphysema, and airway remodeling in the adult murine lung. *Am J Respir Cell Mol Biol* 2005; 32(4): 311-318.
125. Gasse P, Mary C, Guenon I, Noulin N, Charron S, Schnyder-Candrian S, Schnyder B, Akira S, Quesniaux VF, Lagente V, Ryffel B, Couillin I. IL-1R1/MyD88 signaling and the inflammasome are essential in pulmonary inflammation and fibrosis in mice. *J Clin Invest* 2007; 117(12): 3786-3799.
126. Saito F, Tasaka S, Inoue K, Miyamoto K, Nakano Y, Ogawa Y, Yamada W, Shiraishi Y, Hasegawa N, Fujishima S, Takano H, Ishizaka A. Role of interleukin-6 in bleomycin-induced lung inflammatory changes in mice. *Am J Respir Cell Mol Biol* 2008; 38(5): 566-571.
127. Hwang SG, Ryu JH, Kim IC, Jho EH, Jung HC, Kim K, Kim SJ, Chun JS. Wnt-7a causes loss of differentiated phenotype and inhibits apoptosis of articular chondrocytes via different mechanisms. *J Biol Chem* 2004; 279(25): 26597-26604.
128. Wilson MS, Madala SK, Ramalingam TR, Gochuico BR, Rosas IO, Cheever AW, Wynn TA. Bleomycin and IL-1beta-mediated pulmonary fibrosis is IL-17A dependent. *J Exp Med* 2007; 207(3): 535-552.
129. Manzer R, Wang J, Nishina K, McConville G, Mason RJ. Alveolar epithelial cells secrete chemokines in response to IL-1beta and lipopolysaccharide but not to ozone. *Am J Respir Cell Mol Biol* 2006; 34(2): 158-166.
130. Thorley AJ, Ford PA, Giembycz MA, Goldstraw P, Young A, Tetley TD. Differential regulation of cytokine release and leukocyte migration by lipopolysaccharide-stimulated primary human lung alveolar type II epithelial cells and macrophages. *J Immunol* 2007; 178(1): 463-473.
131. Witherden IR, Vanden Bon EJ, Goldstraw P, Ratcliffe C, Pastorino U, Tetley TD. Primary human alveolar type II epithelial cell chemokine release: effects of cigarette smoke and neutrophil elastase. *Am J Respir Cell Mol Biol* 2004; 30(4): 500-509.
132. Dinarello CA. Biologic basis for interleukin-1 in disease. *Blood* 1996; 87(6): 2095-2147.
133. Dinarello CA. The interleukin-1 family: 10 years of discovery. *Faseb J* 1994; 8(15): 1314-1325.
134. Hoshino T, Okamoto M, Sakazaki Y, Kato S, Young HA, Aizawa H. Role of proinflammatory cytokines IL-18 and IL-1beta in bleomycin-induced lung injury in humans and mice. *Am J Respir Cell Mol Biol* 2009; 41(6): 661-670.
135. Ortiz LA, Dutreil M, Fattman C, Pandey AC, Torres G, Go K, Phinney DG. Interleukin 1 receptor antagonist mediates the antiinflammatory and antifibrotic effect of mesenchymal stem cells during lung injury. *Proc Natl Acad Sci U S A* 2007; 104(26): 11002-11007.

136. Wang Z, Shu W, Lu MM, Morrissey EE. Wnt7b activates canonical signaling in epithelial and vascular smooth muscle cells through interactions with Fzd1, Fzd10, and LRP5. *Mol Cell Biol* 2005; 25(12): 5022-5030.
137. Crestani B, Cornillet P, Dehoux M, Rolland C, Guenounou M, Aubier M. Alveolar type II epithelial cells produce interleukin-6 in vitro and in vivo. Regulation by alveolar macrophage secretory products. *J Clin Invest* 1994; 94(2): 731-740.
138. Johnston CJ, Piedboeuf B, Rubin P, Williams JP, Baggs R, Finkelstein JN. Early and persistent alterations in the expression of interleukin-1 alpha, interleukin-1 beta and tumor necrosis factor alpha mRNA levels in fibrosis-resistant and sensitive mice after thoracic irradiation. *Radiat Res* 1996; 145(6): 762-767.
139. Phan SH, Kunkel SL. Lung cytokine production in bleomycin-induced pulmonary fibrosis. *Exp Lung Res* 1992; 18(1): 29-43.
140. Heinrich PC, Behrmann I, Haan S, Hermanns HM, Muller-Newen G, Schaper F. Principles of interleukin (IL)-6-type cytokine signalling and its regulation. *Biochem J* 2003; 374(Pt 1): 1-20.
141. Shahar I, Fireman E, Topilsky M, Grief J, Kivity S, Spirer Z, Ben Efraim S. Effect of IL-6 on alveolar fibroblast proliferation in interstitial lung diseases. *Clin Immunol Immunopathol* 1996; 79(3): 244-251.
142. Vaillant P, Menard O, Vignaud JM, Martinet N, Martinet Y. The role of cytokines in human lung fibrosis. *Monaldi Arch Chest Dis* 1996; 51(2): 145-152.
143. Nakamura Y, Nawata M, Wakitani S. Expression profiles and functional analyses of Wnt-related genes in human joint disorders. *Am J Pathol* 2005; 167(1): 97-105.
144. Vasakova M, Sterclova M, Kolesar L, Slavcev A, Pohunek P, Sulc J, Skibova J, Striz I. Bronchoalveolar lavage fluid cellular characteristics, functional parameters and cytokine and chemokine levels in interstitial lung diseases. *Scand J Immunol* 2009; 69(3): 268-274.
145. Vasakova M, Sterclova M, Kolesar L, Slavcev A, Pohunek P, Sulc J, Striz I. Cytokine gene polymorphisms and BALF cytokine levels in interstitial lung diseases. *Respir Med* 2009; 103(5): 773-779.
146. Takizawa H, Satoh M, Okazaki H, Matsuzaki G, Suzuki N, Ishii A, Suko M, Okudaira H, Morita Y, Ito K. Increased IL-6 and IL-8 in bronchoalveolar lavage fluids (BALF) from patients with sarcoidosis: correlation with the clinical parameters. *Clin Exp Immunol* 1997; 107(1): 175-181.
147. Coker RK, Laurent GJ. Pulmonary fibrosis: cytokines in the balance. *Eur Respir J* 1998; 11(6): 1218-1221.
148. Beklen A, Ainola M, Hukkanen M, Gurgan C, Sorsa T, Konttinen YT. MMPs, IL-1, and TNF are regulated by IL-17 in periodontitis. *J Dent Res* 2007; 86(4): 347-351.
149. Sutton CE, Lalor SJ, Sweeney CM, Brereton CF, Lavelle EC, Mills KH. Interleukin-1 and IL-23 induce innate IL-17 production from gammadelta T cells, amplifying Th17 responses and autoimmunity. *Immunity* 2009; 31(2): 331-341.
150. Zhang K, Phan SH. Cytokines and pulmonary fibrosis. *Biol Signals* 1996; 5(4): 232-239.
151. Budinger GR, Mutlu GM, Eisenbart J, Fuller AC, Bellmeyer AA, Baker CM, Wilson M, Ridge K, Barrett TA, Lee VY, Chandel NS. Proapoptotic Bid is required for pulmonary fibrosis. *Proc Natl Acad Sci U S A* 2006; 103(12): 4604-4609.

152. Sheppard D. Pulmonary fibrosis: a cellular overreaction or a failure of communication? *J Clin Invest* 2001; 107(12): 1501-1502.
153. Kneidinger N, Yildirim AO, Callegari J, Takenaka S, Stein MM, Dumitrescu R, Bohla A, Bracke KR, Morty RE, Brusselle GG, Schermuly RT, Eickelberg O, Konigshoff M. Activation of the WNT/beta-catenin pathway attenuates experimental emphysema. *Am J Respir Crit Care Med*: 183(6): 723-733.

8 DECLARATION

I declare that I have completed this dissertation single-handedly without the unauthorized help of a second party and only with the assistance acknowledged therein. I have appropriately acknowledged and referenced all text passages that are derived literally from or are based on the content of published or unpublished work of others, and all information that relates to verbal communications. I have abided by the principles of good scientific conduct laid down in the charter of the Justus-Liebig-University of Giessen in carrying out the investigations described in the dissertation.

9 ACKNOWLEDGEMENTS

Last, but not least I would like to dedicate this closing chapter to all those people, who have been involved into this period of life with my doctoral thesis in every possible way.

I am thankful to Prof. Dr. Werner Seeger for giving young graduates, like me, from different natural scientific and medical branches the opportunity to enter the exciting world of science, providing an insight into research and teaching us to be cosmopolitan.

I would like to express my sincere gratitude to my supervisor Prof. Dr. Oliver Eickelberg, for giving me the opportunity to work in his laboratory and allowing me to be part of an international research group. I thank him especially for his knowledge and research insights, as well as for his encouragement and guidance throughout my doctoral thesis. During this time, Prof. Dr. Eickelberg has given me the exceptional opportunity to participate in various national and international conferences, supporting my work and self-confidence.

I am deeply grateful to my veterinary supervisor Prof. Dr. Rüdiger Gerstberger for his constant support, encouragement and especially for being receptive to all my questions/problems. His exceptional guidance and patience throughout my doctoral thesis incited me to have an agenda.

Special thanks to Dr. Melanie Königshoff for her constant support, knowledge, enthusiasm and making it clear to me that to be optimistic about achieving a target is the best way to “survive” in the laboratory. And I would like to thank her for the efforts in proof-reading this thesis.

Many, many thanks to my friends Simone Becker and Andreas Jahn for all their help, outstanding technical assistance and all the wonderful and cheerful moments that we had together.

I would also like to thank Marlene Stein and Jochen Wilhelm for their special help and technical assistance.

Special thanks to my friends and “WNT team” members Nele Rensing, Eva Pfaff, Monika Kramer, Izabella Chrobak and Nikolaus Kneidinger for their professional, as

well as emotional support and all the fun, which also made these years of research work in lab and in private life so unique.

I thank my soulmate and “bahen (sister)” Aparna Jayachandran for all her help, support and friendship for life.

I want to thank all the other colleagues of my and collaborating laboratories for fruitful discussions and the opportunity to work with them. There are so many people, very good friends from school and university days who accompanied me during this period of life and I would like to thank all of them by name, but unfortunately this would go beyond the scope - THANKS A LOT TO EVERYONE!!!

I thank my family here and in India for all their love, support and prayers.

Finally, I would like to express my gratitude especially to my parents - the most lovable mom and dad on earth - for their unlimited love, encouragement and support. Without them, especially my mom, I wouldn't be there, where I am today, reached my aims and let my dreams come true. To both of them I dedicate this thesis, and especially to my beloved dad, who always watched over me from “above”, giving me strength and faith in myself. THANK YOU!!!



édition scientifique
VVB LAUFERSWEILER VERLAG

VVB LAUFERSWEILER VERLAG
STAUFENBERGRING 15
D-35396 GIESSEN

Tel: 0641-5599888 Fax: -5599890
redaktion@doktorverlag.de
www.doktorverlag.de

ISBN: 978-3-8359-6054-1



9 7 8 3 8 3 5 1 9 6 0 5 4 1